






Safe Design of Packaging with SFPPy

from Virgin and Recycled Materials

Olivier Vitrac, PhD | *Generative Simulation Initiative*     



Abstract

This document introduces a **tiered framework (M0–M3)** for the safe design of food, cosmetic, and pharmaceutical packaging. The framework progresses from simple conservative balances to complex scenarios integrating diffusion, functional barriers, and recycled materials. It relies on: (i) **explicit indicators** (severity, criticality, release potential); (ii) **constraint-based optimization rules**; (iii) **open databases** (PubChem, ToxTree); and (iv) **Python tools (SFPPy)** to automate calculations and scenarios, including coupling with **generative AI (RAG)** for reasoning and traceability. The goal is **design-for-compliance**: build intrinsically safe, conformant packaging upstream, not only verify ex-post.

See the overview of tiers in Section 6, thermodynamic principles in Section 3, and SFPPy examples in Section 9.

This document is released "AS IS".

The content of this article is intended to be published in French and English in several peer-reviewed journals..

Read this  file in PDF with this link | Access all  files with this link

Note

A glossary of key terms and expressions, as well as a table of acronyms, notations, and symbols used throughout the article, is provided at the end.

Introduction

Motivation

The **safe design** of food packaging consists in integrating **health and safety constraints** from the very beginning. The objective is to ensure that migrating substances from materials remain below regulatory toxicological thresholds, regardless of the complexity of structures or the origin of materials, including **recycled** ones. This proactive approach is decisive, as it steers **formulation** and **design** before market release, in a context where European, American, and Chinese regulations strictly frame compliance requirements.

The proposed method rests on a clear doctrine: translate the **safety problem** into **explainable and verifiable design constraints** that can be tested by humans, AI agents and both. It is structured around four complementary principles.

1. **Formalization of the regulatory constraint**, linking the specific migration of each substance to a toxicological reference value.
2. **Conservative modeling of migration**: a generic thermodynamic model provides robust upper bounds, applicable to any material and any contact condition.
3. **Introduction of risk indicators**, condensing information on substances and components into severities (individual) and criticalities (cumulative), facilitating ranking, optimization, and justification of technical choices.
4. A **tiered approximation method**: a system of “tiers” ranging from the most conservative scenario to refined evaluations by substance and material.

This approach is designed to be operational at multiple scales. It can be implemented simply in a **spreadsheet** for punctual evaluations, but it is also compatible with **automated environments** and **reasoning chains** driven by **Artificial Intelligence (AI)**. It is integrated in the open-source tools *FMECAEngine* (Vitrac 2025) and *SFPPy / SFPPyLite* (Vitrac, 2025a; Vitrac, 2025b). These tools utilize *PubChem* (Kim *et al.*, 2024) as a molecular structure engine and *ToxTree* (Patlewicz *et al.*, 2008) for toxicological classification in a fully automated manner. This dual usage — manual or automated — is deliberate: it aims to foster transparency and auditability, both essential in a regulated domain, while anticipating the industrialization of repetitive calculations and multicriteria explorations, beyond the substances explicitly listed in regulations. In this sense, this article illustrates a philosophy of “**design for compliance**”: the objective is no longer to demonstrate *a posteriori* that a packaging is safe, but to build **intrinsically compliant and safe solutions** from the outset.

This article focuses on the objective construction of **health safety indicators** and their integration in a design logic (optimization of components, formulation, and uses), treated as an engineering mathematical problem. Readers interested in the physics of transfers and their resolution techniques are referred to Zhu *et al.* (2019). Finally, the approaches presented here constitute an important update compared to the last European guide (Brandsch *et al.*, 2015), to which one of us contributed.

Key takeaways

Because this is a **design approach**, it takes place **before experimental testing**. The proposed indicators can accommodate calculated or partial data (composition, decontamination rates, intermediate migration results). They cover:

- **All materials:** while tiers 2 and 3 are particularly suited to thermoplastics and elastomers, an extension is foreseen for paper and board.
- **Virgin and recycled materials**, without distinction of recycling technology.
- **Single-use and repeated-use contexts**, accounting for forming steps that modify substance distribution.
- **All sensitive contact applications:** primarily food, but also pharmaceuticals, cosmetics, medical devices, and household products.

In contrast, this article does not provide a ranking of materials or recommendations on processes/materials. The application of indicators depends on the intended use, without privileging virgin versus recycled plastics or paper. The indicators are generic: they can be combined, if necessary, with other criteria such as economic costs or environmental impacts.

Tip

Readers wishing to explore the concepts while maintaining control over calculation steps may use the *SFPP3* platform (Vitrac, 2025c), which relies on the same computational engine (Nguyen *et al.*, 2013) as *SFPPy* / *SFPPyLite*. Prerequisites for a good understanding of this article can be acquired through the *FitNESS* platform (Vitrac *et al.*, 2024).

1 | General Problem

“It would be ideal if the migration of each additive and monomer into the packed foodstuff could be determined when the package has been filled and stored under normal conditions of practice. This would ensure that no physiologically objectionable plastics material would be admitted and, on the other hand, that no suitable plastics material would be rejected because of a hypercritical assessment.”
— Figge (1980) (Figge 1980)

1.1 | Its evolution

Designing safe packaging remains a challenge because the distinction between **hazard** and **risk** is not always intuitive for designers. Hazard refers to the intrinsic toxicity of substances, whereas risk depends on the quantities actually ingested by the consumer. Two emblematic publications, published more than half a century apart in the prestigious journals *Science* and *Nature*, illustrate the persistence of this problem: Jaeger and Rubin (1970), which highlights migration of major constituents such as monomers and plasticizers, and Monclús *et al.* (2025), which reveals the migration of hundreds of minor substances.

The difficulty is therefore not removed but **shifted**: on the one hand, from controlling a few well-characterized additives to assessing multiple contaminants with uncertain profiles; on the other, from an analytical approach focused on known substances to an **integrated approach** capable of setting priorities and ranking risks.

1.2 | The European regulatory perspective

In Europe, assessment rests on a clear distinction between hazard and risk. Substances are assessed **individually** when their structures differ sufficiently. For homogeneous families (isomers, substituted molecules), they are grouped by **aggregation**. This logic extends to substances sharing a **common toxicological mode of action** such as *phthalates* or *benzophenones*.

Certain effects, however, are **excluded** from the regulatory scope. Synergistic effects, often called “**cocktail effects**,” are not considered. Cumulative exposures to genotoxic or carcinogenic substances are likewise not considered. Thus, the presence of several carcinogens at low levels may be deemed acceptable as long as none individually exceeds its alert threshold.

Note

These rules may evolve, but they do not challenge the **safe design** method presented in this article. The core of the approach—translating the toxicological constraint into a **design constraint**—remains valid regardless of the criteria adopted.

1.3 | Exposure calculation in Europe and the “safety condition”

Exposure calculation relies on a **conservative, simplified hypothesis**. It assumes the daily ingestion of $DI = 1 \text{ kg of food} \cdot \text{day}^{-1}$ contaminated by each substance, by an adult with a body weight $BW = 60 \text{ kg}$. The tolerable daily intake (TDI) expressed in $\text{mg} \cdot \text{kg body weight}^{-1} \cdot \text{day}^{-1}$ is converted to a **maximum allowable concentration in food**, called the specific migration limit (SML).

For a substance i :

$$SML_i = BW \times DI \times TDI_i \quad (\text{SML})$$

Note

SML_i corresponds to the **maximum acceptable exposure** for an adult consuming 1 kg of food daily packaged in the same packaging, **excluding other sources of exposure**.

A package is deemed **safe** if, for every substance i , the estimated concentration in food $C_{i,F}$ results in an exposure below the maximum acceptable exposure:

$$\frac{C_{i,F}}{\rho_F} \leq SML_i \quad (\text{Safety})$$

where ρ_F is the **apparent density** of the food, i.e., the mass of food occupying the food volume. For a granular product such as breakfast cereal, this is the **mass of food in the bag divided by the internal volume** of the bag.

This approach ignores cumulative exposure but **requires aggregation** for substances with a **common toxicological target**. A direct consequence is that a **recycled material**, although richer in contaminants, can be considered as safe as a virgin material as soon as condition **Safety** is satisfied for all substances i it contains. These substances may be **identified and quantified**, only **identified**, or **unknown**.

Note

Here, $C_{i,F}$ is a **volumetric concentration** (SI units: $\text{kg} \cdot \text{m}^{-3}$) consistent with the physical description of transfers: contaminants fill a **volume**, not a mass. This choice is also consistent with the **design problem**, in which volumes are known via the geometry of layers and components.

Conversely, **exposure limits** are expressed per **ingested mass of food**. The ratio $\frac{C_{i,F}}{\rho_F}$ represents the **mass concentration** in food (SI units: $\text{kg} \cdot \text{kg}^{-1}$).

1.4 | Toxicological reference values

When a substance appears on a **positive list**, as in Regulation (EU) No 10/2011, the **regulatory value** of SML_i must be used **as a priority**. When a TDI value is published, it should also be **preferred** over other estimates.

Here, TDI is used in a **generic** sense to denote any **toxicological reference value**. For certain substances, notably those present in recycled materials, other notions may apply, such as the **threshold of toxicological concern (TTC)**.

TTC thresholds (Munro *et al.*, 2008) to be applied to **non-evaluated** substances—and thus usable for **unknown substances**—were set by the **European Food Safety Authority (EFSA)** (EFSA, 2016) and are recalled in Table 1.

Table 1 — TTC thresholds by toxicological class (EFSA) (Source: EFSA, 2016)

Toxicological class	TTC ($\mu\text{g} \cdot \text{kg}^{-1} \cdot \text{bw}^{-1} \cdot \text{day}^{-1}$)
Possible genotoxicity (conservative)	0.0025
Cramer class III (high concern)	1.5
Cramer class II (intermediate toxicity)	9
Cramer class I (low toxicity)	30

Tip

TTC values can be predicted for arbitrary molecules using **ToxTree** (Patlewicz 2008) or its ports in open-source projects such as **SFPy** (Vitrac 2025).

Body weight (BW) and daily ingestion (DI) values vary with the consumer's age. Table 2 illustrates how SML_i values can be **adjusted** for packaging intended for **sensitive populations**.

Table 2 — Recommended BW and DI values by age group

Age group	(kg)	(kg·day ⁻¹)	Source
Newborns (0–16 weeks)	5	0.75	EFSA 2017

Age group	BW (kg)	DI (kg·day ⁻¹)	Source
Infants (0–6 months)	5–6	0.75–1.0	EFSA 2017
Young children (1–3 years)	12	1.0	EFSA 2012
Children (4–9 years)	20	1.0–1.5	EFSA 2012
Adults (≥ 15 years)	60–70	1.0	EU 10/2011

1.5 | Equivalent mathematical problem

The exact calculation of $C_{i,F}$ for **hundreds of substances** and **several components** is costly and unnecessarily precise as long as we can prove that an **over-estimator** $\hat{C}_{i,F}$ satisfies two properties:

(i) **Robust overestimation property:**

$$\begin{aligned} \hat{C}_{i,F} &\geq C_{i,F} \\ \Pr(\hat{C}_{i,F} > \rho_F \cdot SML_i) &\leq \Pr(C_{i,F} > \rho_F \cdot SML_i) \end{aligned} \quad (\text{Equiv-1})$$

(ii) **An explainable and fast calculation of $\hat{C}_{i,F}$.**

Property [Equiv-1](#) guarantees by construction that the inequality $\frac{\hat{C}_{i,F}}{\rho_F} \leq SML_i$ translates into **actual safety** expressed with the **real, experimentally verifiable concentration** $\frac{C_{i,F}}{\rho_F} \leq SML_i$. On the design side, Eq. [Equiv-1](#) imposes **bounds on the initial concentrations** $C_{i,j}^0$ in each component $j = 1, \dots, m$ (food is $j = 0$):

$$C_{i,j}^0 \leq \hat{C}_{i,j}^0 \quad (1)$$

where $\hat{C}_{i,j}^0$ denotes the **maximum acceptable concentration** in component j for substance i , calculated under the conservative hypothesis $\hat{C}_{i,F} = SML_i$ while considering **all possible sources** (layers, inks, adhesives, closures, fibrous backings). Feasibility of a design is then stated as the membership of the vector $\mathbf{C}_i^0 = (C_{i,1}^0, \dots, C_{i,m}^0)$ to an **admissible polytope** defined by these inequalities.

Note

Initial concentrations $C_{i,j}^0$ are also expressed as **volumetric concentrations** (SI: kg · m⁻³). They must be compared to the **mass concentrations** $\frac{C_{i,j}^0}{\rho_j}$ used by industry and formulators/converters, where ρ_j is the **density** of material j .
For porous materials, ρ_j is an **apparent density**. For paperboard, it is defined by the **basis weight divided by the average thickness**.

1.6 | A tiered approach

The same criterion [Equiv-1](#) can be satisfied at **several levels of approximation** that balance **uncertainty**, **compute time**, and **explainability**. We structure these approximations into **tiers** along two independent axes:

- **Toxicology axis (T):** sets SML_i according to substance knowledge. $T0$ corresponds to the **worst case** (genotoxicity TTC: $0.0025 \mu\text{g} \cdot \text{kg}^{-1} \cdot \text{bw}^{-1} \cdot \text{day}^{-1}$); higher levels $T1, T2, \dots$ use TTC by **Cramer classes** and then **published TDI/SML** values. The higher T , the more **informed** and generally **less conservative** SML_i becomes.
- **Transfer axis (M):** sets $\hat{C}_{i,F}$ according to transfer physics. $M0$ assumes **total transfer** ($\bar{v}_i^* \rightarrow 1$ and infinitely favorable partitioning to food); $M1$ introduces **unit partitioning** between phases ($K \simeq 1$); $M2$ uses **realistic partitions** (solubilities, polarity, crystallinity, immobile fractions); $M3$ introduces **diffusion dynamics** (time, temperature, sequences). The higher M , the more **realistic** and thus **less conservative** the estimate.

This $T \times M$ decomposition, reproduced in Table 3, enables tailoring the effort: **improve** T when toxicology progresses, or **improve** M when material/use data become available—**without changing the decision logic**.

Table 3 — Tier matrix for design (T×M)

	T0 — worst case — genotoxic TTC	T1 — TTC — Cramer classes	T2 — published TDI/SML
M0 — total transfer	(T0, M0)	(T1, M0)	(T2, M0)
M1 — unit partition	(T0, M1)	(T1, M1)	(T2, M1)
M2 — realistic partitions (solubility, polarity, crystallinity)	(T0, M2)	(T1, M2)	(T2, M2)
M3 — dynamic diffusion (time, temperature)	(T0, M3)	(T1, M3)	(T2, M3)

The horizontal axis (T) refines toxicology from genotoxic TTC ($T0$) to specific published values ($T2$). The vertical axis (M) refines transfer representation from total transfer ($M0$) to dynamic diffusion ($M3$). Each cell (T, M) is a usable combination to size design thresholds $\hat{C}_{i,j}^0$.

Estimators derived from the **M-tiers** must be constructed to satisfy **monotonicity properties** on concentration scales in food and in materials:

$$\begin{aligned} \{\hat{C}_{i,F}\}_{M=0} &\geq \{\hat{C}_{i,F}\}_{M=1} \geq \{\hat{C}_{i,F}\}_{M=2} \geq \{\hat{C}_{i,F}\}_{M=3} \geq C_{i,F}, \\ \{\hat{C}_{i,j}^0\}_{M=0} &\leq \{\hat{C}_{i,j}^0\}_{M=1} \leq \{\hat{C}_{i,j}^0\}_{M=2} \leq \{\hat{C}_{i,j}^0\}_{M=3} \leq C_{i,j}^0 \end{aligned} \quad (\text{Monotony})$$

Note

In a multilayer design, **each component can be a source** of the same substance: process residues, recycling impurities, ink/adhesive constituents, environmental pickup. The calculation of $\hat{C}_{i,F}$ **adds these contributions conservatively**, including when **no-contact steps** redistribute masses before contact. For **unknown substances**, **substitution rules** are provided: material limits of detection ($DL_{i,j}$), stock levels combined with a decontamination rate ($1 - \Delta_{i,j}$), or dimensioning molecules (e.g., toluene) depending on the chosen tier.

1.7 | Operational formulation of the design problem

For a **given tier pair** (T, M) , the problem reduces to finding $\mathbf{C}_i^0 \in \mathbb{R}_+^m$ such that $\hat{C}_{i,F}^{(T,M)}(\mathbf{C}_i^0) \leq \rho_F \cdot SML_i^{(T)}$ for all i . In practice, we prefer to compute **per-component thresholds** via the sizing equality

$$\begin{aligned} \hat{C}_{i,F}^{(T,M)}(\hat{\mathbf{C}}_i^0) &= \rho_F \cdot SML_i^{(T)} \\ \text{with } \mathbf{C}_i^0 &= (C_{i,1}^0, \dots, C_{i,m}^0) \end{aligned} \quad (\text{FormulationProblem})$$

and deduce **simple constraints** $C_{i,j}^0 \leq \hat{C}_{i,j}^0$ usable in a spreadsheet, in a formulation database, or in a tooled calculation chain (scripts, RAG).

Note

In this article, a **script** denotes a light program that automates calculations for a given tier pair (T, M) and applies them to a large number of substances and components (e.g., in Python or Matlab). **RAG** (Retrieval-Augmented Generation) denotes an AI approach that combines knowledge-base retrieval with the automatic generation of scripts or explanations, used here to document and secure sizing calculations. Finally, the article is written so that it can be directly exploited by **large language models (LLMs)**.

Key takeaways for Section 1

We replace the exact calculation of $C_{i,F}$ with an **explainable over-estimator** $\hat{C}_{i,F}$ and translate safety into **design bounds** $C_{i,j}^0 \leq \hat{C}_{i,j}^0$.

The **tiers** decouple **toxicology** (T : definition of SML_i) from **transfer physics** (M : partitioning then diffusion). **Monotonicity** guarantees **safety by construction**: refining T and/or M enlarges the admissible solution space **without weakening it**.

Tip

The next section (“General model for $C_{i,F}$ and $\hat{C}_{i,F}$ ”) makes explicit the form of $\hat{C}_{i,F}$, the separation of equilibrium/time, and prepares the introduction of indicators (PR , severity/criticality) and tiers $M2$ – $M3$.

2 | General model for the final concentration in food

2.1 | Hierarchical construction and conservative assumptions

The estimators $\{\hat{C}_{i,F}\}_{M=0..3}$ are all built **conservatively**: they aim to **maximize the final contamination** of food. Each tier progressively complicates a common parent model, in order to reduce part of the uncertainty when justified. The representation remains deliberately general to cover any type of material or substance, at least in the lower tiers. Further refinements may then introduce assumptions specific to a family of materials.

All models share a common set of assumptions:

- the total system volume (food + packaging) is additive;
- the system is closed to the outside: no losses, no chemical decomposition, no secondary production;
- use conditions are maximized to reflect the longest contact durations and highest foreseeable temperatures.

2.2 | Isolating the time contribution

The temporal component is the most complex to handle because it depends on:

- geometry (thickness, contact surface),
- use conditions (duration, temperature, type of contact),
- transport and thermodynamic properties of materials.

We introduce a **thermodynamic equilibrium concentration** $C_{i,F}^{eq}$ and a **dynamic term** $\bar{v}_i^*(t)$ that reflects the relative transfer rate (Vitrac and Hayert, 2005; Vitrac and Hayert, 2006):

$$C_{i,F}^{(t)} = C_{i,F}^{(0)} + \bar{v}_i^*(t) (C_{i,F}^{eq} - C_{i,F}^{(0)}) \quad (2)$$

Note

For a monolayer material, $\bar{v}_i^*(t)$ increases monotonically from 0 to 1. For a multilayer material, it may temporarily exceed 1 due to internal redistributions, but never departs by more than an order of magnitude from unity.

2.3 | Equilibrium concentration

At thermodynamic equilibrium, the partial pressures $p_{i,j}$ of substance i are equal in all compartments j . Henry's law gives:

$$p_{i,j} = k_{i,j}^H C_{i,j}, \quad j = 0..m \quad (\text{HenryIsotherm})$$

where $k_{i,j}^H$ is Henry's constant of the substance in compartment j .

Mass conservation imposes:

$$\sum_{j=0}^m V_j C_{i,j}^0 = \sum_{j=0}^m V_j C_{i,j}^{eq} = p_i^{eq} \sum_{j=0}^m \frac{V_j}{k_{i,j}^H} \quad (\text{MassBalance})$$

Thus, the equilibrium concentration in food is:

$$C_{i,F}^{eq} = \frac{p_i^{eq}}{k_{i,0}^H} = \frac{\sum_{j=0}^m V_j C_{i,j}^0}{\sum_{j=0}^m \frac{k_{i,0}^H}{k_{i,j}^H} V_j} \quad (3)$$

2.3.1 | Multiple sources

In the general case, contaminants may come from all packaging components (plastic, adhesive, ink, paper/board), independently of regulations that usually handle substances by material type. It is useful to distinguish the contribution from any **initial food contamination** (before contact) and that from non-food components.

We separate the food contribution ($j = 0$) from those of the other compartments ($j \geq 1$):

$$C_{i,F}^{eq} = C_{i,F}^0 \frac{V_0}{\sum_{j=0}^m \frac{k_{i,0}^H}{k_{i,j}^H} V_j} + \frac{\sum_{j=1}^m V_j C_{i,j}^0}{\sum_{j=0}^m \frac{k_{i,0}^H}{k_{i,j}^H} V_j} \quad (4)$$

In a **conservative approximation**, concentrations are replaced by upper bounds (denoted with a hat, including $\hat{C}_{i,F}^0$ which **ignores dilution** of initial food contamination), and food is assumed to **not recontaminate** the other compartments ($j > 0$):

$$\boxed{\hat{C}_{i,F}^{eq} = \hat{C}_{i,F}^0 + \frac{\sum_{j=1}^m V_j \hat{C}_{i,j}^0}{\sum_{j=0}^m \frac{k_{i,0}^H}{k_{i,j}^H} V_j}} \quad \text{with} \quad \hat{C}_{i,F}^0 \geq C_{i,F}^0, \quad \hat{C}_{i,j}^0 \geq C_{i,j}^0 \quad (5)$$

This introduces **no bias** when the initial food contamination is zero, since then $C_{i,F}^{eq} = \hat{C}_{i,F}^{eq}$.

Specializations by tier (axis M):

- **M0 (total transfer).**
All substances present in packaging fully migrate to food:

$$\boxed{\hat{C}_{i,F}^{eq} = \hat{C}_{i,F}^{(0)} + \frac{\hat{m}_i^0}{V_0}} \quad (6)$$

- **M1 (unit partition).**

All phases are assumed to have the same affinity as food, i.e. $k_{i,j}^H = k_{i,0}^H$ for all j .
The expression simplifies to a volume-weighted mean:

$$\hat{C}_{i,F}^{eq} = \frac{\sum_{j=0}^m V_j \hat{C}_{i,j}^0}{\sum_{j=0}^m V_j} \quad (7)$$

- **M2 (realistic partitions).**
Ratios of Henry's constants $k_{i,0}^H / k_{i,j}^H$ are accounted for to reflect solubility, polarity, and crystallinity of materials.
For prudence, **minimum plausible values** of $k_{i,0}^H / k_{i,j}^H$ are chosen to preserve the conservative nature of $\hat{C}_{i,F}^{eq}$.

Note

If the food has an initial contamination $\hat{C}_{i,F}^{(0)}$, it is convenient to write:

$$\hat{C}_{i,F}^{eq} = \hat{C}_{i,F}^{(0)} + \Delta \hat{C}_{i,F}^{eq} \quad (8)$$

where $\Delta \hat{C}_{i,F}^{eq}$ is obtained with the general formula summing only sources $j \geq 1$. This form simplifies spreadsheet use and contribution traceability.

2.3.2 | Single source and static migration rate

If the substance originates from a single component s , a simplified expression is obtained:

$$\hat{C}_{i,F}^{eq} = \hat{C}_{i,F}^0 + \frac{\hat{C}_{i,s}^0}{\sum_{j=0}^m \frac{k_{i,0}^H}{k_{i,j}^H} \frac{V_j}{V_0}} = \hat{C}_{i,F}^0 + \hat{m}_i^{*,eq} \frac{\hat{m}_i^0}{V_0} \quad (9)$$

where the static migration rate

$$\hat{m}_i^{*,eq} = \frac{1}{\sum_{j=0}^m \frac{k_{i,0}^H}{k_{i,j}^H} \frac{V_j}{V_0}} \quad (10)$$

satisfies $0 \leq \hat{m}_i^{*,eq} \leq 1$ and measures the fraction of substance initially present in packaging \hat{m}_i^0 that is transferred to food at equilibrium.

Note

In recycled materials, it is preferable to adopt a **cautious assumption**: consider multiple potential sources of i and maximize \hat{m}_i^0 .

2.4 | Practical expression of dynamic concentration in food

The conservative concentration in food at time t is:

$$\hat{C}_{i,F}^{(t)} = \hat{C}_{i,F}^{(0)} + \bar{v}_i^*(t) \hat{m}_i^{*,eq} \frac{\hat{m}_i^0}{V_0} \quad (11)$$

This formalism introduces two **release potentials**:

- **dynamic** $PR_i^T = \bar{v}_i^*(t)$,
- **static** $PR_i^E = \hat{m}_i^{*,eq}$,

whose product $PR_i = PR_i^T \times PR_i^E$ represents the total released fraction.

2.5 | Case of porous foods

The food volume, denoted V_0 or V_F , corresponds to the **apparent volume** occupied by food in the case of real food, and to the **experimental volume** imposed in the case of simulants. The concentration $\hat{C}_{i,F}$ must be considered **averaged at the volume scale**.

In porous foods (e.g. bread), since contamination accumulates in condensed phases, the calculated concentration in food will be **lower** than the concentration measured in the solid phase alone (crumb and crust) by extraction. The two measures reconcile if we note that the concentration in the solid phase is:

$$\hat{C}_{i,F,\text{solid}} = \frac{\hat{C}_{i,F}}{1 - \epsilon_F} \quad (12)$$

where ϵ_F is the **porosity** of food, i.e. the void volume fraction.

Key takeaways for Section 2

The general model expresses the final concentration in food as the sum of four components:

- initial contamination,
- a time factor,
- a static migration rate,
- and the total mobilizable amount.

This formulation preserves **thermodynamic rigor** while remaining usable in a spreadsheet. It prepares the introduction of **release potentials** and **ranking metrics**.

Tip

The next section develops the concept of **partial release potentials**, essential for analyzing process sequences and introducing the concept of a **functional barrier**.

3 | Partial release potentials and step sequences

3.1 | Intuition and objective

Within a sequence of steps in a package's life, we aim to assign an **explainable** share of the **total release** of substance i to **each step**. Contrary to common intuition, a **partial potential** may be **non-zero** even if **no direct transfer to food occurs** during the step considered. It is enough that the step **mobilizes** the substance (internal redistribution, surface approach, interface creation, geometry change) so as to **increase** what will be released in a later step.

Examples of “mobilizing” mechanisms without food contact:

- thermoforming that thins a layer and increases the specific surface area;
- thermoforming or any step in which temperature rise changes the internal distribution, notably by bringing substances closer to the exchange surface;
- bringing internal and external surfaces into contact by stacking or roll storage (e.g., contact with printed surfaces);
- folding that puts the packaging into contact with an overwrap;
- sealing or printing that creates active interfaces;
- contamination of contact layers by transfer during storage of components (e.g., cross-contamination with or without physical contact).

Tip

Key point. The concept of a **partial release potential** is independent of the detailed transfer physics and relies on a material balance between a reservoir of contaminants and a receiving phase (e.g., food or simulant). It is useful to trace the **causes and sources** of food contamination.

3.2 | Formal definition for independent steps

We define the **partial potential** of step k by an “with vs without” comparison:

$$PR_{i|k} \equiv 1 - \frac{1 - PR_i^{(N)}}{1 - PR_i^{(N \setminus k)}} \in [0, 1] \quad (13)$$

where $PR_i^{(N)}$ is the global release potential to food after applying an ordered subset of N steps in the execution order, and $PR_i^{(N \setminus k)}$ is the global potential if step k is **omitted** (all else equal). This definition entails the **multiplicative composition of complements**, interpretable as **survival factors** $\sigma_{i,k} = 1 - PR_{i|k}$, i.e., the fraction not yet released at step k :

$$PR_i^{(N)} = 1 - \prod_{k=1}^N (1 - PR_{i|k}) = 1 - \prod_{k=1}^N \sigma_{i,k}. \quad (14)$$

The definition remains valid even if step k **involves no food contact**: if it feeds, structures, or prepares future transfer, then $PR_{i|k} > 0$. In the limiting case where $PR_i^{(N \setminus k)} = 1$ (the “without k ” sequence is already saturating), the ratio $\frac{1 - PR_i^{(N)}}{1 - PR_i^{(N \setminus k)}}$ is undefined. We then adopt the convention $PR_{i|k} = PR_i^k$, where PR_i^k is the release potential **when only step k is considered**.

3.3 | Calculation procedure

Partial release potentials are computed iteratively using the **omission** rule.

1. Define the **actual sequence** of steps and their **conditions** (time, temperature, geometry).
2. Evaluate (by model or data) $PR_i^{(N)}$ for the **full sequence**.
3. For each k , evaluate $PR_i^{(N \setminus k)}$ by **removing step k** (same conditions for the others).
4. Compute $PR_{i|k}$ using Eq. 13.
5. Check consistency for a sequence of **independent** steps:
 $PR_i^{(N)} \stackrel{?}{=} 1 - \prod_k (1 - PR_{i|k})$ (numerical equality within tolerance).
- 6.

Table 4 – Calculation procedure for the estimation of partial potential release associated with independent steps

Step k	$PR_i^{(N \setminus k)}$	$PR_{i k}$	Control : $1 - \prod (1 - PR_{i k})$	Comment (mobilizing/contact/purge)
1				
2				
...				
N				

Mechanisms associated with each step are identified as:

- “mobilizing”: step which redistributes or put closer the substances (e.g. heating, thinning, storage);
- “contact”: step where the packaging material is in contact with food or a food simulant and transfer mobilized substances;
- “purge”: step contribution to the removal of substances from the packaging system (e.g. desorption, washing, outgasing).

Note

Repeated use is a special case where N identical cycles are applied with the same per-cycle potential PR_i^{cycle} :

$$PR_i^{(N)} = 1 - (1 - PR_i^{\text{cycle}})^N. \quad (15)$$

3.4 | Example: storage followed by food contact (2 steps)

Consider a simple situation with a package undergoing two distinct steps; the corresponding release potentials can be obtained experimentally or by simulation:

- **Step 1:** storage of the package at 40 °C for 30 days;
- **Step 2:** an “accelerated” food contact of 10 days at 40 °C.

The full sequence $1 \rightarrow 2$ yields a global transfer of $PR_i^{(2)} = 50\%$ of the initially present substances. Step 2 corresponds to the actual **food-contact** stage. Evaluated alone, step 2 shows a partial potential $PR_{i|2} = 30\%$. Step 1 has **no contact** and corresponds to **stacked storage** of a multilayer article. The contribution of step 1 to total transfer is:

$$PR_{i|1} = 1 - \frac{1 - PR_i^{(2)}}{1 - PR_{i|2}} = 1 - \frac{1 - 0.5}{1 - 0.3} \approx 0.29. \quad (16)$$

This elementary example confirms that **non-contact storage** can have a **significant** effect on the final transfer potential and, by extension, on the risk-assessment outcome.

Now suppose we wish to isolate the effect of **one additional month** of non-contact storage. The description becomes three steps $1 \rightarrow 1' \rightarrow 2$, where $1'$ represents the extra month. The contribution of step 2 alone stays unchanged ($PR_{i|2} = 30\%$). A simulation indicates that adding the month changes the global transfer from $PR_i^{(2)} = 50\%$ to $PR_i^{(2')} = 75\%$. The contribution $PR_{i|1'}$ then follows the “with vs without” relation:

$$PR_{i|1'} = 1 - \frac{1 - PR_i^{(2')}}{(1 - PR_{i|1})(1 - PR_{i|2})} = 1 - \frac{1 - 0.75}{(1 - 0.29)(1 - 0.30)} \approx 49.7\%. \quad (17)$$

Tip

Interpretation.

The value $PR_{i|1'} \approx 50\%$ means that “one additional month of storage contributes to the **transfer of half of the initially present substances** by the end of the $1 \rightarrow 1' \rightarrow 2$ sequence.”

There is no paradox in observing $PR_{i|1'} > PR_{i|2}$, since transfers **initiated** during step $1'$ affect the food concentration C_F **only at the end** of step 2. The composition rule for partial potentials (product of complements) **reconstructs causality** by accounting for the variation of the effective PR **at the end** of

the chain. These variations stem from **dynamic effects** of internal redistribution measured by the temporal potential (mobilization toward interfaces, shorter diffusion paths, increased diffusivity).

Calculation check. One extra month induces a relative increase:

$$\frac{PR_i^{(2')} - PR_i^{(2)}}{PR_i^{(2)}} = \frac{PR_{i|1'}(1 - PR_{i|1})(1 - PR_{i|2})}{PR_i^{(2)}} = PR_{i|1'} \left(\frac{1 - PR_i^{(2)}}{PR_i^{(2)}} \right) \approx 0.497 \times \frac{1 - 0.5}{0.5} \approx 50\%. \quad (18)$$

3.5 | Metrics to rank and prioritize steps

Partial potentials $PR_{i|k}$ provide an explainable **decomposition** of total release. To steer design choices, it is useful to transform them into **metrics** that compare and prioritize steps in a sequence.

Different, complementary metrics are possible:

- **Absolute indicators.** In practice, an additive (log-complement) score is convenient, $A_{i,k}$, monotone with $PR_{i|k}$:

$$A_{i,k} \equiv -\log(1 - PR_{i|k}) \quad (\geq 0). \quad (19)$$

- **Relative scores and elasticities.** A **relative score** normalizes $PR_{i|k}$ by the final value $PR_i^{(N)}$:

$$\text{Score}_{i,k} \equiv \frac{PR_{i|k}}{PR_i^{(N)}}. \quad (20)$$

Elasticities identify the most sensitive parameters for mastering release:

$$E_{i,k} \equiv \frac{\partial PR_i^{(N)}}{\partial \theta_k} \cdot \frac{\theta_k}{PR_i^{(N)}}, \quad (21)$$

where θ_k is a parameter of step k (duration, temperature, thickness).

- **Order-invariant indicators.** When steps are **strongly coupled** (e.g., storage + heating), attributing a unique $PR_{i|k}$ may depend on step order. **Shapley values** provide an “equitable” attribution:

$$\text{Shapley}_{i,k} \equiv \frac{1}{N!} \sum_{\pi} [PR_i^{(\text{previous} + \{k\})} - PR_i^{(\text{previous})}], \quad (22)$$

summing over all permutations π of step order. Each step receives a share proportional to its marginal contribution in all possible configurations.

These metrics (absolute, relative, elasticities, Shapley) can be combined with **health, economic, or environmental weights** to obtain a **multi-criteria ranking** of steps—directly usable to guide safe design and justify decisions to authorities.

Note

Key point. Ranking metrics translate partial potentials into **decision tools**. Absolute metrics support **quick** and intuitive analysis; relative metrics and elasticities give a **comparative/parametric** view; Shapley values and multi-criteria indicators enable **robust analysis** in complex or strongly coupled systems.

3.6 | Dependent steps

When steps are **independent**, their total contribution to release does not depend on order, even though each step's specific contribution may vary with its position. In contrast, introducing **dependent** steps breaks commutativity: steps occurring before or after a dependent step see their contributions modified.

Dependent steps correspond to situations where contaminants are **redistributed, consumed, or produced** inside the material, not necessarily transferred to food. This **symmetry breaking** is the very origin of dependence.

A sequence's degree of dependence can be quantified by the deviation:

$$\text{dependence} = \frac{\prod_k (1 - PR_{i|k})}{1 - PR_i^{(N)}} - 1. \quad (23)$$

Any value significantly different from zero indicates a history effect:

- **Positive dependence:** the theoretical transfer (estimated from individual partial potentials) is **higher** than observed for the full sequence. This reflects an **effective decrease** in transfers to food, e.g., back-flux, crust formation (plasticizer depletion or induced crystallization), or consumption of substances via chemical reactions.
- **Negative dependence:** the effective transfer is **higher** than anticipated from individual contributions. This corresponds to bringing substances **closer to the food interface**, accelerating transfers (plasticization or thermal activation), or generating new substances by chemical reactions.

3.7 | Continuous extension (limit $N \rightarrow \infty$)

3.7.1 | Principles in a nutshell

The discrete formalism of release potentials can be extended to a continuous description by introducing an **instantaneous release rate** $\zeta_i(t)$. The released fraction $PR_i(t)$ follows a **mass-action**-type differential form:

$$\frac{dPR_i(t)}{dt} = (1 - PR_i(t)) \zeta_i(t), \quad PR_i(0) = 0. \quad (24)$$

This approach interpolates a sequence of discontinuous steps (successive times/temperatures) into a continuous profile and evaluates the effect of extended contact. The function $\zeta_i(t)$ encodes the underlying physics (diffusion/partition models in tiers M2 and M3). For a layer in direct contact, $\zeta_i(t) \sim t^{-1/2}$ at **short times** and tends to zero at long times. This framework naturally links the partial potentials $PR_{i|k}$ to **cumulative risk** in an extended scenario.

Tip

Piecewise approximation. The piecewise-constant approximation $\zeta_i(t) \simeq \zeta_{i,k}$ for $t \in (t_{k-1}, t_k]$ lets one interpolate a continuous profile from the $PR_{i|k}$ in a multi-step evolution (e.g., pasteurization or sterilization cycle). An **additive decomposition** of $\zeta_i(t)$ also applies to **multiple sources**, as will be shown at tier M3.

3.7.2 | Demonstration

From discrete to continuous. Let $S_i^{(N)} \equiv 1 - PR_i^{(N)} = \prod_{k=1}^N \sigma_{i,k}$ be the **survival** (fraction not yet released). Define the **cumulative hazard** $H_i^{(N)} \equiv -\ln S_i^{(N)} = \sum_{k=1}^N h_{i,k}$ with $h_{i,k} \equiv -\ln \sigma_{i,k}$. Consider a continuous process parameter τ with partition $\tau_0 < \tau_1 < \dots < \tau_N$, $\Delta\tau_k = \tau_k - \tau_{k-1}$. If $h_{i,k} = O(\Delta\tau_k)$, define the **instantaneous hazard** $\lambda_i(\tau)$ by

$$h_{i,k} = \int_{\tau_{k-1}}^{\tau_k} \zeta_i(u) du = \zeta_i(\zeta_k^*) \Delta\tau_k + o(\Delta\tau_k). \quad (25)$$

Then, as $N \rightarrow \infty$,

$$H_i(\tau) = \int_0^\tau \zeta_i(u) du, \quad S_i(\tau) = \exp(-H_i(\tau)), \quad PR_i(\tau) = 1 - \exp\left(-\int_0^\tau \zeta_i(u) du\right). \quad (26)$$

Compact differential form.

$$\frac{dPR_i}{d\tau} = (1 - PR_i(\tau)) \zeta_i(\tau), \quad PR_i(0) = 0, \quad (27)$$

i.e., survival $S_i(\tau) = 1 - PR_i(\tau)$ satisfies $\dot{S}_i = -\zeta_i S_i$.

Exact link to discrete partial potentials. On an interval $[\tau_{k-1}, \tau_k]$,

$$PR_{i|k} = 1 - \exp\left(-\int_{\tau_{k-1}}^{\tau_k} \zeta_i(u) du\right), \quad \int_{\tau_{k-1}}^{\tau_k} \zeta_i(u) du = -\ln(1 - PR_{i|k}). \quad (28)$$

Tip

If ζ_i is constant over step k , then $\zeta_{i,k} = -\ln(1 - PR_{i|k})/\Delta\tau_k$.

3.7.3 | Extensions

Useful parameterizations. The form of $\zeta_i(\tau)$ encodes the physics/chemistry:

- **Independent pieces (parallel mechanisms).** $\zeta_i(\tau) = \sum_m \zeta_{i,m}(\tau)$ (additivity of hazards).
- **Dependence on process conditions.** $\zeta_i(\tau) = Z_i(T(\tau), RH(\tau), \dot{\zeta}(\tau), \dots)$, e.g., Arrhenius law $\zeta_i(\tau) = \zeta_{0,i} \exp\{-E_{a,i}/(RT(\tau))\} g(\tau)$.
- **Piecewise-constant (calibrated on step data).** $\zeta_i(\tau) = \zeta_{i,k}$ for $\tau \in (\tau_{k-1}, \tau_k]$, with $\lambda_{i,k}$ given above; this lets you interpolate a continuous profile from the $PR_{i|k}$.

Link with mass-transfer models. If release kinetics are aggregated as an **effective first-order** law

$$\dot{M}_{\text{rel}}(t) = k_{\text{eff}}(t) (M_\infty - M_{\text{rel}}(t)),$$

then for $PR_i(t) = M_{\text{rel}}(t)/M_\infty$ we retrieve the above form with $\tau = t$ and $\zeta_i(t) = k_{\text{eff}}(t)$.

For **Fickian diffusion** (planar slab, perfect sink), the **non-released** fraction admits the classical series

$$S_i(t) = 1 - PR_i(t) = \frac{8}{\pi^2} \sum_{n=0}^{\infty} \frac{1}{(2n+1)^2} \exp(-a_n t), \quad a_n = \frac{(2n+1)^2 \pi^2 D_i}{4L^2}. \quad (29)$$

The corresponding instantaneous hazard is

$$\zeta_i(t) = -\frac{d}{dt} \ln S_i(t) = \frac{\sum_{n \geq 0} \frac{a_n}{(2n+1)^2} e^{-a_n t}}{\sum_{n \geq 0} \frac{1}{(2n+1)^2} e^{-a_n t}}, \quad (30)$$

which decreases with t (short-time kinetics $\propto t^{-1/2}$, saturation at long times). Finite external transfer coefficients and a partition K can be handled via **series-resistance** boundary conditions; $\zeta_i(t)$ then depends on B_i and K (or keep the PDE, compute PR_i , then $\zeta_i = -\dot{S}/S$).

Key takeaways for Section 3

Partial potentials decompose total release into step contributions. They can be **non-zero without food contact**, because they measure **mobilization** (preparation for transfer) as well as transfer itself. For independent steps, the “with vs without” definition guarantees the composition $PR_i^{(N)} = 1 - \prod_k (1 - PR_i|_k)$, enabling straightforward spreadsheet implementation.

Partial potentials $PR_i|_k$ feed into **metrics** (absolute impact, elasticity, weighted scores, Shapley value) to **prioritize actions**: modify a step, change its order, add a barrier, tune temperature/duration, etc. They are **compatible** with tiers M : PR can be estimated in **M0–M2** (equilibrium/partition) or in **M3** (explicit diffusion).

Tip

The next section introduces the **functional barrier** concept, which formalizes how a component reduces release. It integrates naturally with partial potentials (barriers in series, cumulative effects, prioritization) and their metrics.

4 | Functional barrier concept

4.1 | Towards a robust definition

The **functional barrier** (FB) concept is central in U.S. (FDA) and EU (Regulation (EU) No 10/2011) frameworks. It enables **derogations**: a recycled material or a debated additive may be used provided that a demonstrated functional barrier keeps the **effective release** below regulatory thresholds.

There is no formal, official definition beyond the idea of “a layer preventing migration”. We propose two **operational** definitions based on **total** (PR) and **partial** release potentials (eqs. 4.1–4.2):

$$(\text{Total PR}) \quad PR_i^{fb} = PR_i^{T,fb} \times PR_i^{E,fb} < PR_i = PR_i^T \times PR_i^E, \quad (4.1)$$

$$(\text{Partial PRs}) \quad PR_i^{fb}(S) = 1 - \prod_{\ell \in S} (1 - PR_i^{fb}|_{\ell}) < PR_i(S) = 1 - \prod_{\ell \in S} (1 - PR_i|_{\ell}), \quad \text{for a significant time } t \leq t_{fb}$$

where the superscript fb denotes the potential **with** a functional barrier. In 4.2, a barrier active on step k is **effective** on $[0, t_{fb}]$ if, for any subsequence S including k , a reduction in transfer potential is observed.

These conditions allow the effect to be limited to a **single step**. The barrier is neither absolute (perfectly tight layer) nor permanent: its effect is **temporary** and of **variable intensity**.

Traditionally seen as a pure diffusion barrier, a functional barrier may actually combine several mechanisms:

- **Reservoir effect**: $PR_i^{T,fb} < PR_i^T$, temporary accumulation upstream (backflow effect).
- **Retention effect**: $PR_i^{E,fb} < PR_i^E$, chemical or physical trapping.
- **Diffusive effect**: combination of a **lag time** t_{lag} and **flux reduction**.

Note

Because the proposed definition is expressed with release potentials (PR), **pure dilution** effects (e.g., blending recycled with virgin) are **excluded** from the FB concept.

Warning

Key point. Poor FB sizing can have **opposite** consequences:

- **Undersized** \Rightarrow potential **health risk** due to uncontrolled transfer from recycled constituents.
- **Oversized** \Rightarrow unnecessary **drag on circularity** (lower recycled content, needless decontamination, poorer recyclability of FB-containing materials).

4.2 | Derived performance indices

FB performance is quantified via **additive gains** $G_{i,k}$:

$$G_{i,k} \equiv \ln \frac{1 - PR_i^{fb}|_k}{1 - PR_i|_k}. \quad (4.3)$$

- $G_{i,k} > 0$ denotes an effective reduction of the **partial** PR at step k .
- Choice of **dimensioning molecules** is critical (e.g., toluene as a reference).
- For homologous series, **lag times** scale with **molar mass squared** (rubbery polymers) or follow **power laws** (glassy polymers).

Note

Worked example. If an FB reduces $PR_i|_2$ from 0.30 to 0.12, then $PR_i^{fb}(1 \rightarrow 1' \rightarrow 2) = 1 - (1 - 0.2857)(1 - 0.50)(1 - 0.12) \approx 57\%$, and $G_{i,2} = \ln \frac{1-0.12}{1-0.30} \approx 0.229$.

4.3 | Functional barrier typology

The FB concept covers **interlayers** between content and contaminants, but may also include **additives**, **micro-/nanoparticles** modifying chemical affinity and/or mobility of potential migrants. **Purge steps** and, more generally, **FB assembly steps** are included insofar as they affect PR_i^{fb} .

1. Classical diffusive barriers

- **Principle:** slow the flux via low diffusivity or large thickness.
- **Example:** virgin PET interlayers between a recycled layer and the food.
- **Indicator:** progressive reduction in $PR_i|_k$; never total.
- **Limit:** $PR_i^{fb} \rightarrow 0$ only if **diffusivity** $\rightarrow 0$ or **infinite thickness** (unrealistic).

2. Trapping barriers

- **Principle:** chemical/physical fixation of contaminants.
- **Example:** scavenger additives, sorptive mineral fillers.
- **Indicator:** sharp but **selective** drop in certain $PR_i|_k$.
- **Limit:** efficiency limited to substances with affinity for the trap.

3. Dilution / redistribution barriers

- **Principle:** disperse the initial contamination within a mass of virgin material.
- **Example:** a virgin polyethylene ply between recycled board and food.
- **Indicator:** reduction in $\hat{C}_{i,F}^{eq}$ **without** removing substances.
- **Limit:** **reversible**; contaminants remain and may migrate later.

4. Dynamic or temporal barriers

- **Principle:** introduce a **delay** shifting transfers to longer times.
- **Example:** saturable absorbent layers, slowly swelling polymers.
- **Indicator:** low PR_i^{fb} at **short times**, converging to PR_i at long times.
- **Limit:** efficiency tied to **use duration** (single-use vs. long storage).

5. Purge steps

- **Principle:** remove part of contaminants **before** use.
- **Example:** thermal degassing of a recycled film; aqueous washing of fibers.
- **Indicator:** **irreversible** decrease in PR_i^{fb} via reduction of $C_{i,j}^0$.
- **Limit:** depends on **industrial reproducibility**.

4.4 | Application to recycled material

Originally, FBs were proposed to enable recycled materials with little or no decontamination. For a fixed use duration t_{contact} , one may theoretically use **less-decontaminated** recycled material if the FB compensates, provided:

$$\frac{1 - \Delta_L}{1 - \Delta_H} \leq \frac{PR_i^T \cdot PR_i^E}{PR_i^{T,fb} \cdot PR_i^{E,fb}} \quad \text{for } t \leq t_{\text{contact}}, \quad (4.4)$$

where $\Delta_L < \Delta_H$ are decontamination efficiencies (e.g., 95% vs 99%).

The left-hand side is the **minimum reduction factor** required from the barrier (dynamic \times static). Example: relaxing from 99% to 95% decontamination imposes a factor $\frac{1-0.95}{1-0.99} = 5$; the FB must reduce $PR_i^T \cdot PR_i^E$ by at least 5 over t_{contact} for a representative set of solutes i .

Tip

Key point. Misestimation of release rates (PR_i^T, PR_i^E or their FB versions) can yield **higher contamination** than without the FB, due to the use of **more contaminated feedstock**. Incorporate uncertainty with **appropriate safety factors**: upper bounds on input contamination, conservative margins on PR values.

4.5 | Points of attention and recommendations

Points of attention

- **Link to recycling.** FBs are often invoked to include recyclates. Poor sizing leads to either (i) **under-protection** (underestimated release, health risk) or (ii) **over-protection** (unrealistic requirements, blocked streams).
- **Measurability.** Effectiveness must be shown via **measurable indicators** (tests, validated simulations), not material assumptions alone.
- **Selectivity.** An FB protects some substances better than others—analyze **per substance** or via **dimensioning migrants**.
- **Identification.** FB-equipped materials should be **identifiable** to route recycling streams; otherwise, risk of **cross-contamination** if non-authorized recyclates are reintroduced into direct-contact loops.

Recommendations

- Favor FBs **implemented cold and as close to the content as possible** to avoid pre-contamination.
- An FB may be **removable** (sachet, inner film, gel) provided it is not confused with the content.
- Typology: diffusive barriers, reservoirs, trapping, or **hybrids**.
- An FB can justify **less-decontaminated** recyclates if it ensures **sufficient reduction** of the **static × dynamic** potential ($PR_i^E \times PR_i^T$).
- FBs are **ephemeral**: sizing must include **all prior steps** (forming, storage, elevated temperatures) that may erode their real effectiveness.

Key takeaways for section 4

Functional barriers are a **core instrument** of safe-by-design: beyond classical diffusion layers, they include trapping, dilution/redistribution, dynamic delay, and purge mechanisms. Evaluation must target **effective reductions** of partial or global PR_i , in **static** PR_i^E and **dynamic** PR_i^T terms. The gains $G_{i,k}$ apply at step level and at sequence level. FBs have **finite service lives** and must be **optimized** for the intended application. Use of FBs should **not** result in introducing materials **unsuitable for food contact** into recycling loops—FB-equipped packaging should be **identified**.

Tip

The next section will integrate FBs into **tier M3 (dynamic tiers)**, where diffusion dynamics are modeled explicitly, showing how differential-equation-based PR predictions confirm or challenge expected FB performance and support regulatory validation.

5 | Severity and criticality scales

The notions of **severity** and **criticality**, rooted in FMECA (Failure Mode Effects and Criticality Analysis) and generalized to mass transfer (see Nguyen 2013), yield **intensive quantities** (severities) and their **cumulants** (criticalities) to compare substances, components, and packages—pinpointing what carries the **highest risk** for consumers.

5.1 | Severity scale

Define the (estimated) severity for substance i using the ratio $\hat{C}_{i,F}/(\rho_0 SML_i)$:

$$\begin{aligned} \hat{s}_i^{(t)} &= 100 \times \frac{\hat{C}_{i,F}}{\rho_0 SML_i} \\ &= \hat{s}_i^0 + 100 \times \bar{v}_i^*(t) \cdot \hat{m}_i^{*,eq} \cdot \frac{\hat{m}_i^0}{\rho_0 V_0 SML_i} \\ &= \hat{s}_i^0 + 100 \times PR_i^T PR_i^E \times \frac{\hat{m}_i^0}{\rho_0 V_0 SML_i}. \end{aligned} \quad (5.1)$$

- $\hat{s}_i^{(t)}$ is **dimensionless** and defined on an **open** scale (can exceed 100).
- Factor **100** flags **severe** or **catastrophic** cases ($\gg 100$).
- It is an **estimate** (hats) and depends on the **tier** (approximation level).
- PR language: $PR_i^T = \bar{v}_i^*(t)$ (**dynamic** potential) and $PR_i^E = \hat{m}_i^{*,eq}$ (**static** potential).

5.1.1 | Partial severity by packaging component

With $\hat{m}_i^0 = \sum_{j=1}^m \hat{m}_i^0|_j$, $\hat{m}_i^{*,eq}|_j$ the static rate for component j , and $\bar{v}_i^*(t)|_j$ its dynamic factor:

$$\hat{s}_i^{(t)}|_j = \hat{s}_i^0|_j + 100 \times \bar{v}_i^*(t)|_j \cdot \hat{m}_i^{*,eq}|_j \cdot \frac{\hat{m}_i^0|_j}{\rho_0 V_0 SML_i}, \quad \hat{s}_i^{(t)} = \sum_{j=1}^m \hat{s}_i^{(t)}|_j. \quad (5.2)$$

Note

(additivity—tier M3). This rigorous definition uses the **additivity** of transfers (see tier M3). Establish realistic orders of magnitude for $\hat{m}_i^{*,eq}|_j$ and $\bar{v}_i^*(t)|_j$ from tier M2–M3 simulations; reuse across similar uses/substances.

5.1.2 | Suspected substances (below LOD)

If substance i is **suspected** but not quantified, bound severity via the **limit of detection** $DL_{i,j}$ of material j :

$$\hat{s}_i^{(t)}|_j = \hat{s}_i^0|_j + 100 \times \bar{v}_i^*(t)|_j \cdot \hat{m}_i^{*,eq}|_j \cdot \frac{\rho_j V_j}{\rho_0 V_0} \cdot \frac{DL_{i,j}^{\text{mass}}}{SML_i}. \quad (5.3)$$

5.1.3 | Mechanically recycled materials

For a mechanically recycled component j from a stream with **maximum contamination** $C_{i,j}^g$ and **minimum** decontamination efficiency $\Delta_{i,j}$:

$$\hat{s}_i^{(t)}|_j = \hat{s}_i^0|_j + 100 \times \bar{v}_i^*(t)|_j \cdot \hat{m}_i^{*,eq}|_j \cdot (1 - \Delta_{i,j}) \cdot \frac{\rho_j V_j}{\rho_0 V_0} \cdot \frac{C_{i,j}^{g,\text{mass}}}{SML_i}. \quad (5.4)$$

Note

Example (mechanical rPET). Commonly $\Delta_{i,j} \geq 0.90$ for $C_{i,j}^{g,\text{mass}} = 3 \text{ mg/kg}$. With $\rho_{PET} \simeq 1380 \text{ kg/m}^3$, $\hat{C}_{i,j=\text{PET}}^0 \approx (1 - 0.9) \times 10^{-6} \text{ kg/kg} \times 1380 \text{ kg/m}^3 = 4.14 \times 10^{-4} \text{ kg/m}^3$.

5.2 | Criticality scale

Criticality aggregates severities across **substances** (and optionally **components**). It is not intensive; it is a **cumulant** used to rank **components**, **packages**, or **designs**.

5.2.1 | Component criticality

From **conditional severities**:

$$\hat{c}^{(t)}|_j = \sum_{i=1}^n \text{pr}(i \in j) \hat{s}_i^{(t)}|_j, \quad j = 1, \dots, m, \quad (5.5)$$

where $\text{pr}(i \in j)$ is the **probability of presence** (intentional) or **likelihood** inferred from identification databases (retention times and/or mass spectra).

Note

Inheritance. Since $\hat{s}_i^{(t)}|_j$ contains PR_i^T , PR_i^E , criticality **inherits** dynamic and equilibrium effects.

5.2.2 | Package criticality

Double sum over **substances** × **components**:

$$\hat{c}^{(t)}|_{\text{packaging}} = \sum_{j=1}^m \hat{c}^{(t)}|_j = \sum_{j=1}^m \sum_{i=1}^n \text{pr}(i \in j) \hat{s}_i^{(t)}|_j. \quad (5.6)$$

$\hat{c}^{(t)}$ in 5.6 is well-suited to compare **design options**: virgin, mechanical/chemical recycling, with/without FB.

Note

Comparability. Always compare criticalities at the **same tier**. If a refinement changes criticality significantly, moving up a tier is **justified**; otherwise it may be **deferred**.

5.2.3 | Step criticality (preview)

To link FMECA with **process sequences**, define a **marginal step criticality** k via the **marginal release gain** $\Delta_{i,k} = PR_i^{(N)} - PR_i^{(N \setminus k)}$:

$$\hat{c}^{(t)}|_k = \sum_{j=1}^m \sum_{i=1}^n \text{pr}(i \in j) \hat{s}_i^{(t)}|_j \cdot \Delta_{i,k}. \quad (5.7)$$

Note

If steps are **coupled**, replace $\Delta_{i,k}$ with the corresponding **Shapley value** (fair attribution). A full development is given at **tier 3** (boundary conditions, kinetics).

Warning

Points of attention

- **Count detected substances** to estimate criticality for **non-identified** ones at/above LOD.
- Reasonable working assumption: **same distribution** of Cramer classes for identified and non-identified substances \Rightarrow a **hierarchy of SML_i** usable for severities.
- Cases with $\hat{s}_i^{(t)} \gg 100$ should trigger a **higher-tier** analysis or be backed by analytical/technical evidence. Exceeding 100 is an **objective alert**, not per se non-compliance.
- Always link $\hat{s}_i^{(t)}$ to the **tiers** used (M0–M3 and T0–T2).
- It is generally acceptable to aggregate severities from **different toxicology tiers** (T0–T2) provided the **same transfer tiers** (M0–M3) were used.
- Document methods and maintain **prudence** regarding criticality calculations.
- Cross $\hat{c}^{(t)}$ with **prioritization metrics** and **FB effectiveness** indicators.

Key Takeaways for Section 5

Severity is a **dimensionless, intensive** indicator, additive across components and incorporating **acceptable exposure**; it naturally expresses via PR_i^T and PR_i^E when available. A severity of **100** corresponds to contamination reaching the acceptable exposure threshold under standardized conditions (e.g., 1 kg food/day for a 60-kg adult).

Criticalities are **cumulants** to **rank** components, packages, and designs by exposure risk. They may include both **identified** and **suspected** substances and decompose along two axes: **components** and **use cycles**.

6 | Principles for constructing tiers M0–M3

6.1 | Objective

Up to this point, the proposed approach has not introduced any simplifying assumptions about package geometry, composition, transfer mechanisms, or interactions among substances. Only the thermodynamic description of transfers has been **linearized** so that **concentrations** can be used as transfer potentials instead of chemical potentials.

In addition, the equilibrium description was adjusted in the case of **pre-existing food contamination**: contaminations are strictly **additive** across steps—put simply, the package never acts to decontaminate the food.

Assigning values to the parameters $\bar{v}_i^*(t)$, $\hat{m}_i^{*,eq}$, \hat{m}_i^0/V_0 , and SML_i nevertheless requires further assumptions—often delicate when many components and substances are involved.

The **tiers** (levels of approximation) therefore aim to identify the **substances** and **components** that most influence the final safety outcome, before optimizing them via design, formulation, or use conditions.

The construction of tiers for transfer physics (**M0** to **M3**) is **artificial** and follows a logic of **decreasing severities and criticalities**: tier 0 provides a very conservative upper bound; subsequent tiers progressively introduce refinements.

6.2 | Overview of tiers

Figure 1 presents the available Tx/Mx options based on what is known about migrants:

- **T0–M0** if the substance is unknown/not detected,
- **T1–M0** or **T1–M1** if the substance is identified but **no material data** are available,
- **T2–M1** or **T2–M2** if **material properties** are available,
- **T2–M3** if a **dynamic** description is required.

The decision tree illustrates the progression from conservative scenarios toward detailed kinetic models by systematically combining a **toxicology tier (Tx)** with a **transfer-modeling tier (Mx)**.

Table 5 provides a concise, progressive view of how assumptions evolve across Mx scenarios. The four transfer-modeling levels (M0–M3) are compared by their required inputs and expected outputs.

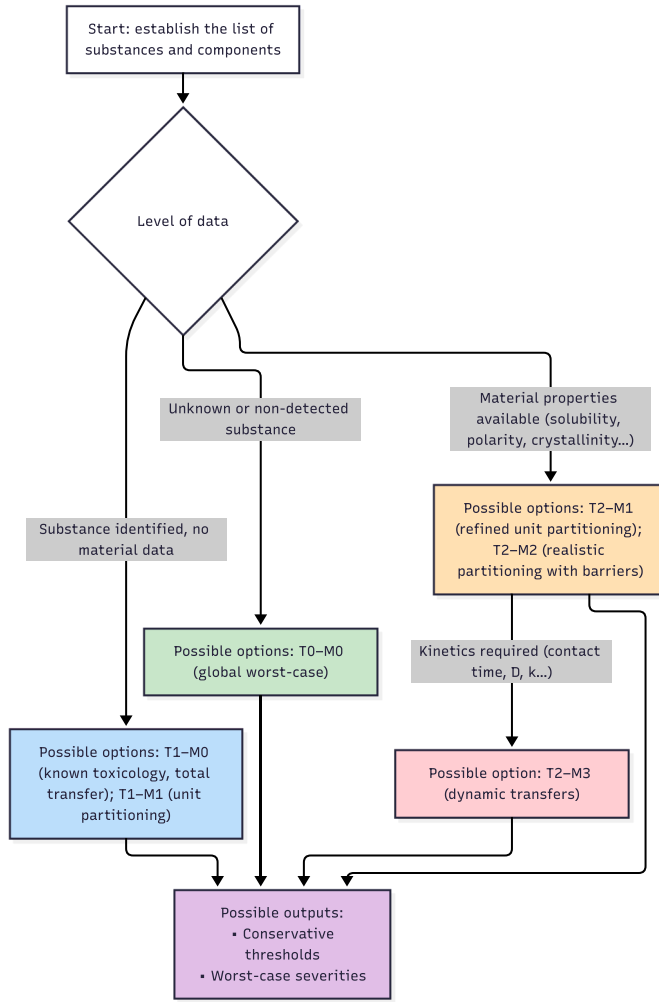


Figure 1 – Decision tree for tier combinations Tx/Mx.
Flow diagram guiding the choice among T0-T2 / M0-M3 according to data availability on substances and materials.

Table 5 – Operational summary of calculations at tiers M0-M3

Tier	Minimal inputs	Condensed calculation procedure	Equations (overview)	Outputs	Notes & conservatism
M0 – Total transfer	BW, DI, V_0, V_j	(1) Set TDI to worst case ($0.0025 \mu\text{g}\cdot\text{kg}^{-1} \cdot \text{bw}\cdot\text{day}^{-1}$). – (2) Compute $SML_i = BW \cdot DI \cdot TDI_i$. – (3) Assume total transfer ($\bar{v}_i^*(t), \hat{m}_i^{*,eq} \rightarrow 1$). – (4) Deduce material thresholds.	$\{\hat{C}_{i,j}^0\}_{M0} = \frac{\rho_F V_0}{V_j} SML_i$	$\hat{C}_{i,j}^{(0)}, \hat{s}_i, \hat{c}_{ j}$	Applies to unknown/undetected substances. Very conservative ($k_j^H \gg k_0^H$).
M1 – Unit partition	BW, DI, V_0, V_j	(1) SML_i as in M0. – (2) Assume $k_0^H \approx k_j^H$. – (3) Volume-weighted distribution.	$\{\hat{C}_{i,j}^0\}_{M1} = \frac{V_0 + \sum_{k=1}^m V_k}{V_j} \rho_F SML_i$ $= \left(1 + \sum_{k=1}^m \frac{V_k}{V_0}\right) \{\hat{C}_{i,j}^0\}_{M0}$	$\hat{C}_{i,j}^{(1)}, \hat{s}_i, \hat{c}$	Less conservative if V_0 is not dominant; does not discriminate materials.
M2 – Realistic partitions	$V_0, V_j; C_{i,j}^{\text{sat}}, P_{i,\text{sat}}, \log P_i, V_{i,\text{mol}}; c_j, \epsilon_j; \theta_{i,j}$	(1) Evaluate $k_{i,j}^H$ (solubility, polarity, crystallinity, porosity). – (2) Derive ratios $K_{i,j_1/j_2}$. – (3) Filter mobile mass $\hat{m}_i^0 = \sum_j V_j (1 - \theta_{i,j}) \hat{C}_{i,j}^0$. – (4) Compute \hat{m}_i^{eq} and $C_{i,F}^{eq}$. – (5) Adjust $\hat{C}_{i,j}^{(2)}$ so that $C_{i,F}^{eq} = SML_i$.	Effective Henry: $k_{i,j}^H = \frac{P_{i,\text{sat}}^{(T_K)} V_{i,\text{mol}}}{(1 - c_j)(1 - \epsilon_j)} \gamma_{i,j}^v$ Partition: $K_{i,j_1/j_2} = \frac{k_{i,j_2}^H}{k_{i,j_1}^H}$. Mobile: $\hat{m}_i^0 = \sum_j V_j (1 - \theta_{i,j}) \hat{C}_{i,j}^0$. Equilibrium: $\hat{C}_{i,F}^{eq} = \hat{C}_{i,F}^0 + \hat{m}_i^{eq} \frac{\hat{m}_i^0}{V_0}$.	$\hat{C}_{i,j}^{(2)}, \hat{s}_i(t), \hat{c}(t);$ barrier-layer diagnostics	Realistic ; supports optimization of material choice and multilayer architecture.

Tier	Minimal inputs	Condensed calculation procedure	Equations (overview)	Outputs	Notes & conservatism
M3 – Dynamic transfers	M2 data + $D_{i,j}$, $k_{i,j}^H$, $T(t)$, t_{contact}	(1) Solve Fick's equations per layer. – (2) Enforce interfacial jumps to reproduce partition at all times. – (3) Compute $\bar{v}_i(t)$ and $\hat{C}_{i,F}^{(t)}$.	Fickian kinetics (1D): $J_{i,j}(t) = -D_{i,j} \frac{\partial C_{i,j}}{\partial x}$. Global transfer: $\hat{C}_{i,F}^{(t)} = \hat{C}_{i,F}^0 + \bar{v}_i(t) \hat{m}_i^{eq} \frac{\hat{m}_i^0}{V_0}$.	Time courses $\hat{C}_{i,F}^{(t)}$, dynamic severities $\hat{s}_i^{(t)}$, transient criticalities $\hat{c}^{(t)}$	Richest tier: introduces time scale and true use conditions (heating, storage). Sensitive to diffusion parameters; requires experimental validation.

6.3 | Tier T0–M0 – Total transfer

The T0/M0 combination is the **most conservative**. The *TDI* is set to cover the **most stringent toxicology scenario**: potentially carcinogenic substance ($0.0025 \mu\text{g kg}^{-1} \text{bw}^{-1} \text{day}^{-1}$) with **total transfer** into food ($\bar{v}_i^*(t) \cdot \hat{m}_i^{*,eq} \rightarrow 1$).

Thus SML_i does not depend on the substance but on the **consumer age group**. One obtains a **factor 16** between adults and newborns. Values are compared in Table 6.

Table 6 – BW, DI, and SML values by age group

Age group	BW (kg)	DI (kg/day)	SML ($\text{kg} \cdot \text{m}^{-3}$) $\times 10^9$
Newborns (0–16 weeks)	5	0.75	9.375
Infants (0–6 months)	5	1	12.5
Young children (1–3 y)	12	1	30
Children (4–9 y)	20	1.5	75
Adults (≥ 15 y)	60	1	150

The interest of the coupled T0 and M0 tiers is to deliver a **per-material concentration threshold** that applies to **any substance**, detected or not, evaluated or not:

$$\{\hat{C}_{i,j}^0\}_{\text{tier=M0}} = \frac{V_0}{V_j} SML_i. \quad (6.1)$$

Note

Tier T0–M0 in practice. A per-material threshold valid for any substance under **total-transfer** and **maximalist toxicology** assumptions. Simple, fast, and safe—but it ignores real material properties and fine geometry.

Strengths

- Per-material threshold, **applicable to any substance** (known or unknown).
- Total transfer + maximal toxicology scenario.
- Simple and fast computation.
- Useful for **screening** substances/projects without data.

Tip

Moving to tier M1 incorporates **volume partitioning** between food and packaging to obtain more realistic yet broadly conservative thresholds.

6.4 | Tier M1 – Unit partition coefficients

Tier 1 keeps the **equilibrium** assumption ($\bar{v}_i^*(t) \rightarrow 1$) but replaces the extreme approximation $k_j^H \gg k_0^H$ (tier 0) by **equivalence** $k_0^H \approx k_j^H$.

This amounts to assuming a **homogeneous partition** proportional to volumes:

$$\{\hat{C}_{i,j}^0\}_{\text{tier=M1}} = \frac{1}{V_j} \sum_{k=0}^m V_k \cdot SML_i = \left(1 + \sum_{j=1}^m \frac{V_j}{V_0}\right) \cdot \{\hat{C}_{i,j}^0\}_{\text{tier=0}}. \quad (6.2)$$

Tiers 0 and 1 yield similar results as long as the **food volume dominates** over the packaging components.

Note

Tier M1 in practice. Introduces global geometry (relative volumes) and a **unit partition** between phases, refining thresholds according to the actual configuration. Still conservative because it does **not** discriminate materials by physicochemical properties.

Strengths

- Introduces **global geometry** (relative volumes).

- Still conservative, but less severe than M0.
- Does **not yet** discriminate materials by chemistry.
- Prepares tier **M2**, which introduces polarity, solubility, and barrier effects.

Tip

Tier M2 will enrich the calculation with **realistic partition coefficients** derived from solubilities, polarities, and material structures—opening the way to optimization via retention layers or barriers.

6.5 | Additional data required for tiers M2 and M3

Tiers M2 (see § M2) and M3 (see § M3) explicitly introduce **sorption** and **diffusion** properties into the transfer-risk evaluation. These properties are directly tied to the identity of the considered substances (migrants/contaminants, polymers, simulants or food components).

To keep the assessment exhaustive, property-estimation methods should apply equally to:

- **identified** contaminants,
- **probable** substances inferred from mass-spectral and/or retention-time matches,
- **unknown** compounds represented by **typical, well-characterized physicochemical proxies**.

This framework justifies using coarse **estimators** correlated with diffusion/sorption properties and available from public databases or easily computable: **molar mass**, **logP**, **molar volume**, **van der Waals volume**. Links between these descriptors and the target properties used in transport equations are summarized in Table 7.

Table 7 — Minimal data for computing thermodynamic and transport properties of an arbitrary solute

Required data	Use	Target properties
Molar mass M_i	Molar volume $V_{i,\text{mol}}$	$k_{i,j}^H, \gamma_{i,j}^v, K_{i,F/P}, D_{i,j}^{\text{Piringer}}$
Optimized 3D geometry (.sdf , .mol , .pdb)	van der Waals volume $V_{i,\text{vdW}}^\dagger$, parameter ξ_i	$D_{i,j}^{\text{Welle}}$, by extension $D_{i,j}^{\text{hFV}}$
logP (octanol/water)	Polarity index P'	$k_{i,j}^H, \gamma_{i,j}^v, K_{i,F/P}$

[†] $V_{i,\text{vdW}}$ is obtained by summing atomic spheres $\frac{4}{3}\pi r_{\text{vdW}}^3$ with overlap corrections. Robust implementations exist in RDKit (Landrum 2022), OpenBabel (O'Boyle 2011), and in SFPPy (Vitrac 2025a, Vitrac 2025b).

Important

The approach is **not limited** to known **monomers** and **additives**; it extends to **emerging contaminants** and **potential migrants** from recycled inputs. Descriptors are purposely simplified to allow **rapid, automatable** calculations across hundreds of substances. **Macroscopic effects** (porosity, crystallinity, plasticization, trapping) must also be considered.

Key takeaways (Section 6)

- **M0** and **M1** are simple tiers, easy to implement in a spreadsheet. Coupled with **T0**, they allow decisions on risks from **identified** and **non-evaluated** substances.
- For **identified** substances, they help shortlist those that must be analyzed with **detailed transfer scenarios**, accounting for **material nature**, **substance identity**, and **use conditions**.
- **M2** and **M3** progressively add **realistic partitions** and **dynamic diffusion**, enabling **design optimization** (materials, multilayers, barriers) and supporting **regulatory justification** with quantified severities and criticalities.

7 | Advanced Tier M2: realistic partition coefficients, retention layers, and solubility barriers

7.1 | Objective

The goal of **Tier M2** is to provide a **realistic yet conservative** estimate of equilibrium contamination by introducing **physicochemical rules** on affinities (Henry-type notations) and **immobile fractions**, without requiring the partial differential equations of Tier M3.

M2 primarily informs the **static release potential** $PR_i^E = \hat{m}_i^{*,eq}$; the **dynamic release potential** $PR_i^T = \bar{v}_i^*(t)$ is kept bounded (often set to 1 in M2) or approximated by simple time tiers, and will be fully developed in Section 8.

7.2 | Positioning and assumptions

The assumptions are aligned with those already used in the literature (Nguyen *et al.*, 2016; Zhu *et al.*, 2019a; Vitrac *et al.*, 2022) to describe transfers between packaging/polymer materials and foods/liquids. See Zhu *et al.*, 2019a for a comprehensive review.

- **Framework:** multi-source, multi-layer, multi-material systems (plastics, adhesives, inks, papers/boards, elastomers), virgin and recycled, single-use and repeated-use.
- **Purpose of M2:** discriminate **food** ↔ **material affinities** and **weight the mobile mass** by component, to obtain an $\hat{C}_{i,F}^{eq}$ that is both **explainable** and **conservative**.
- **Principle of conservatism:** select **minimally plausible affinity ratios** (Henry ratios) from the perspective of transfer *toward food* so as to **maximize** the final concentration in food.
- **Separation of scales:** microstructural/supramolecular effects (crystallinity, trapping) are treated by homogenization separately from molecular mean-field effects.
- **Simplified molecular framework:** molecular theory provides parameterization of $k_{i,j}^H$ values from chemical databases, usable in automated calculation workflows.

Notations (recall):

- $k_{i,j}^H$: Henry-type affinity coefficient of substance i in compartment j (food $j = 0$; layers $j = 1..m$).
- V_j : volume of compartment j ; $\hat{C}_{i,j}^0$: initial (estimated) concentration.
- $K_{i,j/F} \equiv \frac{k_{i,0}^H}{k_{i,j}^H}$: partition coefficient between layer j and the contacting food (F).
- $\theta_{i,j} \in [0, 1]$: **immobile fraction** (effective crystallinity, trapping, occlusion, inaccessibility).
- Linearized equilibrium with **multiple sources** and **immobile fractions**:

$$\hat{C}_{i,F}^{eq} = \hat{C}_{i,F}^{(0)} + \frac{\sum_{j=1}^m V_j (1 - \theta_{i,j}) \hat{C}_{i,j}^0}{V_0 + \sum_{j=1}^m \bar{K}_{i,j/F} V_j (1 - \theta_{i,j})} \quad (31)$$

7.3 | Macroscopic scale: apparent partition coefficients

7.3.1 | Definitions

Partition coefficients between compartments j_1 and j_2 ,

$$K_{i,j_1/j_2} = \frac{C_{i,j_1}^{eq}}{C_{i,j_2}^{eq}}, \quad (32)$$

approximate more complex thermodynamic equilibria (non-linear sorption isotherms, elastic energy in constrained polymers). They emerge from equality of partial vapor pressures between j_1 and j_2 :

$$K_{i,j_1/j_2} = \frac{k_{i,j_2}^H}{k_{i,j_1}^H}, \quad j_1 \neq j_2, j_1, j_2 \geq 0 \quad (33)$$

Extrapolating Henry's law up to saturation:

$$k_{i,j}^H = \frac{P_{i,v}^{\text{sat}}(T_K)}{C_{i,j}^{\text{sat}}}, \quad j \geq 0 \quad (34)$$

where $P_{i,v}^{\text{sat}}(T_K)$ is the saturated vapor pressure at temperature T_K , and $C_{i,j}^{\text{sat}}$ the solubility/saturation concentration in phase j .

Thus the partition coefficient between food and layer j is:

$$K_{i,F/j} = \frac{k_{i,j}^H}{k_{i,0}^H} = \frac{C_{i,F}^{\text{sat}}}{C_{i,j}^{\text{sat}}} \quad (35)$$

Food-favoring migration occurs if solubility in food is greater than in the material. With volume ratios included:

$$\hat{C}_{i,F}^{eq} = \frac{\hat{C}_{i,j}^0}{(V_0/V_j) + (C_{i,j}^{\text{sat}}/C_{i,F}^{\text{sat}})} \quad (36)$$

and is significantly constrained only if:

$$C_{i,j}^{\text{sat}} \gg \frac{V_0}{V_j} C_{i,F}^{\text{sat}} \quad (37)$$

7.3.2 | Link to solubility barriers

Unit partition coefficient (M1) does not allow optimizing designs with **retention layers** or **solubility barriers**. Table 8 contrasts the two strategies.

Table 8 – Differences between a retention layer and a solubility barrier

Strategy (source layer $s > 0$)	Condition	Interpretation	Limitation	Example
Source layer s as retention layer	$K_{i,F/s} \ll 1$	Layer s retains its own substances	Strong/persistent if $K_{i,F/s} \ll V_j/V_0$	Hydrophobic polymer for hydrophobic contaminants
Upstream layer $j > s$ as reservoir	$K_{i,j/s} \gg K_{i,F/s}$	Substances accumulate opposite to food side	Temporary (depends on diffusion time)	Waxy external coating
Downstream layer $j < s$ as solubility barrier	$K_{i,j/s} \gg 1$	Interposed layer reduces driving force	Temporary (diffusion time across s)	Dense polar film, or air gap

7.3.3 | Non-partition cases – example of inks

Partition coefficients apply only to **exchangeable fractions**. Substances **co-crystallized**, trapped in pigments, or embedded in nanoparticles are excluded and described by an **immobile fraction** $\theta_{i,j}$. Transferable mass is:

$$\hat{m}_i^0 = \sum_{j=1}^m V_j (1 - \theta_{i,j}) \hat{C}_{i,j}^0 \quad (38)$$

Proof of immobilization ($\theta > 0$) must be experimental (extraction, DSC). Pigments often qualify; soluble dyes typically do not.

Fraction $\theta_{i,j}^{(T_K)}$ may be estimated from DSC melting enthalpy:

$$\theta_{i,j}^{(T_K)} = \frac{A_{i,j}^{T_K \rightarrow}}{\phi_{i,j} H_i^{\text{ref}}} \quad (39)$$

where $\phi_{i,j}$ is the volume fraction of i in phase j .

7.3.4 | Ready-to-use spreadsheet procedure

Table 9 gives a spreadsheet framework to compute equilibrium concentrations $\hat{C}_{i,F}^{eq}$ across layers and food.

Table 9 – Spreadsheet template for Tier M2 macroscopic effects

Col.	Content	Example formula
A	Layer j (0=food, 1..m)	0,1,2,...
B	Volume V_j	thickness × area
C	Init. conc. $\hat{C}_{i,j}^0$	input
D	Immobile fraction $\theta_{i,j}$	0–1
E	Mobile mass $\hat{m}_{i,j}^{0,\text{mob}}$	=B*(1-D)*C
F	Affinity $k_{i,j}^H$	proxy/score
G	Ratio $\hat{K}_{i,j/F}$	=k0H/kjH
H	Num. term	=B*(1-D)*C
I	Den. term	=IF(j=0;B;G*B*(1-D))
J	Sum num.	=SUM(H[j≥1])
K	Sum den.	=V0+SUM(G*B*(1-D) [j≥1])
L	$\hat{C}_{i,F}^{eq}$	=C_F0+J/K

7.4 | Parameterization of molecular effects

This section explains how molecular effects are translated into Henry-type partition coefficients $k_{i,j}^H$ or its aggregated version PubChemLite (see Schymanski *et al.*, 2025). The approach relies on well-known techniques from the scientific literature (see Gillet *et al.*, 2009, Gillet *et al.*, 2010, Vitrac and Gillet, 2010, Nguyen *et al.*, 2016, Nguyen *et al.*, 2017, Vitrac *et al.*, 2022), but is deliberately simplified and automatable, so it can be applied to hundreds or even thousands of substances using a spreadsheet or an online query.

The method has been implemented in SFPPy (see Vitrac 2025a) and SFPPyLite (see Vitrac 2025b) and integrated into AI agents built on top of them. It provides an operational framework (for risk assessment and regulatory modeling) while retaining a solid theoretical foundation that supports updates, extensions to new families of compounds, and generalization to other migration and material–content interaction domains.

7.4.1 | Link to activity coefficients

The coefficients $k_{i,j}^H$ depend on the solute only in condensed phases j . In gaseous phases, molecules are treated as point masses and $k_{i,j}^H$ depends only on j . In condensed phases, attractive or repulsive interactions between neighbors modify heats of mixing: exothermic (attraction, spontaneous dissolution) or endothermic (dissolution requiring heat input). Even without specific interactions, any solute whose size differs from the polymer's rigid unit (the monomer) imposes a local reorganization, changing the entropy of mixing compared with the pure components.

The free-energy difference between the mixture $i+j$ and the pure components of i and j governs the chemical potentials and the fugacity of i in j . The compressible Flory–Huggins theory at the atomic scale properly describes these attraction/repulsion and compaction/excess-free-volume effects (see Gillet *et al.*, 2010, Vitrac and Gillet, 2010). However, it requires heavy molecular modeling and is not suitable for evaluating hundreds of substances within seconds.

We therefore apply a simplified, robust Flory–Huggins formulation based on data accessible in public databases (PubChem, PubChemLite), interoperable with substance identification. The formal link between $k_{i,j}^H$ and activity coefficients $\gamma_{i,j}^v$ is:

$$k_{i,j}^H = \frac{P_{i,\text{sat}}^{(T_K)} \cdot V_{i,\text{mol}}}{(1 - c_j)(1 - \epsilon_j)} \cdot \gamma_{i,j}^v \quad (40)$$

where $V_{i,\text{mol}}$ is the molar volume of i , approximating its partial molar volume under an incompressibility assumption. The crystallinity c_j and porosity ϵ_j of layer j reduce the accessible fraction. The saturation vapor pressure $P_{i,\text{sat}}^{(T_K)}$ matters only if a gas phase is present; for all-dense systems one sets $P_{i,\text{sat}}^{(T_K)} = 1$.

7.4.2 | Link to compressible Flory–Huggins theory

At infinite dilution, the Flory–Huggins theory generalized to compressible mixtures allows estimation of $\gamma_{i,j}^v$ from the dimensionless heat of mixing χ_{i+j} (Flory–Huggins parameter) and the size ratio $r_{i,j} \simeq V_{i,\text{mol}}/V_{j,\text{mol}}$ between solute i and the representative molecule of polymer j . A correction term $n(r_{i,j})$ accounts for the effective compressibility of j within the solute's interaction sphere. We obtain:

$$\ln \gamma_{i,j} \approx \chi_{i+j} + 1 - [r_{i,j} - n(r_{i,j})] \quad (41)$$

Parameterization of entropic effects (volume and reorganization)

For polymers much larger than the solute, $r_{i,j} = n(r_{i,j}) \rightarrow 0$.

For solutes, food simulants, or solid ink solvents, we use Miller's empirical approximation for molar volume:

$$V_{k,\text{mol}} = 0.997 \cdot M_{k,\text{mol}}^{1.03} \quad (k = i, j) \quad (42)$$

where $M_{k,\text{mol}}$ is the molar mass from the chemical formula.

For large, flexible solutes ($r_{i,j} \geq 1$), solvent molecules can reorganize and reduce the effective number of molecules displaced as the solute is introduced. A compressibility correction is then applied:

$$n(r_{i,j}) = \frac{r_{i,j}}{3} - 1 \quad \text{for } r_{i,j} \geq 3 \quad \text{else } 0 \quad (43)$$

This correction reflects that bulky solutes occupy an effective space smaller than their geometric volume thanks to flexibility and possible rearrangements in the surrounding matrix.

Parameterization of enthalpic effects (interactions)

Enthalpic effects associated with specific interactions between solute i and reference phase j cover both van der Waals and electrostatic interactions, including potential hydrogen bonding. As contact energies and coordination are not available without a 3D molecular representation, we resort to the quadratic regular-solution (Hildebrand–Scatchard) approximation as in Gillet *et al.* (2009):

$$\chi_{i+j} = \frac{V_{\text{ref}}}{RT_K} (\delta_i - \delta_j)^2 \quad (44)$$

where V_{ref} is a reference molar volume, taken as the volume of the rigid segment j exchangeable with solute i .

The parameter $\delta_k = \sqrt{\frac{\Delta H_{k,\text{mol}}^{\text{vap}}}{V_{k,\text{mol}}}}$ is the Hildebrand solubility parameter, i.e., the square root of the cohesive energy density—energy needed to vaporize molecule k (at zero pressure) normalized by its molar volume.

Eq. \ref{eq:chi_delta} essentially expresses differences in the energy needed to create a sorption volume V_{ref} , but it does not capture binary specific interactions between i and j . To estimate partition coefficients, it is preferable to use solubility indices P' . These indices are defined as the natural logarithm of the product of partition coefficients of reference solutes i between a solvent and a gas phase.

Along these lines, we introduce polarity estimators \hat{P}' correlated with octanol/water partition coefficients ($\log P$), widely available in databases:

$$\chi_{i+j} \approx \alpha \left[\hat{P}'(\log P_i, V_{i,\text{mol}}) - \hat{P}'(\log P_j, V_{j,\text{mol}}) \right]^2 \quad (45)$$

7.4.3 | Building a polarity index scale inspired by Snyder

Snyder's scale (see Snyder, 1974) defines polarity indices P' from solvent/air partition coefficients of three probe solutes (ethanol, dioxane, nitromethane) (see Rohrschneider, 1973). It is adapted here because (i) it is familiar in analytical chemistry, (ii) it reflects dipole–dipole interactions, hydrogen bonding, and other polar interactions, and (iii) it covers the main contaminants of recycled plastics.

Reference values used for calibration are given in Table 10. The lower bound (0) corresponds to n-hexane, and the upper bound (10.2) to water (neutral molecules). Ionic species or metal solvates can exceed this bound.

Table 10 — Reference values to calibrate a P' polarity scale, based on logP and Miller molar volumes.

Solvent	Polarity index P'	logP	Miller molar volume ($\text{cm}^3 \cdot \text{mol}^{-1}$)
n-hexane	0.0	3.90	98.2
toluene	1.8	2.73	105.2
dichloromethane	3.1	1.25	96.7
acetone	5.6	-0.21	65.4
ethanol	6.0	-0.24	51.5
acetonitrile	6.8	-0.22	45.8
methanol	8.1	-0.77	35.4
water	10.2	-1.38	19.6

To avoid bias in estimating $\gamma_{i,j}$ and thus $k_{i,j}^H$, the evaluation of P' uses the same Flory–Huggins theory applied to the octanol/water partition coefficient:

$$\ln 10 \cdot \log P_k + (r_{k,w} - r_{k,o}) \approx \chi_{k+w} - \chi_{k+o} = \Delta\chi_{k,ow} = \alpha \left[(P'_k - P'_w)^2 - (P'_k - P'_o)^2 \right] \quad (46)$$

which expands to:

$$\Delta\chi_{k,ow} = \alpha \left[-2P'_k(P'_w - P'_o) + (P'_w + P'_o)(P'_w - P'_o) \right] = \alpha(P'_w - P'_o)(P'_w + P'_o - 2P'_k) = C_1 - C_2P'_k \quad (47)$$

with fitted constants C_1 and C_2 . The scale parameter is $\alpha = \frac{C_2}{2(P'_w - P'_o)}$.

A linear regression on the data in Table 10 validates the model, with $C_1 \approx 11.7$ and $C_2 \approx 1.49$. The octanol index is then $P'_o = 2\frac{C_1}{C_2} - P'_w \approx 5.5$, between dichloromethane ($P' = 3.1$) and acetone ($P' = 5.6$). We obtain $\alpha \approx 0.163$.

Because the linear model assumes uniform compressibility and a single scaling law across the polarity range, we add a quadratic component to better separate very hydrophobic solutes (strong van der Waals interactions, $P' \rightarrow 0$):

$$\Delta\chi_{k,ow} = AP'^2 + BP' + C \quad (48)$$

with a calibration on the eight reference solvents and the α value determined above. The fitted values are $A = 0.181613$, $B = -3.412679$, $C = 13.079540$. The polarity estimator is then:

$$\hat{P}'_k(\log P_k, V_{k,\text{mol}}) = \begin{cases} 10.2, & \text{if } \Delta\chi_{k,ow} \leq \Delta\chi_{k,ow}^{\min} \approx -4.11 \\ \frac{-B - \sqrt{B^2 - 4A(C - \Delta\chi_{k,ow})}}{2A}, & \text{if } \Delta\chi_{k,ow}^{\min} \leq \Delta\chi_{k,ow} \leq \Delta\chi_{k,ow}^{\max} \approx 13.08 \\ 0, & \text{if } \Delta\chi_{k,ow} > \Delta\chi_{k,ow}^{\max} \end{cases} \quad (49)$$

Note

Calibration update.

A recalibration of α on the eight solvents yields a marginal revision ($\alpha = 0.162$).

7.4.4 | Polarity indices for polymers

Polymers are not soluble and thus lack usable $\log P$ values. A robust estimate can nevertheless be obtained from their monomer or, more faithfully, from a **saturated analogue/proxy**. This molecular-modeling approach replaces the polymerizable function by hydrogens to reproduce the local steric environment of the repeating unit.

Table 11— Molecular homologues/proxies to estimate the effective polarity P' of common polymer repeat units.

Polymer	Monomer	Substitute / analogue	Remark
LDPE / HDPE / LLDPE	ethylene	4.7 n-hexane (LD/HD), iso-pentane (LLD)	0.2 / 1.8 Saturated, apolar chains (linear vs. slightly branched)
PP (isotactic)	propylene	3.9 iso-pentane (tert-butyl-like branching)	1.8 Reflects branching of PP
PS	styrene	0.9 ethylbenzene (saturated styrylic motif)	0.7 Faithful proxy of phenyl-alkyl group

Polymer	Monomer	P'	Substitute / analogue	P'	Remark
HIPS	styrene	0.9	ethylbenzene (matrix) + butadiene (rubber)	0.7 / 2.8	Bicontinuous (PS + PB)
SBS	styrene	0.9	ethylbenzene (PS) + isopentane (PB)	0.7 / 1.8	PS/PB blocks
PMMA	methyl methacrylate	2.8	isobutyl acetate (compact ester)	2.0	Represents pendant ester function
PVC	vinyl chloride	3.3	1-chlorobutane (chlorinated alkane)	1.5	Increased polarity due to chlorine
PVAc	vinyl acetate	3.9	ethyl acetate (acetate ester)	3.9	Same functional family
PET	ethylene terephthalate	0.0	dimethyl terephthalate (DMT)	0.4	Aromatic ester proxy (DMT)
PBT	butylene terephthalate	0.1	dibutyl terephthalate	0.0	DMT usable as lower bound
PEN	ethylene naphthalate	0.0	dimethyl 2,6-naphthalene dicarboxylate	0.0	Faithful proxy of naphthalene-ester motif
PA6	caprolactam	4.5	n-hexanamide	2.6	Linear amide, realistic local proxy
PA66	hexamethylenediamine + adipic acid	0.7–3.6	adipamide (amide motif)	5.5	Di-functional amide, highly polar

Note

Usage notes

- Proxies are **not** the actual monomers but **local solvation homologues/proxies** to approximate P' at **Tier M2**.
- P' values rely on calculated $\log P$ reported in PubChem (XLOGP3), consistent with the simplified Flory–Huggins approach embedded in **SFPy**.
- Using proxies better discriminates apolar polymers (PE, PP) from polar ones (PA, PVAc, PMMA), especially in multilayer systems.

7.4.5 | Validation and prediction-error estimates

The choice of solutes/solvents and reference values aims to **deliberately overestimate** $\Delta\chi_{k,ow}$ for most neutral organic compounds, i.e., to favor transfer toward octanol because $\chi_{i,w} > \chi_{i,o}$ and $\frac{dP'}{d\Delta\chi_{k,ow}} < 0$. This is conservative for chemical risk assessment since it promotes migration into lipophilic phases.

Robustness was tested on 35 independent substances relevant to recyclates (see Figure 2). The calibration shows that this setting overestimates the expected value in over 80% of cases (tolerance $\pm 20\%$), aligned with the objective. Estimated/tabulated P' values are compared in Figure 3. The RMSE is 1.16 with $R^2 = 0.713$.

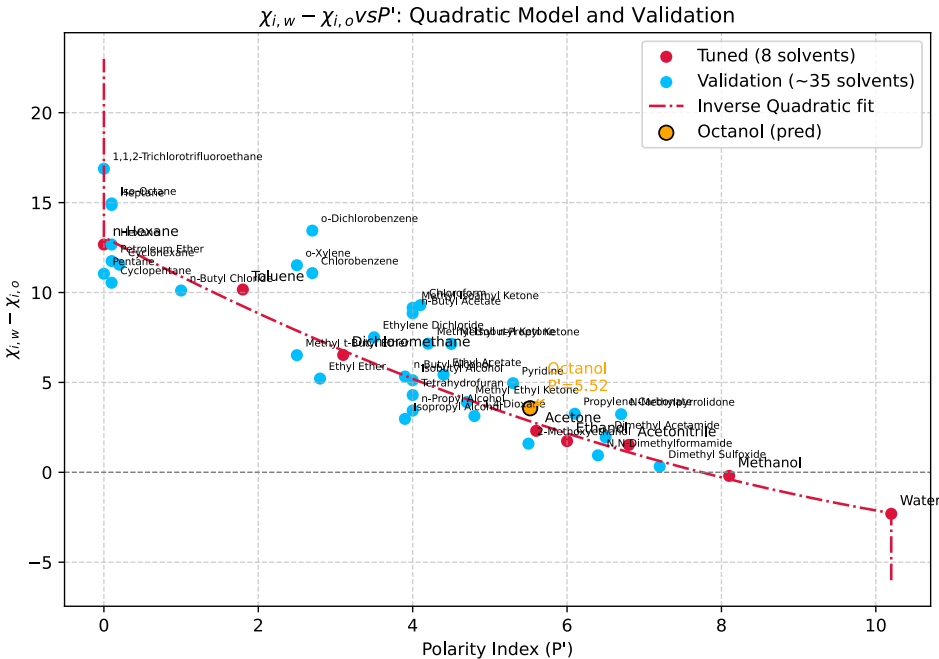


Figure 2 — Comparison of estimated $\chi_{k,w}-\chi_{k,o}$ with tabulated P' values. Calibration data in red; validation data (35 substances) in blue. The model curve and its theoretical asymptotes at the bounds of P' are shown. The octanol estimate is highlighted in orange.

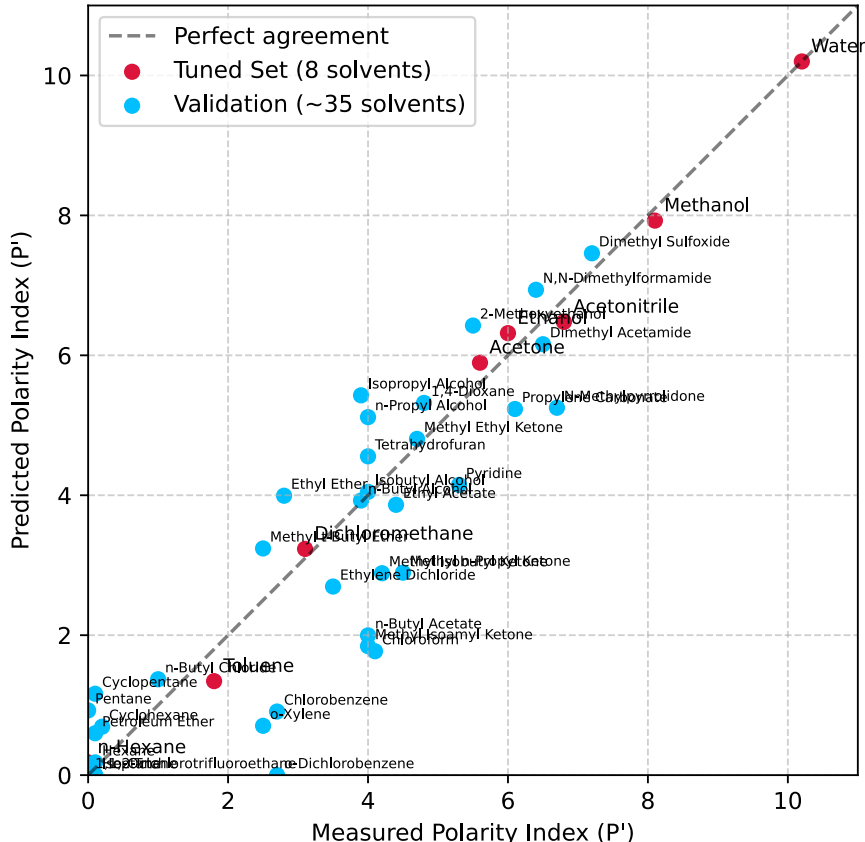


Figure 3 – Comparison of estimated and calculated P'. The dashed line is the 1:1 line.

Note

PubChem error on water $\log P$ (2025 version).

PubChem values (see Kim *et al.*, 2024) use the XLOGP3 algorithm (see Cheng *et al.*, 2007). For water an inconsistency appears:

- **PubChem value:** $\log P = -0.5$ (XLOGP3, 87 atom/group types).
- **Expected value:** from solubility in octanol $[H_2O]_{\text{octanol}} \approx 2.3 \text{ mol} \cdot \text{L}^{-1}$, $\log_{10}\left(\frac{2.3}{55}\right) \approx -1.38$, confirmed by AlogPS and ChemAxon.
- **Consequence:** with $\log P = -0.5$, the polarity index is $P' = 8.00$ (near methanol, $P' \approx 7.4$) instead of the theoretical upper bound 10.2.
- **Impact:** overestimation of partitioning toward water equivalent to $0.1663 \cdot (10.2 - 8.00)^2 \simeq 14.7$. This limitation remains acceptable as it yields a more conservative scenario (increased transfer to aqueous phases).

7.4.6 | Ready-to-use procedure to parameterize molecular effects

Table 12 – Calculation template for molecular effects (ready-to-use in a spreadsheet).

Col.	Content	Example cell (pseudo-Excel/Calc)
A	Substance i	"limonene"
B	$\log P_i$	input (PubChem)
C	$V_{i,\text{mol}}$ (cm ³ ·mol ⁻¹)	input (Miller or DB)
D	Phase j	"amorphous PET", "PP (C=0.30)", "ethanol", "water"
E	$V_{j,\text{mol}}$ (if condensed)	input (monomer/analogue proxy)
F	$r_{i,j} = V_{i,\text{mol}}/V_{j,\text{mol}}$	=C/E
G	$n(r)$	=IF(F>=3, F/3-1, 0)
H	$\Delta\chi_{i,ow}$	=LN(10)*B + (r_i,w - r_i,o)
I	P'_i (positive root)	=(-B - SQRT(B^2 - 4*A*(C - H)))/(2*A) bounded to [0; 10.2]
J	P'_j	input (proxy for phase j)
K	$\chi_{i+j} = \alpha(P'_i - P'_j)^2$	=0.163*(I-J)^2
L	$\ln \gamma_{i,j} \approx \chi_{i+j} + 1 - [r_{i,j} - n(r)]$	=K+1-(F-G)
M	$\gamma_{i,j} = \exp(\ln \gamma)$	=EXP(L)

Col.	Content	Example cell (pseudo-Excel/Calc)
N	c_j (cryst.), ϵ_j (porosity)	input (0–1)
O	$k_{i,j}^H$ (condensed phase)	$=M^*V_{-i}/((1-c_{-j})*(1-\epsilon_{\text{solid}_{-j}}))$ (use $P_{\text{sat}} = 1$)
P	$k_{i,0}^H$ (food/simulant F)	same with $j = 0$
Q	$K_{i,F/j} = k_{i,j}^H/k_{i,0}^H$	$=O/P$
R	$K_{i,j/F} = k_{i,0}^H/k_{i,j}^H$	$=P/O$
S	Justification	source, version, assumptions

Computation steps

1. Estimate P' from $(\log P, M_i \text{ or } V_{i,\text{mol}})$ via the octanol/water calibration (constant parameters provided).
2. Compute $\gamma_{i,j}$ (simplified Flory–Huggins, infinite dilution).
3. Derive $k_{i,j}^H$ including c_j and ϵ_j .
4. Obtain $K_{i,F/j} = k_{i,j}^H/k_{i,0}^H$.

Calibration constants

- Scale parameter: $\alpha = 0.163$
- Quadratic form for $\Delta\chi_{k,ow}$: $A = 0.181613$, $B = -3.412679$, $C = 13.079540$
- Bounds: $\Delta\chi_{\min} \approx -4.11$ (gives $P' = 10.2$); $\Delta\chi_{\max} = C$ (gives $P' = 0$)

Implementation notes

1. **Gas phases:** implement $k_{i,\text{air}}^H = RT_K$.
2. **Condensed phases only:** using $P_{\text{sat}} = 1$ is consistent (thermodynamic equilibrium without a vapor phase).
3. **Semi-crystalline polymers and porous media** (paper/board): crystallinity c_j and porosity ϵ_j **reduce the available phase**: the **amorphous/solid fraction** hosts the migrating substance and affects $k_{i,j}^H$ via
$$\sim \frac{1}{(1-c_j)(1-\epsilon_j)}.$$
4. **Ionizable substances:** out of the M2 domain (or $K_{i,F/j} \rightarrow \infty$ for aqueous contact); document separately.

7.4.7 | Worked example

Table 13 — Examples of Henry and partition coefficients ($K_{i,F/j}$) for limonene under typical conditions (SFPPy outputs).

Case	Pair (j/F)	$k_{i,j}^H$	$k_{i,F}^H$	$K_{i,F/j} = k_{i,j}^H/k_{i,F}^H$
1	PET ($c = 35\%$) / Ethanol	0.845	3.612	0.234
2	PET ($c = 35\%$) / Water	0.845	5.805	0.146
3	PP ($c = 50\%$) / Ethanol	1.351	3.612	0.374
4	PP ($c = 50\%$) / Water	1.351	5.805	0.233

Note

M2 reading. Limonene shows stronger affinity for PET than for ethanol or water ($K < 1$). Water is the least favorable solvent, confirming the molecule's hydrophobic nature. PP and PET behave similarly here and illustrate that fruit-juice terpenes sorb readily into most plastics.

7.5 | Comment on the temperature effect on partitioning

At Tier M2 (thermodynamic control), transfers between two condensed phases j_1 and j_2 do not depend on saturation vapor pressure but on the difference in excess sorption energies $\chi_{i,j_1} - \chi_{i,j_2}$. Temperature effects are weak because there is usually compensation between phases: thermal expansion and thermal agitation simultaneously reduce the occurrence of favorable interactions in both j_1 and j_2 . The main cases are summarized in Table 14.

Table 14 — Temperature effect on partition coefficients.

Situation	Expected effect
Two endothermic mixtures (common case)	Compensation of thermal effects; K_{j_1/j_2} overall stable.
Specific interaction with one phase only	Increasing T_K favors transfer to the other phase; decreasing T has the opposite effect.
Presence of a gas layer	T_K dominates: activation proportional to latent heat of vaporization. Volatiles migrate uniformly; low-volatiles show a marked threshold .

7.6 | Identified limitations

Tier M2 enables:

- Incorporation of solubility, polarity, crystallinity, porosity, immobile fractions.
- Differentiation of partition coefficients between layers.
- Evaluation of barrier/retention layers, supporting recycled/multilayer design.
- Routine application via spreadsheets or automated agents.

But: limitations include handling of ions/zwitterions, non-linear sorption, poorly characterized immobile fractions, multiphase tie-layers, food matrix effects, multi-solute competition, and recycled material variability. Table M2-4 summarizes the main limitations and best practices.

Fast, explainable partition values come with limits that must be documented. They are summarized in Table 1.

Tip

Operational recommendations

1. Use the molecular substitutes listed above to parameterize polymer $k_{i,j}^H$.
2. Apply conservative rules: take the minimal plausible $K_{i,F/j}$ from the “food ← material” perspective.
3. Document immobilized fractions $\theta_{i,j}$ **only** if supported by experimental data (extraction, DSC).
4. Check consistency by cross-referencing criticalities $\hat{c}(t)$ and potentials PR_i^E .

Table 15 — Main limits of Tier M2 and practical consequences.

Aspect	Limit	Consequence / Good practice
P' indices, logP	Valid for neutral migrants. Out of scope for ions, zwitterions, siloxanes, heavy halogenated species, etc.	Document the source (PubChem/XLOGP3). If anomalies arise (e.g., water), retain the more solvating phase.
Henry's law	Assumes a linear isotherm. Ignored: dual-mode sorption, plasticization, swelling.	Keep the unfavorable slope. Move to M3 when strong non-linearities are present.
Immobilized fractions $\theta_{i,j}$	Hard to estimate (DSC, extraction, NMR). Strong dependence on thermal history.	Accept $\theta > 0$ only with analytical evidence. Otherwise, use a lower bound.
Multiphase systems & interphases	Tie-layers, micro-domains, actual porosity not explicit.	Add an interphase compartment or bias toward the more solvating phase.
Real matrices vs simulants	pH, proteins, co-solvency not captured.	Adjust P' to the matrix or choose the unfavorable scenario.
Multi-solute competition	Additivity simplified. Ignored: competition, co-solvency, complexation.	Use the most mobile migrant for screening. Switch to M3/experiments for critical cases.
Recycled materials	Variability, NIAS, pre-contamination.	Choose conservative $C_{i,j}^0$ (P90–P95). Include NIAS present at the LOD [†] .
Temperature and time	Static M2. Thermal cycles and headspace change $K, \theta, C^{\text{sat}}$.	Move to M3 for long storage, pasteurization, or temperature cycling.
Adhesives, inks, varnishes	Oligomers, residual solvents, pigments.	Distinguish slow diffusion/trapping. Keep θ minimal unless strongly evidenced.
Extensive quantities	Risk of mass/volume confusion, A/V, heterogeneous thicknesses.	Always reduce to V_0 ; document the calculation chain.
Uncertainties	Poorly quantified. Risk of over- or under-estimation.	Report ranges (low, central, high). Separate screening (M0–M2) from validation (M3).
Switch to M3	Justified when: barriers, low-diffusivity substances, uncertain K , dimensioning T/t , plasticization, critical interphases, high health stakes.	Couple M2+M3 for higher accuracy.

[†]LOD: limit of detection. A value of 0.3 mg kg^{-1} is generally a good approximation.

Key takeaways (Section 7)

- **Tier M2 enriches M1** by incorporating **material/solute-specific properties** (solubility, polarity, crystallinity, porosity, immobile fractions).
- Partition coefficients become differentiated per layer and included in a **filtered mass balance**, enabling the evaluation of barrier or retention layers.
- M2 and M3 are **complementary**: M2 addresses thermodynamic sharing, while M3 adds dynamics ($\bar{v}_i^*(t)$).
- M2 is suitable for **screening and design justification**, while M3 refines results under **real usage conditions** (time, temperature, cycling).

8 | Advanced Tier M3: Diffusion dynamics, barrier layers, and functional barriers

Note

Micro-recap of what changes at M3

M1 gives you a mass balance; M2 adds realistic equilibrium partitioning; **M3 adds time**. It brings in diffusion kinetics via $\bar{v}_i^*(t)$ and $D_{i,j}$, and leverages two powerful properties: **temporal commutativity** (sum of Fourier numbers) and **spatial additivity** (superposition by layer). Use M3 together with M1/M2.

8.1 | Introduction

Tier **M3** extends M1 and M2. While M1 provides a global mass balance and M2 refines it with thermodynamic partitioning at equilibrium, **M3 explicitly introduces transfer kinetics**. It couples equilibrium quantities with diffusive phenomena and ties real contact conditions (duration, temperature, sequences) to the effective migration.

M3 is never used alone: its results only make sense when combined with M1/M2, which supply thermodynamic framing and mass-balance coherence. It is indicated when:

- contact time is short or variable (transport, forming, thermal treatments);
- temperature varies strongly (processing, storage, use);
- the effectiveness of one or more barrier layers must be demonstrated;
- contamination is governed by diffusion kinetics rather than equilibria;
- polymer plasticization, swelling, or aging affects diffusion;
- recycled/aged materials make kinetics critical.

M3 introduces the cumulative transfer fraction $\bar{v}_i^*(t)$ and uses several predictive models for diffusivity $D_{i,j}$. Two fundamental properties structure the approach:

- temporal commutativity** (sequences are equivalent via cumulative Fo),
- spatial additivity** (superpose per-layer contributions).

This section develops: molecular bases, invariance and additivity properties, models for $\hat{D}_{i,j}$, then a summary emphasizing complementarity with M2. For overviews see Fang 2015, Zhu 2019; for molecular descriptors used in learning-based models see Vitrac 2006. Mathematical properties for mono- and multilayers appear in Vitrac 2005 and Nguyen 2013.

Important

Key idea.

Because diffusion laws are linear in time, two key properties follow: (i) **temporal commutativity**, letting you replace a succession of isothermal or thermally varying steps by a single equivalent step defined by a **cumulative Fourier number** $Fo^{(N)}$; (ii) **spatial additivity**, allowing you to **decompose the final contamination** into distinct contributions from each source layer. These greatly simplify complex scenarios (multiple barriers, storage/processing sequences) and partial severities by step or layer.

Note

A diffusive transport description is also assumed applicable to paper and board in a mean-field sense, though the microscopic picture involves diffusion plus sorption/desorption at fiber surfaces.

8.2 | Diffusive phenomena

In earlier tiers, kinetics was ignored: results were identical whether contact was brief or prolonged. At equilibrium, microscopic fluxes between compartments j_1 and j_2 balance; off-equilibrium, a net flux appears from the source layer to others.

The same mechanisms operate at the molecular scale (barring secondary effects such as plasticization, swelling, aging). Diffusion arises from random walks of solutes i through free-volume pockets created by thermal agitation of rigid polymer segments. Jump length and frequency depend on:

- the ratio of molecular volumes (solute vs rigid segment),
- the renewal rate of free volume, linked to $T - T_g$,
- the fraction of free volume, linked to polymer density.

Important

Thermal activation stems from polymer volumetric expansion: in rubbery matrices ($T > T_g$) it is strong; in glassy matrices ($T < T_g$) it is moderate.

8.3 | Invariance and temporal commutativity

Diffusion laws with constant D are linear in time: several transfer steps can be reordered or replaced by an equivalent one.

For m layers ($l_j = V_j/A$), kinetics is controlled by the limiting layer:

$$j_{\min} = \arg \min_{1 \leq j \leq m} \left\{ \frac{D_{i,j}}{k_{i,j}^H l_j} \right\}. \quad (50)$$

Define the cumulative Fourier number:

$$Fo^{(N)} = \sum_{k=1}^N \Delta Fo_k, \quad \Delta Fo_k = \frac{D_{j_{\min}}(T_k)}{l_{j_{\min}}^2} t_k. \quad (51)$$

Note. j_{\min} remains the same across steps, at least for the same solute i .

The cumulative contamination after N steps writes:

$$\hat{C}_{i,F}^{(N)} = \hat{C}_{i,F} \left(Fo^{(N)} \right). \quad (52)$$

The **relative severity** of step ℓ is:

$$\hat{s}_i|_{\ell} = 100 \times \frac{\max \left(\hat{C}_{i,F}^{(N)} - \hat{C}_{i,F}^{(N \setminus \ell)}, \hat{C}_{i,F}|_{\ell} \right)}{\rho_0 \cdot \text{SML}_i}. \quad (53)$$

8.4 | Spatial additivity (superposition of contributions)

By linearity, total contamination in M3 decomposes into elementary contributions of each layer s :

$$\hat{C}_{i,F}^{(N)} = \sum_{j=1}^m \hat{C}_{i,j \rightarrow F}^{(N)}, \quad \hat{s}_{i,s} = 100 \times \frac{\hat{C}_{i,s \rightarrow F}^{(N)}}{\rho_0 \cdot \text{SML}_i} \quad (54)$$

where $\hat{C}_{i,j \rightarrow F}$ is component j 's contribution to F , and $\hat{s}_{i,j}$ its associated severity.

This comes from the linear Fick equation and its convolution solution. The final concentration in F is the superposition of impulse responses $G_{j \rightarrow F}(t)$ (Green's functions) weighted by initial conditions $C_{i,j}^0$:

$$C_{i,F}(t) = \sum_{j=1}^m (G_{j \rightarrow F} \otimes C_{i,j}^0)(t), \quad (55)$$

with \otimes the convolution operator.

Each layer/component behaves as an independent source; contributions add without artificial interaction as long as the **tracer diffusion** assumption holds (properties independent of concentration).

Important

Practical note.

Superposition is valid only if all else is unchanged (number of layers, properties, boundary conditions). Only the initial contamination conditions may vary. **This property applies to any source arrangement**—1D, 2D or 3D; in series, in parallel, or any combination.

8.5 | Diffusivity prediction models

8.5.1 | Physical definitions

The diffusivity $D_{i,j}$ of tracer i in medium j (SI units m^2s^{-1}) is the long-time rate of increase of the mean-squared displacement $\mathbf{r}(t)$, averaged over directions (Fang 2015):

$$D_{i,j} = \lim_{t \rightarrow \infty} \frac{\langle \|\mathbf{r}(t) - \mathbf{r}(0)\|^2 \rangle}{6t}. \quad (56)$$

The average $\langle \cdot \rangle$ is over a statistical ensemble of tracers and all start times $t = 0$. Displacements are relative to the system's center of mass to remove drift.

In condensed phases, three regimes are distinguished:

- (i) **tracer diffusion** (infinite dilution, D constant),
- (ii) **mutual diffusion** (high concentration/co-solutes, D depends on composition),
- (iii) **self-diffusion** (pure medium, D constant).

Beyond molecular times, several theories describe $D_{i,j}$: hydrodynamic **Stokes–Einstein**, **free-volume theory** (solute translation + polymer relaxation), and **WLF** (frequency vs temperature).

Important

We restrict to **concentration-independent** D . Concentration effects can be handled by the **hFV model**; here they enter only indirectly via changes to polymer T_g .

8.5.2 | Model taxonomy

Three operational models are proposed—**Piringer**, **Welle**, **hFV (hole Free-Volume)**—with the following conservative hierarchy:

$$\hat{D}_{i,j}^{\text{Piringer}} \geq \hat{D}_{i,j}^{\text{Welle}} \geq \hat{D}_{i,j}^{\text{hFV}} \approx D_{i,j}. \quad (57)$$

A usage comparison is given in Table 16.

Note

Model precedence (as in SFPPy; see Vitrac 2025a, Vitrac 2025b):

- **hFV** whenever the **toluene/polymer** couple is covered;
- **Welle** where polymer-specific parameters exist;
- **Piringer** as the universal envelope elsewhere.

Using **hFV with toluene** is preferred to qualify **functional barrier** effectiveness, notably for recycled/aged materials.

Table 16 — Compared properties of diffusivity prediction models

Model / effect	$\hat{D}_{i,j}^{\text{Piringer}}$	$\hat{D}_{i,j}^{\text{Welle}}$	$\hat{D}_{i,j}^{\text{hFV}}$
Principle	Empirical envelope (M_i, T)	Correlation V_{vdW}, T	Physical model (free volume, $T - T_g$)
Parameters	$M, T, (A_{pp}, \tau)$	$V_{\text{vdW}}, T, (a, b, c, d)$	$T, T_g, (D_0, \xi, K_a, K_b, r)$
Accounts for T_g	No	Via parameter sets	Yes (continuous)
Plasticization	No	No	Yes (tracer \rightarrow self-diffusion)
Polymers covered	Broad (universal)	PET, PS/HIPS	PE, polyesters, PA, PV, etc.
Solutes covered	Organics $M > 40 \text{ g}\cdot\text{mol}^{-1}$	Organics $M > 40 \text{ g}\cdot\text{mol}^{-1}$	Rigid/linear solutes
Pros	Simplicity, upper bound	Tuned for glassy polymers	High realism, T effects
Limits	Variable over-prediction; not conservative for very small solutes in glassy polymers	Spherical solutes; no plasticization	More complex; needs fine parametrization
SFPPy status	complete	complete	partial (toluene)

8.5.3 | Piringer model: a near-universal envelope

The Piringer model (Begley 2005) is simple: it uses solute molar mass M_i as sole descriptor; polymer effects via A_{pp} and τ :

$$D_{i,j}^{\text{Piringer}}(M, T) = \exp \left[\left(A_{pp} - \frac{\tau}{T_K} \right) - 0.135 M_i^{2/3} + 0.003 M_i - \frac{10454}{T_K} \right] \quad (58)$$

with $T_K = T [^\circ\text{C}] + 273.15$, M in $\text{g}\cdot\text{mol}^{-1}$.

Parameters (A_{pp}, τ) are **material-specific** (e.g., LDPE: (11.5, 0); gPET: (3.1, 1577); rPET: (6.4, 1577); PP: (13.1, 1577)). No T_g nor plasticization.

Note

Use vs limits.

Use: broad coverage, robust upper envelope when specifics are missing.

Limit: may be non-conservative for very small molecules in glassy polymers. Applicability to paper/board is limited.

Table 17 — Polymer parameters for the Piringer model

Key†	className†	material†		
HDPE	HDPE	high-density polyethylene	14.5	1577
LDPE	LDPE	low-density polyethylene	11.5	0
LLDPE	LLDPE	linear low-density polyethylene	11.5	0
PP	PP	isotactic polypropylene	13.1	1577
aPP	PPrubber	atactic polypropylene	11.5	0
oPP	oPP	biooriented polypropylene	13.1	1577
pPVC	plasticizedPVC	plasticized PVC	14.6	0
PVC	rigidPVC	rigid PVC	−1.0	0
HIPS	HIPS	high-impact polystyrene	1.0	0
PBS	PBS	styrene-based polymer PBS	10.5	0

Key†	className†	material†	A_{pp}	τ
PS	PS	polystyrene	-1.0	0
PBT	PBT	polybutylene terephthalate	6.5	1577
PEN	PEN	polyethylene naphthalate	5.0	1577
PET	gPET	glassy PET (below T_g)	3.1	1577
rPET	rPET	rubbery PET (above T_g)	6.4	1577
wPET	wPET	(duplicate of rPET)	6.4	1577
PA6	PA6	polyamide 6	0.0	0
PA6,6	PA66	polyamide 6,6	2.0	0
Acryl	AdhesiveAcrylate	acrylate adhesive	4.5	83
EVA	AdhesiveEVA	EVA adhesive	6.6	-1270
rubber	AdhesiveNaturalRubber	natural rubber adhesive	11.3	-421
PU	AdhesivePU	polyurethane adhesive	4.0	250
PVAc	AdhesivePVAc	PVAc adhesive	6.6	-1270
sRubber	AdhesiveSyntheticRubber	synthetic rubber adhesive	11.3	-421
VAE	AdhesiveVAE	VAE adhesive	6.6	-1270
board_polar	Cardboard	cardboard (polar migrants)	4.0	-1511
board_apol	Cardboard	cardboard (apolar variant)	7.4	-1511
paper	Paper	paper	6.6	-1900
gas	air	ideal gas	-	-

† SFPPy nomenclature: material key, class name, material.

8.5.4 | Welle model: specific for PS/HIPS (and PET)

The Welle model (Ewender and Welle, 2022) corrects over-estimation in glassy polymers (notably PET). It replaces molar mass with van-der-Waals volume $V_{i,\text{vdW}}$:

$$D_{i,j}^{\text{Welle}}(V_{\text{vdW}}, T) = 10^{-4} b \left(\frac{V_{i,\text{vdW}}}{c} \right)^{\frac{a-1/T_K}{d}} \quad (59)$$

where a, b, c, d are polymer-specific (e.g., gPET: $a = 1.93 \cdot 10^{-3}$, $b = 2.27 \cdot 10^{-6}$, $c = 11.1$, $d = 1.50 \cdot 10^{-4}$). T_g effects are implicit through distinct parameter sets.

③ Note

Use vs limits.

Use: validated accuracy for PET and PS/HIPS; uses true 3D size.

Limit: needs rigorous V_{vdW} (atomic connectivity). Parameters established for dry polymers, not equilibrated with ambient humidity.

Table 18 — Polymer parameters for the Welle model

Polymer key†	a (1/K)	b (cm ² /s)	c (Å ³)	d (1/K)
gPET	1.93×10^{-3}	2.27×10^{-6}	11.1	1.50×10^{-4}
PS	2.59×10^{-3}	7.38×10^{-9}	55.71	2.73×10^{-5}
rPS	2.44×10^{-3}	6.46×10^{-8}	25.51	7.55×10^{-5}
HIPS	2.55×10^{-3}	9.21×10^{-9}	73.28	2.04×10^{-5}
rHIPS	2.46×10^{-3}	2.07×10^{-7}	45.00	2.07×10^{-7}

† SFPPy nomenclature: polymer key.

8.5.5 | hFV model: rigid blob in free-volume theory

The reformulated free-volume theory (Fang *et al.*, 2013; Zhu *et al.*, 2019b) includes a **smoothed glass transition** and a **scaling law** for linear probes (rigid blobs). It is parameterized here for **toluene** on several polymers.

Smoothed transition around T_g :

$$H(T) = \frac{1}{2} \left(1 + \tanh \frac{4}{\Delta T} [T_K - T_g] \right), \quad \Delta T \simeq 2 \text{ K} \quad (60)$$

Thermal dilations:

$$\alpha(T) = 1 + \frac{K_a}{T_K - T_g + K_b}, \quad \alpha_g(T) = 1 + \frac{K_a}{r(T_K - T_g) + K_b} \quad (61)$$

Mixture:

$$\alpha_T(T) = (1 - H)\alpha_g(T) + H\alpha(T) \quad (62)$$

Free-volume measure:

$$P_{j,\text{like}}(T) = \frac{\alpha_T(T) + \beta_{\text{lin}}}{0.24}, \quad \beta_{\text{lin}} = 1 \quad (63)$$

Diffusivity:

$$D_{i,j}^{\text{hFV}}(T) = D_{i,0} \exp\left(-\frac{E_{i,j}}{RT_K}\right) \exp(-\xi_i P_{j,\text{like}}(T)) \quad (64)$$

Note

Use vs limits.

Use: good accuracy over many conditions (polar/apolar solutes; glassy/rubbery polymers).

Limit: more complex; needs careful parameterization for arbitrary solutes.

Table 19 — Polymer parameters for the blob model applied to toluene

Polymer key†	T_g (K)	$D_{i,0}$ (m ² /s)	ξ_i	K_a (K)	K_b (K)	$E_{i,j}$ (J/mol)	r
LDPE	148.15	1.87×10^{-8}	0.6150	144	40	0	0.5000
PMMA	381.15	1.87×10^{-8}	0.5600	252	65	0	0.5000
PS	373.15	4.80×10^{-8}	0.5840	144	40	0	0.5000
PVAc	305.15	1.87×10^{-8}	0.8600	142	40	0	0.5000
gPET	349.15	1.02×10^{-8}	0.6761	252	65	0	0.6153
wPET	316.15	1.02×10^{-8}	0.6761	252	65	0	0.2777

† SFPPy nomenclature: polymer key.

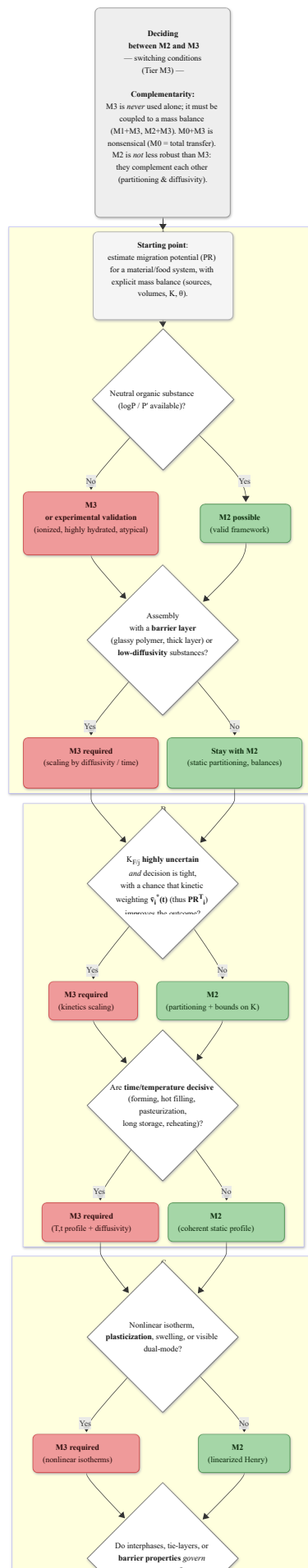
8.6 | When to use Tier M3?

Using M3 entails numerical solutions of diffusion equations, which lack closed forms once more than two layers are present. You need initial distributions and values of $\hat{D}_{i,j}$ and $\hat{k}_{i,j}^H$.

Thanks to tools such as **FMECAengine** or **SFPPy** (built for this compute load), a function $\bar{v}^*(t)$ can be computed in **< 0.1 s**, enabling analysis of dozens/hundreds of substances across designs.

Do **not** switch to M3 if all substances satisfy $\hat{s}_i \leq 100$ or if setting $\bar{v}^*(t) \rightarrow 1$ would not change your decision. Switch to **M3** if:

- the final decision depends on the limiting value of $\bar{v}^*(t)$ or on its optimization;
- transfer mechanisms require explicit kinetics;
- multiple layers function as barriers and need dynamic coupling.



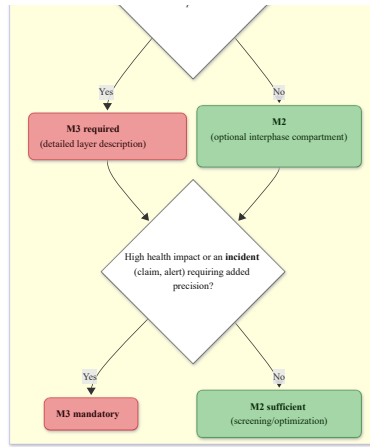


Figure 4 – Decision guide for choosing M2 alone vs M2+M3

Key takeaways for Section 8

Blue box – What to remember.

M3 enriches M2 by introducing **diffusion kinetics**, indispensable when time, temperature, or barrier performance governs migration. Three model families are available: **Piringer** (universal envelope, conservative), **Welle** (PET/PS/HIPS-specific correlations, more realistic), and **hFV** (free-volume physics, accurate but more complex).

Tip

Their **hierarchical combination**, already implemented in **SFPpy** (Vitrac 2025a, Vitrac 2025b), yields **explainable, consistent predictions** for both screening and in-depth evaluation of recycled materials, with uncertainties appropriately framed.

9 | Risk reduction by optimization

9.1 | Objective and stakes

Risks arise from **formulation** (substances, concentrations), **use** (food, duration, temperature), and **design** (materials, stack-up, geometry). Some parameters are tunable, others imposed. Constrained optimization aims, for each substance i , to ensure $\hat{s}_{i,\max} \leq 100$, equivalently $\hat{C}_{i,F} \leq \hat{C}_{i,F}^{\max}$ (maximum admissible concentration in food).

Contamination from **multiple sources** is common (layers of the same material, multiple printings, multi-function additives such as benzophenones, use of recyclates). It requires **linked** decisions across components.

Note

Operational note. Optimization is applied **substance by substance**, targeting the most **critical** compounds due to quantity, toxicity, or propensity to migrate. An **equivalent** approach minimizes risk for **surrogate/proxy molecules** representative of the critical substances (similar orders of magnitude for D and k).

An article/package is rarely designed for a single product/use. Conception should therefore remain **robust** across several use cases.

A large-scale example (multi-criteria, multiple constraints and parameters) for a bottle-type packaging can be found in Zhu 2019.

9.2 | Useful properties and identities

Two indicators help rank layers/components to target first, assuming the food is not pre-contaminated:

- the **current relative contribution** of layer s :

$$u_{i,s} = \frac{\hat{C}_{i,s \rightarrow F}^{(N)}}{\hat{C}_{i,F}^{(N)}}, \quad 0 \leq u_{i,s} \leq 1, \quad \sum_{s=1}^m u_{i,s} = 1 \quad (65)$$

- the **propensity to transfer** of layer s , i.e., its marginal leverage:

$$w_{i,s} = \frac{V_0}{V_s} \cdot \frac{\hat{C}_{i,s \rightarrow F}^{(N)}}{\hat{C}_{i,s}^0}, \quad 0 \leq w_{i,s} \leq 1 \quad (66)$$

Total contamination and the associated severity are:

$$\hat{C}_{i,F}^{(N)} = \sum_{s=1}^m w_{i,s} \cdot \frac{V_s}{V_0} \cdot \hat{C}_{i,s}^0, \quad \hat{s}_i^{(N)} = \frac{100}{SML_i} \hat{C}_{i,F}^{(N)} \quad (67)$$

The general optimization constraint is:

$$\sum_{s=1}^m \frac{V_s}{V_0} w_{i,s} \hat{C}_{i,s}^{0,new} \leq C_{i,F}^{\max} \quad (68)$$

Two levers (marginal sensitivities) follow:

$$\eta_{i,s} = \frac{\partial \hat{C}_{i,F}^{(N)}}{\partial \hat{C}_{i,s}^0} = \frac{V_s}{V_0} w_{i,s}, \quad \frac{\partial \hat{C}_{i,F}^{(N)}}{\partial w_{i,s}} = \frac{V_s}{V_0} \hat{C}_{i,s}^0. \quad (69)$$

Note

Reading the levers. $\eta_{i,s}$ is the marginal sensitivity of **total contamination** to a change in initial content. The second lever quantifies sensitivity to a change in transfer rate via design or use. Its effect scales with the **initial contaminant load**, confirming that such modifications should first target the most formulated or most contaminated parts/components.

9.3 | Mitigation rules (content and transfer)

9.3.1 | General principles

For a single source, options are straightforward:

- avoidance: **substitute the substance** or **remove the source**;
- mitigation: **reduce content**, **add a barrier**, **adapt use conditions**.

With multiple sources, it is essential to distinguish:

- $u_{i,s}$: current contribution,
- $w_{i,s}$: latent risk of future transfer.

The joint reading is illustrated in Table 20.

Table 20 – Joint reading of indicators $u_{i,s}$ (current contribution) and $w_{i,s}$ (future propensity).

Configuration	Interpretation	Comment
large u , large w	Priority layer	Already contributes and transfers strongly
large u , small w	Contribution due to high content	Content reduction is effective
small u , large w	“Hot” layer with latent risk	Act on transfer (barrier, reduce Fo) before rise
small u , small w	Low priority	Marginal contribution

Note

On the indicators. $u_{i,s}$ is composite: it includes mass-action (transfer \propto amount present) plus design effects. $w_{i,s}$ is more specific to **causes** (physico-chemistry and design), independent of the present quantities.

9.3.2 | Uniform content reduction

The simplest rule reduces concentrations uniformly across all layers/components. With λ the reduction factor:

$$\hat{C}_{i,s}^{0,new} = \lambda \hat{C}_{i,s}^0, \quad \lambda = \min \left(1, \frac{C_{i,F}^{\max}}{\sum_r \frac{V_r}{V_0} w_{i,r} \hat{C}_{i,r}^0} \right). \quad (70)$$

Practical note (recyclates). This closed-form, auditable rule may be hard to apply where certain substances cannot be reduced in specific components or suppliers refuse changes. For recyclates, it maps directly to the contamination level. The updated decontamination rate Δ_2 is:

$$\Delta_2 = 1 - \lambda (1 - \Delta_1), \quad (71)$$

where Δ_1 is the initial decontamination rate.

9.3.3 | Selective prioritization by marginal impact (step-by-step)

Rank components/layers by decreasing $\eta_{i,s}$ (Eq. \ref{eq:sensitivities}) and reduce content first where $\eta_{i,s}$ is largest.

If a cost κ_s (€/ppm, losses, feasibility) is available, replace $\eta_{i,s}$ by a **cost-effectiveness** index

$$\nu_{i,s} = \frac{\eta_{i,s}}{\kappa_s}. \quad (72)$$

Iterate mitigation until

$$\sum_s \frac{V_s}{V_0} w_{i,s} \hat{C}_{i,s}^{0,\text{new}} \leq C_{i,F}^{\text{max}}. \quad (73)$$

9.3.4 | Priority indices that combine u and w

Ranking solely by $\eta_{i,s} = \frac{V_s}{V_0} w_{i,s}$ ignores current contributions $u_{i,s}$. Table 21 introduces composite indices covering both aspects.

Table 21 — Prioritization indices combining $u_{i,s}$ and $w_{i,s}$.

Indicator	Interpretation	Properties
$R_{i,s}^{(\times)} = u_{i,s} \eta_{i,s}$	Priority to layers that already contribute and transfer strongly	Bounded, monotone in u and w (i.e., never mis-prioritizes)
$R_{i,s}^{(\alpha)} = u_{i,s}^\beta \eta_{i,s}^{1-\beta}$	Tunable weighting (β)	$\beta \uparrow$: emphasize dominant layers; $\beta \downarrow$: emphasize marginal leverage
$R_{i,s}^{(\times, \text{Euros})} = \frac{u_{i,s} \eta_{i,s}}{\kappa_s}$	Cost-effectiveness index	Impact per euro invested

Note

Coupling content & design. Costs κ_s may come from a cost matrix for **content reduction (C)** and/or for **barrier improvement (w)**. This couples optimization of content and design in one framework.

9.3.5 | Acting on the transfer propensity w

When content reduction is limited, act on $w_{i,s}$:

- reduce Fo (time/temperature),
- change partition $K_{F/s}$ (material choice),
- insert/optimize a barrier to enforce j_{\min} ,
- increase $\theta_{i,s}$ (immobilization, crystallinity).

Caution

Focusing on $u_{i,s}$ alone (“who contributes **today**”) can miss a high $w_{i,s}$ (“who will transfer **tomorrow**”). Combine both via $\eta_{i,s} = (V_s/V_0) w_{i,s}$.

9.4 | Safe design as a linear programming problem

Introducing a cost κ_s not only prices design modifications on an existing package, it also prioritizes solutions that are technically/economically feasible (available and effective).

Safe design becomes a cost-minimization problem with a health-safety constraint. The cost may include raw material, package mass, recycling, etc. Compactly:

$$\min_{\{\Delta C_s\}} \sum_{s=1}^m \kappa_s \Delta C_s \quad \text{s.t.} \quad \sum_{s=1}^m \frac{V_s}{V_0} w_{i,s} (\hat{C}_{i,s}^0 - \Delta C_s) \leq C_{i,F}^{\text{max}}. \quad (74)$$

A variant includes variables that reduce $w_{i,s}$ (barriers, design), at the cost of a **sequential** solve (fix w , optimize C , then vice-versa). The computation chain is summarized in Figure 5.

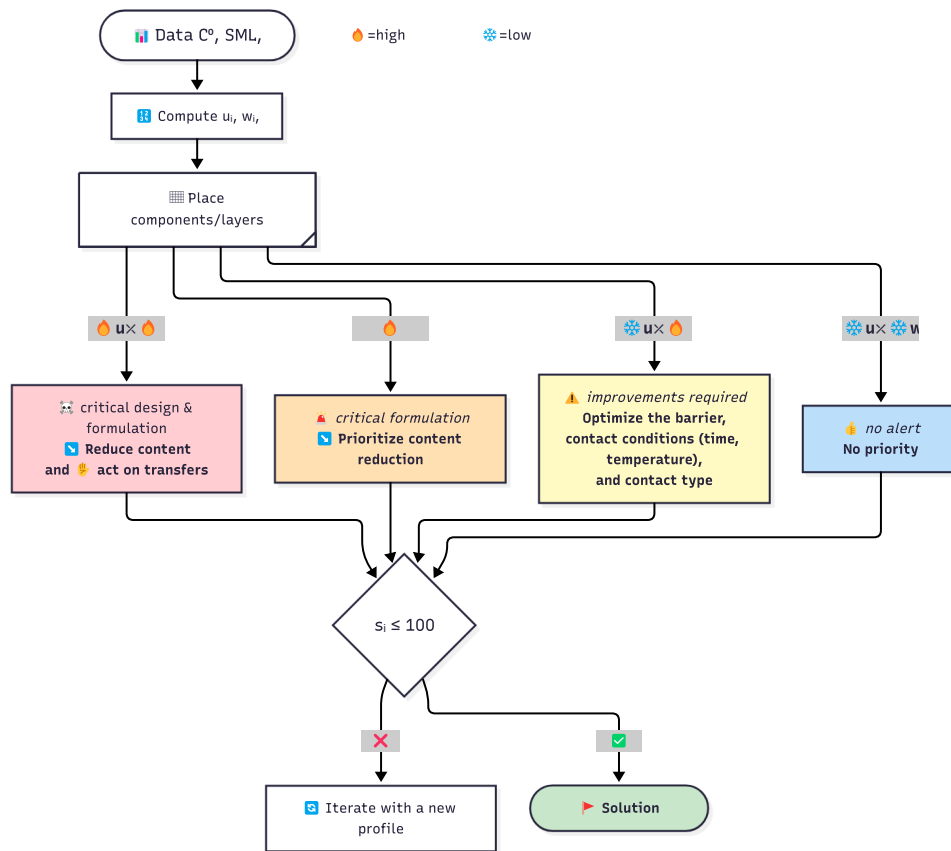


Figure 5 — Optimization chain driven by the joint values of u_i and w_i .

Key takeaways (Section 9)

The optimization framework formalizes risk reduction through **targeted actions**: content reduction, **barriers**, and **use conditions**. Indicators $u_{i,s}$ (current load) and $w_{i,s}$ (transfer propensity) guide prioritization, while $\eta_{i,s}$ quantifies marginal gain. With a cost κ_s , safe design becomes a **linear programming** problem that reconciles safety and feasibility—either **substance-wise** or via **homologues/proxies** representative of critical migrants.

10 | Application perspectives with SFPPy and Python

This section illustrates how to operationalize the concepts of tiers M1–M3 with **SFPPy** (Vitrac 2025a, 2025b) and Python, through five progressive examples. Code snippets follow the idioms in `example1.py`–`example5.py` and the project `README`. They cover the full chain: (i) defining migrants and layers, (ii) M2 partitioning, (iii) M3 dynamics (time/temperature sequences), (iv) visualization, and (v) automation (fitting, optimization, AI integration).

Note

The **SFPPy** project (*Safe Food Packaging Portal in Python*) is an open-source initiative that implements the principles presented in this article as Python scripts and notebooks. Based on a finite-volume solver (Patankar method, see Nguyen *et al.*, 2013) and interfaced with public databases (PubChem Kim *et al.*, 2024, ToxTree Patlewicz *et al.*, 2008, EU/US/CN regulations), SFPPy bridges theory and operational simulation in a few lines of code — or without local installation via online notebooks (e.g., Google Collab) or browser-based WebAssembly builds (Vitrac 2025b).

10.1 | Example 1 — Transfer simulation through a monolayer

Objective of example 1

Estimate partitioning and potential migration of an additive (e.g., Irganox 1076) from a thin LDPE film wrapping a sandwich, then quickly evaluate the effect of duration/temperature (simplified M3).

Table 21 summarizes the studied configurations.

Table 21 — Parameters of Example 1.

Properties	Values
Film	LDPE, $l = 100 \mu\text{m}$
Food (simulant)	Cylindrical shape ($\varnothing=19 \text{ cm}$, $L=19 \text{ cm}$), ethanol 95%
Migrant	Irganox 1076 (CAS 2082-79-3), properties from public DBs
Outputs	$K_{F/LDPE}$, $\hat{C}_{i,F}$, \hat{s}_i after 10 days at 7°C , plus 4 h at 25°C

Listing 1 – Simulation of transfers between LDPE film and a sandwich

```

1 # Listing 1 - Simulation of transfers between LDPE film and a sandwich
2
3 # =====
4 # ////////////////////////////////////////////////// Minimalist version ///////////////////////////////////
5 # =====
6 # Inspired by example1.py (SFPPy distribution)
7 from patankar.layer import LDPE
8 from patankar.loadpubchem import migrant
9 from patankar.geometry import Packaging3D
10 import patankar.food as food
11
12 # Geometry: cylinder (h=19 cm, r=30 mm)
13 internal_volume, surface_area = Packaging3D(
14     "cylinder", length=(19, "cm"), radius=(30, "mm")
15 ).get_volume_and_area()
16
17 # Migrant + film
18 m = migrant("irganox 1076")
19 film = LDPE(migrant=m, l=(100, "um"))
20
21 # Food proxy: fatty semi-solid sandwich
22 class Sandwich(food.realfood, food.semisolid, food.fat): name = "sandwich"
23 F = Sandwich(volume=internal_volume, surfacearea=surface_area,
24     contacttime=(10, "days"), contacttemperature=(7, "C"),
25     substance=m, simulant="ethanol")
26
27 # Tier M2 - partition
28 K_F_over_P = film.k / F.k0
29
30 # Tier M3 - kinetics
31 kin = F.migration(film)
32 CF = kin.CFtarget
33 s = 100 * CF / m.SML
34
35 # =====
36 # ////////////////////////////////////////////////// Detailed version ///////////////////////////////////
37 # =====
38 # --- Imports -----
39 from patankar.layer import LDPE # LDPE model
40 from patankar.loadpubchem import migrant # PubChem + props
41 from patankar.geometry import Packaging3D # 3D geometry
42 import patankar.food as food # food/simulants
43
44 # --- 1) Geometry: cylinder (height x radius) -----
45 # Units as tuples (value, "unit"), handled by SFPPy.
46 internal_volume, surface_area = Packaging3D(
47     "cylinder", length=(19, "cm"), # height = 19 cm
48     radius=(30, "mm") # radius = 30 mm (diam = 60 mm)
49 ).get_volume_and_area()
50 print(f"[Geometry] V = {internal_volume.item():.6g} m^3")
51 print(f"[Geometry] A = {surface_area.item():.6g} m^2")
52
53 # --- 2) Migrant + LDPE film -----
54 # Example: Irganox 1076 (phenolic AO) from public DBs.
55 m = migrant("irganox 1076")
56 film = LDPE(migrant=m, l=(100, "um")) # 100 um
57 print(f"[Migrant] {m.compound} | CAS={m.CAS} | "
58     f"M={m.M} g/mol | logP={m.logP}")
59
60 # --- 3) Food proxy: semi-solid, fatty sandwich -----
61 class Sandwich(food.realfood, food.semisolid, food.fat): name = "sandwich"
62 F = Sandwich(volume=internal_volume, surfacearea=surface_area,
63     contacttime=(10, "days"), contacttemperature=(7, "C"),
64     substance=m, simulant="ethanol") # fatty matrix proxy
65
66 # --- 4) Equilibrium partition (Tier M2) -----
67 # K_{F/P} = k_P / k_F
68 K_F_over_P = film.k / F.k0

```

```

69 print(f"[M2] K_(F/LDPE) = {K_F_over_P.item():.4g} "
70       "<1: stronger LDPE affinity)")
71
72 # --- 5) kinetics (Tier M3): 10 d @ 7 C -----
73 # SFPPy couples partition + diffusion with T,t.
74 kin = F.migration(film)
75 CF = kin.CFtarget
76 s = 100 * CF / m.SML
77 print(
78     f"[M3] 10 d @ 7 C: C_F = {CF.item():.6g} mg/kg, "
79     f"severity = {s.item():.2f}")
80 )
81 # Optional plots: time course + layer profiles
82 kin.plotCF() # kinetics
83 kin.plotCx() # concentration profiles
84
85 # --- 6) Step 2: +4 h @ 25 C (warming before use) -----
86 F2 = F.copy().update( contacttime=(4, "hours"),contacttemperature=(25, "C"))
87 kin2 = kin >> F2 # simulation chaining with ">>"
88 s2 = 100 * kin2.CFtarget / m.SML # updated severity
89 print(f"[M3] +4 h @ 25 C: C_F = {kin2.CFtarget.item():.6g} mg/kg, "
90       f"severity = {s2.item():.2f}")
91 # Cumulative kinetics over both steps
92 (kin + kin2).plotCF()

```

Typical outputs (Listing 2):

Output 1 – outputs of listing 1

```

1 [Geometry] V = 0.000537212 m^3
2 [Geometry] A = 0.041469 m^2
3 [Migrant] irganox 1076 | CAS=['2082-79-3'] | M=530.9 g/mol | logP=[13.8]
4 [M2] K_(F/LDPE) = 6.741 (<1: stronger LDPE affinity)
5 [M3] 10 d @ 7 C: C_F = 5.22691 mg/kg, severity = 87.12
6 [M3] +4 h @ 25 C: C_F = 5.56426 mg/kg, severity = 92.74

```

Takeaway. This example shows the SFPPy syntax and basic M2/M3 calculations from just the compound's name. Severities are computed automatically. While 4 h at 25 °C breaks cold chain for microbiological risk, it has minor impact on chemical risk.

10.2 | Example 2 – Functional barrier in recycled materials

Objective of example 2

Assess migration of *toluene* from a 300 µm recycled polypropylene (rPP) bottle wall into a fatty liquid food, then evaluate the efficiency of a PET functional barrier (FB) of various thicknesses).

Table 22 gives the setup; Listing 3 shows the script.

Table 22 – Parameters of Example 2.

Properties	Values
Geometry	Bottle, $V \approx 1$ L (cylinder + neck)
Migrant	Toluene (CAS 108-88-3), typical NIAS proxy
Wall	rPP, $l = 300$ µm, $C_0 = 10$ mg/kg
Barrier	PET FB, base case 30 µm, variants 2–60 µm
Food	Fatty liquid, 450 d @ 20 °C
Outputs	$\hat{C}_{i,F}(t)$, profiles, severity, FB efficiency

Listing 2 – Optimizing FB thickness for a PP bottle (SFPPy, example2.py)

```

1 # Listing 2 – Optimizing FB thickness for a PP bottle (SFPPy, example2.py)
2 # =====
3 # // Minimalist version //
4 # =====
5 from patankar.loadpubchem import migrant
6 from patankar.geometry import Packaging3D
7 import patankar.food as food
8 import patankar.layer as polymer
9 from patankar.migration import senspatankar, CFSimulationContainer
10
11 # Bottle geometry (1 L)
12 bottle = Packaging3D("bottle",
13                     body_radius=(40,"mm"), body_height=(0.2,"m"),

```

```

14     neck_radius=(1.8,"cm"), neck_height=0.05)
15 Vint, Acontact = bottle.get_volume_and_area()
16
17 # Migrant + rPP wall
18 to1 = migrant("toluene")
19 PP = polymer.PP(l=(300,"um"), substance=to1, C0=10, T=(20,"C"))
20
21 # Food proxy
22 class FattyLiquid(food.realfood, food.liquid, food.fat): name="fattyFood"
23 F = FattyLiquid(volume=Vint, surfacearea=Acontact,
24     contacttime=(450,"days"), contacttemperature=(20,"C"))
25
26 # Simulation without FB
27 ref = senspatankar(PP, F)
28
29 # Add 30 µm PET FB
30 PETfb = polymer.wPET(l=(30,"um"), substance=to1, C0=0, T=(20,"C"))
31 walls_FB = PETfb + PP
32 fb = senspatankar(walls_FB, F)
33
34 # =====
35 # //////////////// Detailed version ////////////////
36 # =====
37 # --- Imports -----
38 from patankar.loadpubchem import migrant      # migrants (PubChem)
39 from patankar.geometry import Packaging3D      # 3D bottle geometry
40 import patankar.food as food                  # food/simulants
41 import patankar.layer as polymer              # polymer layers
42 from patankar.migration import senspatankar   # solver
43 from patankar.migration import CFSimulationContainer as store
44 from patankar.layer import _toSI
45
46 # --- 1) Bottle geometry (1 L) -----
47 bottle = Packaging3D("bottle",
48     body_radius=(40,"mm"), body_height=(0.2,"m"),
49     neck_radius=(1.8,"cm"), neck_height=0.05)
50 Vint, Acontact = bottle.get_volume_and_area()
51 print(f"[Geometry] V={Vint.item():.3e} m3, A={Acontact.item():.3e} m2")
52
53 # --- 2) Migrant + rPP wall -----
54 to1 = migrant("toluene")
55 PP = polymer.PP(l=(300,"um"), substance=to1, C0=10, T=(20,"C"))
56
57 # --- 3) Food proxy -----
58 class FattyLiquid(food.realfood, food.liquid, food.fat): name="fattyFood"
59 F = FattyLiquid(volume=Vint, surfacearea=Acontact,
60     contacttime=(450,"days"), contacttemperature=(20,"C"))
61
62 # --- 4) Simulation without FB -----
63 ref = senspatankar(PP, F, name="rPP_bottle")
64 ref.plotCF(); ref.plotCx()
65
66 # --- 5) Add PET functional barrier (30 um) -----
67 PETfb = polymer.wPET(l=(30,"um"), substance=to1, C0=0, T=(20,"C"))
68 walls_FB = PETfb + PP
69 fb = senspatankar(walls_FB, F, name="rPP_bottle_FB")
70 fb.plotCF(); fb.plotCx()
71
72 # --- 6) Compare with/without FB -----
73 comp = store(name="bottles")
74 comp.add(ref, "without FB", "b"); comp.add(fb, "with PET FB", "m")
75 comp.plotCF()
76
77 # --- 7) Systematic study: FB thickness (2-60 um) -----
78 study = store(name="FBthickness")
79 study.add(ref, "without FB", "k")
80 for lfb in range(2,61,4):
81     walls_FB.l[0] = _toSI(lfb,"um").item()
82     sim = senspatankar(walls_FB, F, name=f"FB{lfb}um")
83     study.add(sim, f"PET {lfb} um")
84 study.plotCF()

```

Results. Figure 6 shows kinetic profiles for varying PET FB thickness. Key points:

- rapid contamination without FB (reference),
- drastic reduction with 30 µm PET (even plasticized “wPET”),
- only moderate pure lag effect (weeks).

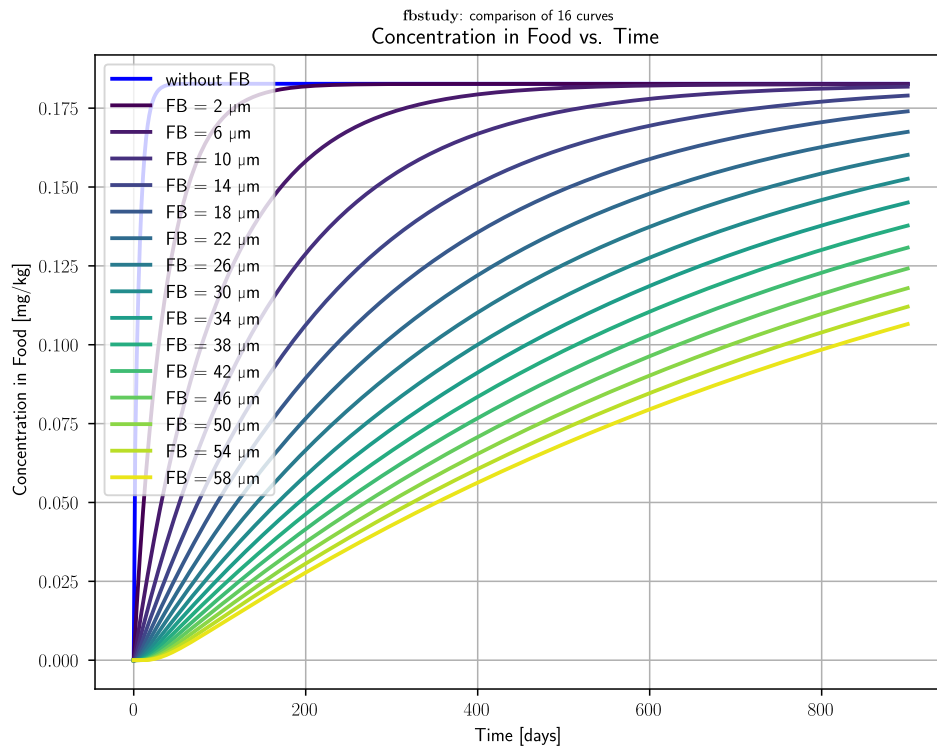


Figure 6 — Simulated kinetics for various PET FB thicknesses (Example 2).

Tip

Takeaway. SFPPy models **functional barriers** (FB) without extra equations: same M2/M3 solvers apply. Thickness sweeps directly size the FB needed for compliance. Full script: `example2.py`.

10.3 | Example 3 — Multilayer structure and sequential scenarios

Objective of example 3

Simulate limonene migration from a 500 μm rPP core through a PET/PP/PET (ABA) tray, across 3 steps: (1) 4 mo @ 20 °C storage, (2) hot fill @ 90 °C with fatty food, (3) 6 mo @ 30 °C storage.

Variants: (v1) substitute with toluene, (v2) halve PET layers (20 \rightarrow 10 μm), (v3) combine v1+v2.

Table 23 summarizes the studied configurations.

Table 23 — Parameters of Example 3.

Properties	Values
Geometry	Open box 19 \times 10 \times 8 cm (rectangular prism)
Migrant	Limonene, $C_0 = 200$ mg/kg; variant: toluene
Structure	ABA: PET 20 μm / rPP 500 μm / PET 20 μm
Steps	(1) 4 mo @ 20 °C, (2) hot fill 90 °C, (3) 6 mo @ 30 °C
Outputs	Concentration profiles, cumulative kinetics, variant comparisons

Key findings (Figure 6):

- PET 20 μm stabilizes contamination (steady permeability regime),
- toluene (v1) migrates more (higher mobility),
- thinner PET (v2) worsens migration,
- v3 is worst case.

Listing 3 — Multilayer structure and sequential scenarios (SFPPy, `example3.py`)

```

1 # Listing 3 — Multilayer structure and sequential scenarios
2 # Imports
3 from patankar.loadpubchem import migrant
4 from patankar.layer import gPET, wPET, PP
5 from patankar.geometry import Packaging3D
6 from patankar.food import setoff, ambient, hotfilled, realfood, liquid, fat
7 from patankar.migration import CFSimulationContainer as store

```

```

8
9 # --- 1) Geometry -----
10 box = Packaging3D("box_container", length=(19,"cm"),
11                 width=(10,"cm"), height=(8,"cm"))
12 Vint, Acontact = box.get_volume_and_area()
13
14 # --- 2) Migrant and layers -----
15 m = migrant("limonene")
16 A1 = wPET(l=(30,"um"), migrant=m, C0=0)
17 B = PP(l=(0.5,"mm"), migrant=m, CP0=200) # CP0 or C0 are aliases
18 A2 = gPET(l=(30,"um"), migrant=m, C0=0)
19 ABA = A1 + B + A2 # trilayer structure
20
21 # --- 3) Contact conditions -----
22 class Step1(setoff,ambient): contacttime=(4,"months"); contacttemperature=
23 (20,"C")
24 class Step2(hotfilled,realfood,liquid,fat): pass
25 class Step3(ambient,realfood,liquid,fat): contacttime=(6,"months");
26 contacttemperature=(30,"C")
27 F1,F2,F3 = Step1(), Step2(), Step3()
28 box >> F1 >> F2 >> F3 # propagate geometry
29
30 # --- 4) Chained simulation (>> operator) -----
31 F1 >> ABA >> F1 >> F2 >> F3
32 sol_ref = F1.lastsimulation + F2.lastsimulation + F3.lastsimulation
33
34 # --- 5) Variants -----
35 # operator % is used to inject substances
36 m2 = migrant("toluene")
37 m2 % F1 >> ABA >> F1 >> F2 >> F3
38 sol_v1 = F1.lastsimulation + F2.lastsimulation + F3.lastsimulation
39 m % F1 >> ABA.copy(l=[10e-6,0.5e-3,10e-6],migrant=m) >> F1>>F2>>F3
40 sol_v2 = F1.lastsimulation + F2.lastsimulation + F3.lastsimulation
41 m2 % F1 @ ABA.copy(l=[10e-6,0.5e-3,10e-6],migrant=m2) >> F1>>F2>>F3
42 sol_v3 = F1.lastsimulation + F2.lastsimulation + F3.lastsimulation
43
44 # --- 6) Compare all cases -----
45 comp = store(name="ABA study")
46 comp.add(sol_ref, "Limonene with 20 um thick FB (ref)", "Teal", linewidth=3,
47          linestyle='--')
48 comp.add(sol_v1, "Toluene with 20 um thick FB (v1)", "Crimson", linewidth=3)
49 comp.add(sol_v2, "Limonene with 10 um thick FB (v2)", "deepskyblue",
50          linewidth=2, linestyle='--')
51 comp.add(sol_v3, "Toluene-FB with 10 um thick FB (v3)", "tomato", linewidth=2)
52 hfig = comp.plotCF()
53 hfig.print('cmp_pltCF_container_with_FB',destinationfolder="tmp/",overwrite=True)

```

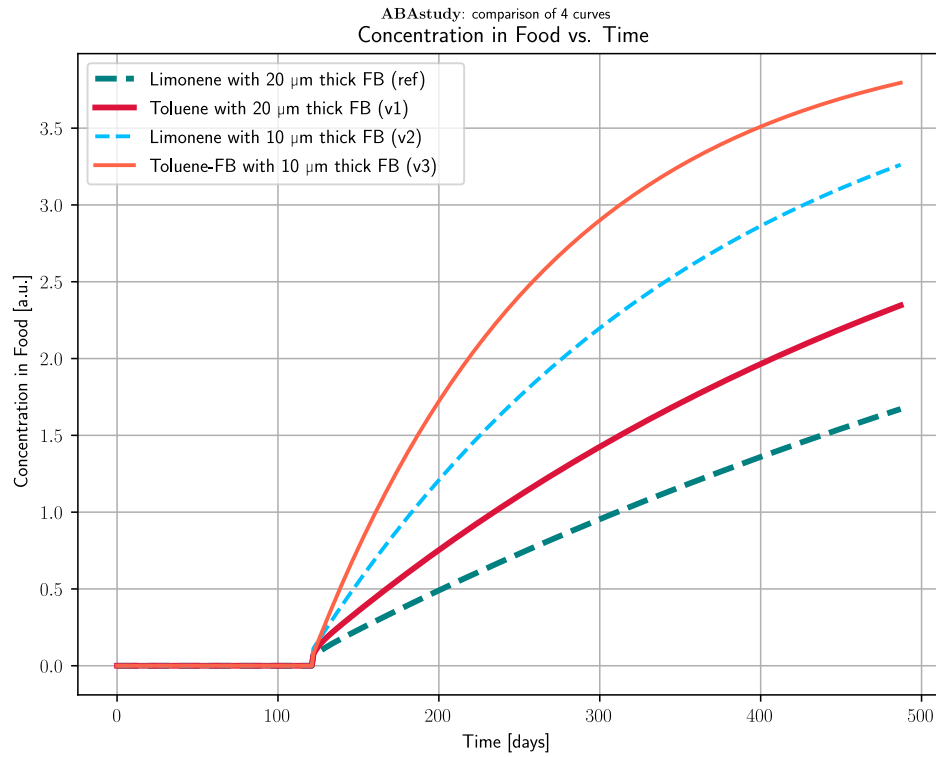


Figure 6 — Simulated kinetics for ABA tray and variants (Example 3).

[Note]

Takeaway. SFPPy's symbolic operators: + (layer assembly/sum), >> (step chaining), % (migrant substitution), @ (thermal reinit). Applicable at M3 for kinetics and release potentials.

10.3.1 | Intrinsic Release Potentials

The extension proposed in Listing \ref{lst:Ex3multilayerPR} computes the *intrinsic potential releases per step* $PR_{i|k}$ for the complete package (with the initial contaminant distribution unchanged), using both full and “amputated” sequences (Eq. \ref{eq:PRw-o}). It then decomposes the *intrinsic potentials per layer* $PR_{i,j|k}$ by assuming that the contaminant is initially localized in each layer j in turn. Comparison with the full sequence allows the specific contribution of each step or layer to be inferred (see Eq. \ref{eq:PRdependence}).

Listing 4 — Calculate potential release corresponding to listing 3

```

1  # %% Example 3 - Extension (1/2) - Potential Release (PR)
2  # -----
3  """
4  Analysis at the scale of the full packaging (the initial distribution of
5  contaminants is preserved)
6      PR = PRE * PRT
7
8  PR : ndarray of shape (n_steps,)
9      Array of intrinsic potential release values for each step in the
10     current sequence of transfer (e.g. storage, hot fill, long-term storage).
11 """
12
13 import numpy as np
14
15 # effective potential release of steps 1+2+3, 2+3, 1+2
16 # Fj @ ABA or Fj >> ABA = thermalize
17 # ABA >> Fj >> Fj+1 propagates migration from ABA to Fj and then Fj+1
18 sim123 = m2 % F1 >> ABA >> F1 >> F2 >> F3
19 PRall123 = np.array([m.lastsimulation.PR.PRTtarget_effective for m in
20 [F1,F2,F3]])
21
22 F2 @ ABA >> F2 >> F3 # step 1 omitted
23 PRall23 = np.array([m.lastsimulation.PR.PRTtarget_effective for m in [F2,F3]])
24 F1 @ ABA >> F1 >> F3 # step 2 omitted
25 PRall13 = np.array([m.lastsimulation.PR.PRTtarget_effective for m in [F1,F3]])
26
27 # intrinsic potential release for steps: 1=1+2+3\2+3, 2=1+2+3\1+3, 3=1+2+3\1+2
28 PR = np.zeros((len(PRall123)), dtype=float)
29 PRN = PRall123[-1,0] # potential release with all steps
30 PR[0] = 1.0 - (1.0-PRN)/(1.0-PRall123[1,0])
31 PR[1] = 1.0 - (1.0-PRN)/(1.0-PRall13[1,0])
32 PR[2] = 1.0 - (1.0-PRN)/(1.0-PRall123[1,0])

```

```

29 print("PR =", PR)
30 print("PRT =", PR/F3.lastsimulation.PR.PRE_effective)
31 print("score = PR/PRN =", PR/PRN)
32 # compute dependency error on intrinsic PR
33 PRNcontrol = (1-np.prod(1-PR))
34 print(f"PR dependency ~ {(PRNcontrol/PRN - 1).item()*100:0.3f} %")
35
36
37 # %% Example 3 - Extension (2/2) - layer-based Potential Release (PR)
38 # -----
39 """
40 Analysis at the scale of each layer (j=1,2,3).
41
42 PR_layers : ndarray of shape (n_steps, n_layers)
43     Array of intrinsic potential release values per step and per layer
44     in a multilayer system, reconstructed by comparison of full and
45     step-omitted sequences.
46 """
47 R123 = F1.potentialRelease(ABA) >> F2 >> F3
48 R23 = F2.potentialRelease(ABA) >> F3
49 R13 = F1.potentialRelease(ABA) >> F3
50
51 # intrinsic layer-based potential release
52 PR_layers = np.zeros((len(R123), len(ABA)), dtype=float) # nsteps x nlayers
53 PRN_layers = R123.PR[2,:]
54 PR_layers[0,:] = 1.0 - (1.0-PRN_layers)/(1.0-R23.PR[1,:])
55 PR_layers[1,:] = 1.0 - (1.0-PRN_layers)/(1.0-R13.PR[1,:])
56 PR_layers[2,:] = 1.0 - (1.0-PRN_layers)/(1.0-R123.PR[1,:])
57 PRN_layers_control = 1 - np.prod(1-PR_layers, axis=0)

```

10.3.2 | Results and Interpretation (Package Scale)

The computed release potentials for the ABA tray are summarized in Table 24.

The value $\text{PRN} \approx 0.338$ indicates that roughly one third of the initial toluene mass ends up in the food phase during the complete sequence ($F_1 + F_2 + F_3$).

Step F_3 alone accounts for about **97 %** of the cumulative release ($\text{score}[2]$), while F_2 is negligible ($\text{score}[1]$) and F_1 (storage without contact) still contributes about **11 %**, moving the contaminant closer to the contact interface.

The dependency check (Eq. \ref{eq:PRdependence}) shows a positive deviation of **4.29 %** between the migration reconstructed from the $PR_{i|k}$ values and the full sequence $PR_i^{N=F_1+F_2+F_3}$, revealing slight interdependence between steps.

Step F_1 is *composite*: it loads A_1 (contact side) but also induces a *partial backflow* (~4 %) toward A_3 , i.e., the opposite surface. Asymmetrical structures or longer F_1 durations significantly alter these contributions.

Table 24 — Release potentials per step (script extension 1/2).

↓ Variable / index o →	0	1	2	Interpretation
PRa11123[o]	0	0.0154	PRN = 0.3375	$PR_i^{(N=F_1,F_1+F_2,F_1+F_2+F_3)}$
PRa1123[o]	2.887×10^{-6}	0.3134	–	$PR_i^{(N=F_2,F_2+F_3)}$
PRa1113[o]	0	0.3361	–	$PR_i^{(N=F_1,F_1+F_3)}$
PR[o]	0.0350	0.0020	0.3271	$PR_i _{k=F_1,F_2,F_3}$
PRT[o]	0.0362	0.0020	0.3381	$PR_i^T _{k=F_1,F_2,F_3}$
score[o]	0.1039	0.0059	0.9692	$PR_i _k/PR_i^{(F_1+F_2+F_3)}$

† In Python, the index o = k - 1 (step index). Variables PRa11123, PRa1123, and PRa1113 capture cumulative effects up to step k. PR, PRT, and score are intrinsic to each step k.

10.3.3 | Results and Interpretation (Layer Scale)

The computation of $PR_{i,j}|_k$ (variable PR_layers) follows the same logic by introducing the contaminant (m_2) successively into A_1 ($j = 1$), B ($j = 2$), and A_3 ($j = 3$).

Results (Table \ref{tab:Ex3Ext2}) confirm that the column PR_layers[:,1] ($j = 2$) reproduces PR (the real source).

Values for A_1 are similar except for F_1 , where PR_layers[0,0] is strongly negative: storage without contact causes a backflow toward B_2 , limiting final release.

Very small values for A_3 confirm that contaminants initially located on the external side have a low transfer risk toward the food.

Note

Practical note: this analysis yields a *component-wise release indicator*, highly useful for recycled materials. It identifies the parts that are *structurally prone* to releasing the most (for a given content) and thus where to install or optimize barriers.

When a layer is protected, the barrier *imposes* its resistance on the global transfer; conversely, a *reservoir*

layer behaves almost neutral and contributes little to the total release.

Table 25 — $\text{PR}_{\text{layers}}[\text{o}, \text{p}]$ values per step (o) and per layer (p) (script extension 2/2).

↓ Index o / Index p →	A _i (p = 0)	B _i (p = 1)	A _i (p = 2)
F ₁ (o = 0)	-0.89269	0.03505	0.00293
F ₂ (o = 1)	0.00195	0.00198	0.00699
F ₃ (o = 2)	0.32807	0.32706	0.02125

† Python indices start at 0 → o = k - 1 (step) and p = j - 1 (layer). The smallest index corresponds to the layer in contact with the food.

10.4 | Example 4 — Parametric identification

Objective of example 4

Estimate diffusivity D and partition coefficient k of a monolayer directly from kinetic data (real or noisy simulated). Generate pseudo-experimental kinetics, then recover true values by non-linear fit.

Table 6 details the case; Listing 4 shows the script.

Table 26 — Parameters of Example 4.

Properties	Values
Layer	Monolayer P: $l = 100 \mu\text{m}$, $D = 1 \times 10^{-10} \text{ cm}^2/\text{s}$, $C_0 = 1000$ (a.u.), $k_P = 0.1$
Medium	Food simulant F: $V = 1 \text{ L}$, $A = 6 \text{ dm}^2$, $h = 10^{-6} \text{ m/s}$, $k_F = 1$
Data	Noisy $C_F(t)$ kinetics (30 pts, $\sigma=1\%$)
Outputs	Nonlinear fit of D, k ; compare fitted vs. true

Note

Result Overview. Despite noise, fitted D, k are close to true values (e.g., $D \simeq 9.9 \times 10^{-15} \text{ m}^2/\text{s}$ vs. 1.0×10^{-14} , $k \simeq 0.108$ vs. 0.10).

Listing 5 — Script to identify D and k from experimental data (adapted from `example4.py`)

```

1 # Listing - Script to identify D and k from experimental data (adapted from
  # example4.py)
2
3 # --- Imports -----
4 from patankar.layer import layer, layerLink
5 from patankar.food import foodlayer
6
7 # --- 1) Define layer P and food F -----
8 P = layer(l=(100,"um"), D=(1e-10,"cm**2/s"), C0=1000, k=0.1)
9 F = foodlayer(contacttime=(10,"days"), volume=(1,"L"),
10               surfacearea=(6,"dm**2"), h=(1e-6,"m/s"), CF0=0, k=1)
11
12 # --- 2) Link parameters (D,k) for external control -----
13 Dref, kref = P.D, P.k
14 P.Dlink = layerLink("D", indices=0, values=Dref)
15 P.klink = layerLink("k", indices=0, values=kref)
16
17 # --- 3) Baseline simulation + pseudo-experiment -----
18 R = F.migration(P) # reference kinetics
19 E = R.pseudoexperiment(npoints=30, std_relative=0.01) # noisy data
20
21 # --- 4) Sensitivity scan (optional visual check) -----
22 R.comparison.update(0, label="**Reference**", color="black")
23 for _ in range(10):
24     P.Dlink[0] /= 1.1 # decrease D
25     P.klink[0] *= 1.1 # increase k
26     R.rerun(name=f"{P.Dlatex()[0]}, {P.klatex()[0]}",
27             color=R.comparison.jet(10)[_])
28 R.comparison.add(E, label="Pseudo Experiment", discrete=True)
29 R.comparison.plotCF()
30
31 # --- 5) Fit D and k on the experimental kinetics -----
32 d2 = R - E # squared-distance callable
33 print("Before fit:", d2())
34 res = R.fit(E) # non-linear optimization of D and k

```

```

35 print("After fit:", d2())
36 print("Fitted D:", P.Dlink.values, "| True:", Dref)
37 print("Fitted k:", P.klink.values, "| True:", kref)
38 R.comparison.plotCF()           # show fitted curve vs. data

```

Key result. Despite added noise, the method recovers D and k very close to the true values (e.g., $D \simeq 9.89 \times 10^{-15} \text{ m}^2/\text{s}$ vs. 1×10^{-14} ; $k \simeq 0.108$ vs. 0.10). Figure 7 shows the fitted kinetics superimposed on the experimental points, as well as successive deviations from the reference solution ($D/1.1^\ell$ and $k \times 1.1^\ell$, $\ell = 1 \dots 10$).

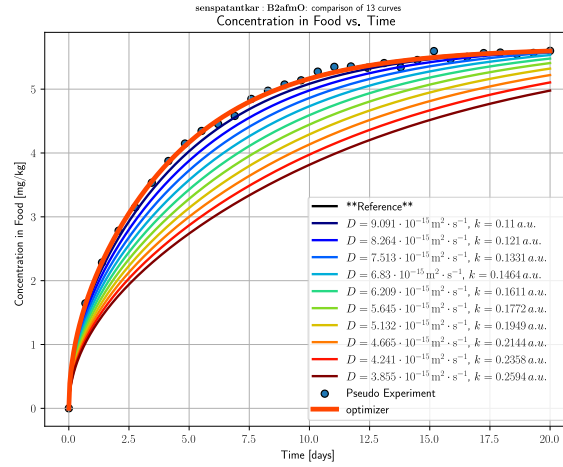


Figure 7 — Joint fit of D and k from a noisy kinetic (“pseudo-experiment”) using Listing 5. The optimized curve (orange) overlays both the simulated experimental points and the noise-free reference. Other curves illustrate sensitivity to D and k .

Tip

Real data. The procedure works identically with experimental series ($E = R.from_csv(\dots)$ or by creating an equivalent “experiment” object). The `layerLink` mechanism *binds* any targeted parameter (here D, k) for non-linear fitting on $C_F(t)$ while preserving the M2/M3 physics. The only constraint is to remain within the linear (tracer) regime presented in Section 8 (properties independent of concentration).

Note

Takeaway. The `layerLink` mechanism links targeted parameters (here D, k) and estimates them via nonlinear fit on $C_F(t)$, while keeping M2/M3 physics intact. Applies equally to real datasets (`from_csv`). Domain validity: tracer regime (concentration-independent properties, see §8).

10.5 | Example 5 — AI integration with local knowledge base (RAG)

Automating calculations and verifying regulatory thresholds with AI becomes possible by integrating local document bases (*Retrieval-Augmented Generation*, RAG) and Python scripts. The whole stack can run offline, with confidentiality and auditability—key conditions for safe-by-design workflows.

Objective of example 5

Couple SFPPy with a local regulatory Q/A engine by indexing a Markdown knowledge base (regulations, internal guides, Python scripts). Documents are vectorized using *HuggingFace embeddings*, then queried via `LlamaIndex/ollama` with a `mistral` model.

A minimal setup can be built from open tools and modest hardware (an 8–16 GB VRAM GPU is recommended). Components are summarized in Table 27.

Table 7 shows minimal setup; Listing 5 demonstrates.

Table 27 — Components of RAG system coupled to SFPPy.

Properties	Values
KB (source)	Markdown files under <code>./docs/KB</code>
Index	Persistent <code>vectorStoreIndex</code> (Chroma)
Embeddings	<code>BAAI/bge-small-en-v1.5</code> (HuggingFace)
LLM	<code>mistral</code> via <code>ollama</code>
I/O	User question → synthetic answer + cited sources

Outputs. Table 8 compares EU vs. US definitions of “functional barrier.” SFPPy models them by low D , thickness, partitioning.

Listing 6 — Minimal RAG configuration (adapted from `example5.py`)

```

1 # Listing - Minimal RAG configuration (adapted from example5.py)
2
3 from llama_index.core import SimpleDirectoryReader, VectorStoreIndex
4 from llama_index.embeddings.huggingface import HuggingFaceEmbedding
5 from llama_index.llms.ollama import Ollama
6
7 # 1) Load the Markdown/Python KB (recursive)
8 documents = SimpleDirectoryReader(input_dir="./docs/KB",
9 recursive=True).load_data()
10
11 # 2) Embeddings (HuggingFace) then vector index
12 embed_model = HuggingFaceEmbedding(model_name="BAAI/bge-small-en-v1.5")
13 index = VectorStoreIndex.from_documents(documents, embed_model=embed_model)
14
15 # 3) Declare the local LLM (ollama)
16 llm = Ollama(model="mistral") # other models may be installed
17
18 # 4) Query (RAG) with source citations
19 query_engine = index.as_query_engine(llm=llm, similarity_top_k=3)
20 response = query_engine.query("what is the definition of a functional barrier
21 in EU 10/2011?")
22 print(response.response)
23 for src in response.source_nodes:
24     print(" -", src.metadata.get("file_path", "unknown"))

```

Note

Good practices.

Store regulatory excerpts and Python scripts in `./docs/KB`, rebuild the persistent index, and preserve source citations. The SFPPy–RAG coupling enables *hybrid agents* where the LLM’s answer directly steers physical simulation and design choices.

10.5.1 | A Practical Illustration: Legal Definition of Functional Barriers in the EU and US

Table 28 — Comparison of “functional barrier” definitions in the EU and US, as returned by a RAG system built on the SFPPy KB.

Question (EU)	Question (US)
What is the definition of a functional barrier in EU 10/2011?	What is the definition of a functional barrier in the US?
RAG answer	RAG answer
Definition in EU Regulation 10/2011 (Art. 3): “Functional barrier means a layer which prevents migration of substances from behind that barrier into food.” Implications: (i) very low D ; (ii) very low/negligible permeability; (iii) use <code>nofood()</code> or <code>setoff()</code> boundaries in SFPPy.	In the US, “functional barrier” is not legally defined , but FDA recognizes the concept in FCS Notifications. <i>Informal definition:</i> a layer that prevents or significantly reduces migration so that exposure is below levels of safety concern. Key points: migration < 0.5 ppb (0.5 $\mu\text{g/kg}$); accepted in FDA ToR policy and FCNs; modeled in SFPPy by low D , high thickness, and partitioning conditions. Also see FDA ToR policy, FCNs, and CFR 21 Parts 174–179.

In SFPPy. Model a functional barrier by setting (i) very low D ; (ii) sufficiently high thickness; and (iii) partitioning such that downstream migration remains < 0.5 $\mu\text{g/kg}$.

10.5.2 | Advanced Use: Asking a RAG System to Build Predictions

Extension request (to the RAG agent).

“Generate a simulation example with a functional barrier applied in a multilayer system, justify your choice.”

The RAG system can combine example strategies and known documentation to generate new simulations. Listing 7 is auto-generated and can be executed in the SFPPy environment to produce Figure 8 and the interpretation summarized in Table 28.

The selections (migrant = toluene; recycled PP as the source layer; glassy PET as the barrier; simulant = ethanol) are consistent with SFPPy recommendations. Ethanol is intentionally chosen as a fatty-food simulant: it provides a severe and reproducible stress, although other options like `oliveoil` are available. Keep in mind these are numerical calculations: ethanol does not interact with glassy PET (“gPET”) as it might experimentally.

Value for SMEs.

Such auto-generations provide concrete technical support—both executable scripts and expert interpretations. They do not replace regulatory evaluation, but they speed up preparation of credible, well-argued scenarios. Limitations remain: for instance, the agent proposes an un-plasticized PET barrier without discussing

plasticization risk (see Example 2, Section 10.2) or polymer-compatibility issues.

Listing 7 – Multilayer with a Functional Barrier

```

1  """
2  SFPPy demo - Multilayer with a Functional Barrier
3  -----
4  Scenario: Toluene in a recycled PP core, with/without a PET functional barrier
5  Contact: ethanol, 60 days @ 40oC
6  Outputs: CF(t) curves, snapshots, and a small thickness study for the FB
7  """
8  # --- Imports ---
9  from patankar.loadpubchem import migrant
10 from patankar.layer import PP, gPET
11 from patankar.food import ethanol
12 from patankar.migration import senspatankar, CFSimulationContainer
13 import matplotlib.pyplot as plt
14
15 # --- Define Migrant (Toluene) ---
16 tol = migrant("toluene")
17
18 # --- Define Layers ---
19 PPcore = PP(l=500e-6, C0=200, substance=tol) # 500 um PP with 200 mg/kg
    toluene
20 PETbarrier = gPET(l=30e-6, C0=0, substance=tol) # 30 um PET barrier, initially
    no migrant
21
22 # --- Build Multilayer Systems ---
23 multilayer_with_FB = PETbarrier + PPcore # PET on food side
24 multilayer_no_FB = PPcore # no barrier
25
26 # --- Define Food (Ethanol, 40oC, 10 days) ---
27 food_contact = ethanol(contacttime=(60, "days"), contacttemperature=(40,
    "degC"))
28
29 # --- Run Simulations ---
30 result_no_FB = senspatankar(multilayer_no_FB, food_contact, name="No Barrier")
31 result_with_FB = senspatankar(multilayer_with_FB, food_contact, name="With 30
    um PET FB")
32
33 # --- Plot & Compare ---
34 result_no_FB.plotCF()
35 result_with_FB.plotCF()
36 comparison = CFSimulationContainer(
37     name="Toluene Migration into Fatty Food (Ethanol)",
38     SML=0.15e-3, SMLunit="mg/kg")
39 comparison.add(result_no_FB, label="No Barrier", color='red')
40 comparison.add(result_with_FB, label="With 30 um PET FB", color='blue')
41 comparison.plotCF()
42 plt.yscale("log") # log-scale for better visibility
43 plt.ylim(1e-10,10) # concentration range (mg/kg)
44 plt.axhline(0.5e-3, color='black', linestyle='--', label="FDA ToR (0.5
    ug/kg)")
45 plt.title("Toluene Migration into Fatty Food")
46 plt.ylabel("C_F (mg/kg)")
47 plt.xlabel("Time (days)")
48 plt.legend()
49 plt.grid(True)
50 plt.tight_layout()
51 plt.show()

```

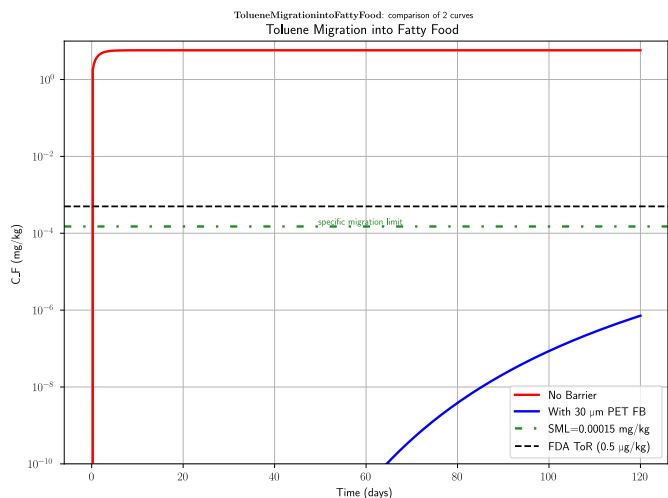


Figure 8. Output figure produced by the auto-generated script in Listing 7.

Table 29 — RAG system’s interpretation of the results from Listing 7 and Figure 8.

Question	Answer
Why these inputs.	(i) rPP core (500 µm) as a realistic volatile reservoir; (ii) PET 30 µm FB (low <i>D</i> for aromatics at moderate <i>T</i>); (iii) toluene as a classic surrogate; (iv) ethanol at 40 °C for 60 days as a severe, reproducible stress; (v) <i>C</i> ₀ = 200 mg/kg to stress the barrier; (vi) SML line at 0.15 µg/kg; (vii) FDA ToR line at 0.5 µg/kg.
How to read the figure.	The blue curve (30 µm PET FB) lies orders of magnitude below red (no barrier): clear functional-barrier effect (lag + reduced flux). On the log scale: staying below both SML and ToR at 60 days meets both criteria; between the lines meets ToR but fails SML; above ToR fails both.
Is 60 days sufficient?	Depends on intended use. Simulate the full profile (hot-fill → cooling → storage). If life exceeds 60 days, extend duration or increase PET thickness. Align simulant choice to the actual food (e.g., ethano195() or a real-fat model as needed).

10.6 | Integrating Other Capabilities: Analytical Fingerprints and Neo-formed Compounds

SFPPy Vitrac 2025a is an *AI-ready* open-source project already integrating molecular-modeling modules, a dynamic PubChem client (Kim *et al.*, 2024), EU/US/CN regulatory bases, and a ToxTree port (Patlewicz *et al.*, 2008). It is compatible with Vitrac 2025b, dedicated to predicting oxidation products and their kinetics under controlled thermo-oxidative conditions—thus enabling realistic migrant scenarios from degradation processes (oxidative scission, more polar low-MW products).

The Vitrac 2025c project—aimed at recycled-material management—leverages chemical fingerprints to recognize/classify contaminants from chromatograms or spectroscopic signals. These tools pave the way to an integrated approach that combines modeling, automated recognition, and release scenarios.

More broadly, SFPPy sits within a rich ecosystem of complementary tools (Table 30) orchestrable in Python. This ecosystem is now usable by large language models (LLMs), which can directly operate these software bricks to answer targeted questions. Coupled with **RAG** techniques, these capabilities enable repeatable, traceable answers grounded in vetted internal guides and examples.

Table 30 — Ecosystem of tools combinable with SFPPy for extended computation, analysis, and decision support.

Tool / Library	Primary role	Use with SFPPy
sig2dna	Analytical-signal interpretation; chemical fingerprints	Map GC/LC–MS peaks to likely chemical families; feed SFPPy with “migrant/NIAS” candidates.
radigen	Neo-formed product generation (oxidation, thermolysis)	Enumerate plausible oxidation products in polymer or food at arbitrary <i>T</i> ; test worst-cases in SFPPy.
OpenChrom*	GC/LC(/MS) data management & processing	Import, filter, integrate chromatograms; export peak lists to SFPPy (CSV).
pymzML, pyteomics	MS data I/O (mzML, mzXML)	Python pipeline for intensities and m/z; couple to sig2dna/matchms, then SFPPy.
matchms	Spectral matching	Rapid candidate annotation (public libs); prioritize migrants to simulate.
RDKit	Cheminformatics (structures, 3D, descriptors)	Generate 3D structures, <i>V</i> _{vdW} , computed log <i>P</i> ; feed M2/M3 modules.
Open Babel	Chemical-format conversion/optimization	Normalize .sdf/.mol/.pdb; complement geometric properties for diffusion (Welle/hFV).
PubChemPy	Programmatic PubChem access	Retrieve formulas, masses, IDs, log <i>P</i> ; auto-complete SFPPy “migrant” sheets.

Tool / Library	Primary role	Use with SFPPy
SciPy (optimize)	Deterministic optimization (LS, simple constraints)	Fit D and k from kinetics (cf. Ex. 4); small design optimizations.
Pyomo, cvxpy	Mathematical programming (LP, QP, MIP)	Cast “safe design” as LP/MILP (costs κ_s , constraints $\hat{C}_{i,F}^{\max}$).
scikit-optimize, DEAP/pymoo	Bayesian / evolutionary optimization	Multi-objective search (migration, cost, mass); explore complex, gradient-free surfaces.
SALib	Global sensitivity analysis (Sobol, Morris)	Rank parameters (D, k, Fo, K) and target measurement/qualification effort.
PyMC	Bayesian inference & uncertainty	Fit D, k with credible intervals; propagate uncertainties to severities \hat{s}_i .
pandas, DuckDB	Tables, joins, analytics	Aggregate M2/M3 outputs; build dashboards across trials/variants; fast local queries.
Matplotlib, Plotly/Dash, Streamlit	Visualization / light apps	CF curves, $C(x, t)$ profiles, parametric studies; mini-apps for quality engineers.
Dask, joblib	Parallelization, batch	Sweep hundreds of substances/designs; accelerate Monte-Carlo/sensitivity.
Prefect, Snakemake	Workflow orchestration	Reproducible studies (data ETL → M2/M3 → optimization → report).
pint	Robust units handling	Secure I/O (μm , dm^2 , mg/kg); align with SFPPy units.
LlamaIndex, LangChain + Ollama	Local RAG/LLMs	Regulatory Q/A, study generation; hybrid agents (code + regulation) around SFPPy (cf. Ex. 5).
unstructured, pdfplumber	PDF/HTML ingestion	Extract tables/normative excerpts for RAG; build parameter sets.

* OpenChrom (like ToxTree) is a Java application; integration is via CSV/Mass-List export and command-line calls.

Key takeaways (Section 10)

The five examples show that M2–M3 simulations, continuous with T0–T2, can be **automated and coupled to AI agents** in Python. Key properties ($\hat{D}_{i,j}, \hat{k}_{i,j}^H$) are extracted from substance/material names. Literature data and scripts can be indexed and exploited by LLMs. The Python ecosystem integrates diverse libraries — from data analysis to analytical chemistry — building pipelines from experimental fingerprints to design scenarios. This capability enables **safe designs**, adaptable to recylcate variability and interoperable among industry and regulators.

11 | Conclusion

This article proposes the main ingredients of a safe-by-design approach, progressing from the simplest indicators to complex scenarios where formulation, design, and use interact. These two levels are not opposed: one helps prioritize when not everything can be controlled, the other integrates all real constraints (geometry, format, presence of contaminants).

Safe design can be framed as a constrained optimization problem, high-dimensional (\mathbb{R}^n in \mathbb{R}^n when n substances are considered). While computations at the different tiers remain fast, collecting and integrating physico-chemical and toxicological data is the main challenge. For simple cases, spreadsheets suffice; for realistic ones (recyclates, $n > 100$, diverse polymers and contact conditions), scripted automation becomes essential.

The proposed formulation is thus suited to managing recycled feedstock and usage diversity. It paves the way for environments where the paper itself can serve as a **RAG** (Retrieval-Augmented Generation) knowledge base, building scenarios and optimizations in natural language. Relying on **open and interoperable** tools and databases, the proposed ecosystem (SFPPy, Python, PubChem, ToxTree...) enables rapid adoption without prior modeling expertise and lends itself to the development of **hybrid agents** combining physical simulation, regulatory bases, and artificial intelligence.

Hence, this approach provides a robust and extensible foundation for research, industry, and regulation—combining scientific rigor, operational requirements, and openness to digital innovation.

12 | Acronyms, notations, and symbols

12.1 | Notations and symbols

Table 31 — Notations and symbols used.

Symbol	Definition (FR; *EN*)	Units
i	Index de la substance / soluté i ; <i>solute index</i> .	—
j	Index de phase (0: référence, F : aliment, s : couche); <i>phase index</i> .	—
s	Index d'une couche / composant d'emballage; <i>layer index</i> .	—
A	Surface de contact; <i>contact area</i> .	m^2
l_s	Épaisseur de la couche s ; <i>layer thickness</i> .	m
V_F, V_s	Volume de l'aliment / d'une couche; <i>food/layer volume</i> .	m^3
ρ_j	Densité de la phase j ; <i>density</i> .	$kg \cdot m^{-3}$
$C_{i,j}, C_{i,j}^0$	Concentration de i dans j (initiale 0); <i>concentration (initial)</i> .	$mol \cdot m^{-3}$ or $mg \cdot kg^{-1}$
$\hat{C}_{i,F}^{(N)}$	Concentration prédite dans l'aliment (itération N); <i>predicted food concentration</i> .	$mol \cdot m^{-3}$ or $mg \cdot kg^{-1}$
$w_{i,s}, \theta_{i,j}$	Poids/fraction mobilisée de la source s ; fraction de disponibilité dans j ; <i>weight / availability fraction</i> .	—
$D_{i,j}(T)$	Diffusivité de i dans la phase j ; <i>diffusivity</i> .	$m^2 \cdot s^{-1}$
$D_{0,i,j}, E_{a,i,j}$	Pré-exponentielle et énergie d'activation (Arrhenius); <i>pre-exponential, activation energy</i> .	$m^2 \cdot s^{-1}$; $J \cdot mol^{-1}$
$k_{i,j}^H$	Coefficient de Henry apparent (réf. $j=0$); <i>apparent Henry coefficient</i> .	—
$K_{i,F/j}$	Coefficient de partage aliment/phase j ($= k_{i,j}^H / k_{i,0}^H$); <i>partition coefficient</i> .	—
$\gamma_{i,j}, a_{i,j}$	Coefficient d'activité et activité; <i>activity coefficient & activity</i> .	—
χ_{i+j}	Paramètre d'interaction de Flory–Huggins; <i>Flory–Huggins interaction</i> .	—
δ_j	Paramètre de solubilité (Hildebrand/Hansen); <i>solubility parameter</i> .	$(MPa)^{1/2}$
P'	Indice de polarité dérivé de $\log P$; <i>polarity index</i> .	—
$\log P$	Partage octanol/eau (base 10); <i>octanol/water partition</i> .	—
Fo	Nombre de Fourier $\int D dt / l^2$; <i>Fourier number</i> .	—
Bi_m, h_m	Nombre de Biot de masse; coeff. de transfert convectif; <i>mass Biot number; mass transfer coeff.</i>	—; $m \cdot s^{-1}$
Sh, Pe	Nombres de Sherwood et de Péclet; <i>Sherwood, Péclet</i> .	—
$M_{i,mig}(t)$	Masse cumulée migrée dans l'aliment; <i>cumulative migrated mass</i> .	mol or mg
$m_{i,0}$	Masse initiale disponible dans la source; <i>initial available mass</i> .	mol or mg
$s_{i,max}$	Sévérité maximale visée (critère d'optimisation); <i>target maximal severity</i> .	—
SML_i, OML	Limites de migration spécifique / globale; <i>SML / OML</i> .	$mg \cdot kg^{-1}$; $mg \cdot dm^{-2}$
Q_M	Teneur autorisée dans le polymère; <i>quantity in material</i> .	$mg \cdot kg^{-1}$ (polymer)
R, T	Constante des gaz et température absolue; <i>gas constant, temperature</i> .	$J \cdot mol^{-1} \cdot K^{-1}$; K
t	Temps de contact; <i>contact time</i> .	s, h, d
A_{pp}, τ	Paramètres polymère (corrélations de Piringer : diffusivité et facteur thermique); <i>Piringer polymer/thermal parameters</i> .	—; K
$V_i, V_{i,mol}$	Volume (molaire) de la molécule i ; <i>molecular (molar) volume</i> .	m^3 ; $cm^3 \cdot mol^{-1}$
ε, τ_{por}	Porosité et tortuosité effectives; <i>porosity, tortuosity</i> .	—
PR_i^T, PR_i^E, t_{fb}	Potentiels de relargage dynamique/statique; durée de service de la barrière fonctionnelle; <i>dynamic/static release potentials; FB service life</i> .	—; —; s

12.2 | Indices and exponents

Table 32 — Indices and exponents used.

Index/Exponent	Meaning (FR; *EN*)
i	Substance/soluté; <i>solute</i> .
j	Phase (0: référence; F : aliment; s : couche polymère); <i>phase (reference/food/layer)</i> .
s	Couche/composant d'emballage; <i>layer/component</i> .
F	Aliment (ou simulant); <i>food (or simulant)</i> .
0 (zero)	Référence thermodynamique (air/eau ou phase de référence); <i>reference phase</i> .
0 (superscript)	Valeur initiale; <i>initial value</i> .
(N)	Itération / ordre d'approximation; <i>iteration/order</i> .
fb	Barrière fonctionnelle; <i>functional barrier</i> .
eq	Équilibre thermodynamique; <i>thermodynamic equilibrium</i> .
ref	Référence (condition/état de référence); <i>reference</i> .

13 | Literature cited

- [1] Vitrac, O.. *FMECAengine: FMECA software developed in the framework of the project SafeFoodPack Design (version v0.45)*. GitHub repository. Last commit: 2019 (commit 3a9f417); available at: <https://github.com/ovitrac/Fmeaengine>. (2019). URL.
- [2] Vitrac, O.. *SFPPy: Python Framework for Food Contact Compliance and Risk Assessment (version v1.42)*. GitHub repository. Last commit circa mid-2025; available at <https://github.com/ovitrac/SFPPy> (accessed on July 27, 2025). (2025). URL.
- [3] Vitrac, O.. *SFPPyLite: lightweight browser-based version of SFPPy (version v1.42)*. GitHub repository. Lightweight browser-based version of SFPPy. Last commit circa mid-2025; available at <https://github.com/ovitrac/SFPPyLite> (accessed on July 27, 2025).. (2025). URL
- [4] Kim, S.; Chen J.; Cheng, T.; Gindulyte, A.; He, J.; He, S.; Li, Q.; Shoemaker, B.; Thiessen, P.; Yu, B.; Zaslavsky, L.; Zhang, J.; Bolton, E.. – Pubchem 2025 update. *Nucleic Acids Research*, 53(D1) :D1516–D1525 (Nov 2024). doi
- [5] Patlewicz, G.; Jeliaskova, N.; Safford, R.; Worth, A.; Aleksiev, B. An evaluation of the implementation of the cramer classification scheme in the toxtree software. *SAR and QSAR in Environmental Research*, 19(5–6) :495–524 July 2008 ;doi, available at URL (accessed on July 27, 2025).
- [6] Zhu, Y.; Nguyen, P.; Vitrac, O.. *Risk assessment of migration from packaging materials into food*. Elsevier. (2019). doi.
- [7] Brandsch, Rainer; Dequatre, Claude; Mercea, Peter; Milana, Maria Rosaria; Stoermer, Angela; Trier, Xenia; Vitrac, Olivier; Schaefer, Annette; Simoneau, C. *Practical guidelines on the application of migration modelling for the estimation of specific migration..* IRC Report IRC98028, Publications Office, LU. (2015). doi.
- [8] Vitrac, O.. *SFPP3: Safe Food Packaging Portal – migration simulation and decision framework (version 1.28)*. Web-based platform. Access: <https://sfpp3-simulation.contactalimentaire.fr/>; default login credentials: user: demouser , password: inramig .Platform hosted by LNE (accessed on July 27, 2025).. (2016). URL.
- [9] Nguyen, P.; Goujon, A.; Sauvegrain, P.; Vitrac, O.. *A computer-aided methodology to design safe food packaging and related systems*. *AIChE Journal*, 59(4): 1183–1212. (mar 2013). doi.
- [10] Vitrac, O.; Ouadi, S.; Hayert, M.; Domenek, S.; Cornuau, G.; Nguyen, P. *FitNESS an E-learning platform to design safe and responsible food packaging*. *Journal of Chemical Education*, 101(8): 3179–3192. (aug 2024). doi. URL.
- [11] Figge, K.. *Migration of components from plastics-packaging materials into packed goods — test methods and diffusion models*. *Progress in Polymer Science*, 6(4): 187–252. (jan 1980). doi.
- [12] Jaeger, R. J.; Rubin, R. J.. *Plasticizers from plastic devices: extraction, metabolism, and accumulation by biological systems*. *Science*, 170(3956): 460–462. (oct 1970). doi.
- [13] Monclús, L.; Arp, H. P. H.; Groh, K. J.; Faltynkova, A.; Løseth, M. E.; Muncke, J.; Wang, Z.; Wolf, R.; Zimmermann, L.; Wagner, M.. *Mapping the chemical complexity of plastics*. *Nature*, 643(8071): 349–355. (jul 2025). doi.
- [14] Munro, I.; Renwick, A.; Danielewska-Nikiel, B.. *The Threshold of Toxicological Concern (TTC) in risk assessment*. *Toxicology Letters*, 180(2): 151–156. (aug 2008). doi.
- [15] Authority, E. F. S.; Organization, W. H.. *Review of the Threshold of Toxicological Concern (TTC) approach and development of new TTC decision tree*. *EFSA Supporting Publications*, 13(3). (Mar 2016). doi.
- [16] Patlewicz, G.; Jeliaskova, N.; Safford, R.; Worth, A.; Aleksiev, B.. *An evaluation of the implementation of the Cramer classification scheme in the Toxtree software*. *SAR and QSAR in Environmental Research*, 19(5–6): 495–524. (jul 2008). doi. URL.
- [17] Committee, E. S.; Hardy, A.; Benford, D.; Halldorsson, T.; Jeger, M. J.; Knutsen, H. K.; More, S.; Naegeli, H.; Noteborn, H.; Ockelford, C.; Ricci, A.; Rychen, G.; Schlatter, J. R.; Silano, V.; Solecki, R.; Turck, D.; Bresson, J.; Dusemund, B.; Gundert-Remy, U.; Kersting, M.; Lambré, C.; Penninks, A.; Tritscher, A.; Waalkens-Berendsen, I.; Woutersen, R.; Arcella, D.; Court Marques, D.; Dorne, J.; Kass, G. E.; Mortensen, A.. *Guidance on the risk assessment of substances present in food intended for infants below 16 weeks of age*. *EFSA Journal*, 15(5). (May 2017). doi.
- [18] Committee, E. S.. *Guidance on selected default values to be used by the EFSA Scientific Committee, Scientific Panels and Units in the absence of actual measured data*. *EFSA Journal*, 10(3). (Mar 2012). doi. [19] Commission. *Commission Regulation (EU) No 10/2011 of 14 January 2011 on plastic materials and articles intended to come into contact with food*. *Official Journal of the European Union*, L 12: 1–89. (2011). URL.
- [20] Vitrac, O.; Hayert, M.. *Risk assessment of migration from packaging materials into foodstuffs*. *AIChE Journal*, 51(4): 1080–1095. (feb 2005). doi.
- [21] Vitrac, O.; Hayert, M.. *Identification of Diffusion Transport Properties from Desorption/Sorption Kinetics: An Analysis Based on a New Approximation of Fick Equation during Solid-Liquid Contact*. *Industrial & Engineering Chemistry Research*, 45(23): 7941–7956. (oct 2006). doi.
- [22] Landrum, G.; Tosco, P.; Kelley, B.; Ric, Sriniker; Gedeck; Vianello, R.; NadineSchneider; Kawashima, E.; Dalke, A.; N, D.; Cosgrove, D.; Cole, B.; Swain, M.; Turk, S.; AlexanderSavelyev; Jones, G.; Vaucher, A.; Wójcikowski, M.; Take; Probst, D.; Ujihara, K.; Scalfani, V. F.; Godin, G.; Pahl, A.; Berenger; JIVarjo; Strêts123; JP; DoliathGavid. *rdkit/rdkit: 2022_03_1b1 (Q1 2022) Release*. Zenodo. ; available at <https://www.rdkit.org/> (accessed July 27, 2025).. (2022). doi. URL.
- [23] O'Boyle, N. M.; Banck, M.; James, C. A.; Morley, C.; Vandermeersch, T.; Hutchison, G. R.. *Open Babel: An open chemical toolbox*. *Journal of Cheminformatics*, 3(1). (oct 2011). doi. URL.
- [24] Nguyen, P.; Guiga, W.; Vitrac, O.. *Molecular thermodynamics for food science and engineering*. *Food Research International*, 88: 91–104. (oct 2016). doi.
- [25] Vitrac, O.; Nguyen, P.; Hayert, M.. *In silico prediction of food properties: a multiscale perspective*. *Frontiers in Chemical Engineering*, 3. (jan 2022). doi.
- [26] Kim, S.; Chen, J.; Cheng, T.; Gindulyte, A.; He, J.; He, S.; Li, Q.; Shoemaker, B. A.; Thiessen, P. A.; Yu, B.; Zaslavsky, L.; Zhang, J.; Bolton, E. E.. *PubChem 2025 update*. *Nucleic Acids Research*, 53(D1): D1516–D1525. (nov 2024). doi. URL.
- [27] Schymanski, E.; Kondic, T.; Elapavalore, A.; Bolton, E.; Thiessen, P.; Zhang, J.; Kim, S.; Krinsky, A. M.; Ross, D. H.; Xu, L.. *PubChemLite for Exposomics + predicted CCS from CCSbase - 2 August 2025*. Zenodo. (2025). doi.

- [28] Gillet, G.; Vitrac, O.; Desobry, S.. *Prediction of solute partition coefficients between polyolefins and alcohols using a generalized Flory-Huggins approach*. Industrial & Engineering Chemistry Research, 48(11): 5285–5301. (may 2009). doi.
- [29] Gillet, G.; Vitrac, O.; Desobry, S.. *Prediction of partition coefficients of plastic additives between packaging materials and food simulants*. Industrial & Engineering Chemistry Research, 49(16): 7263–7280. (jul 2010). doi.
- [30] Vitrac, O.; Gillet, G.. *An off-lattice flory-huggins approach of the partitioning of bulky solutes between polymers and interacting liquids*. International Journal of Chemical Reactor Engineering, 8(1). (jan 2010). doi.
- [31] Nguyen, P.; Guiga, W.; Dkhissi, A.; Vitrac, O.. *Off-lattice Flory–Huggins approximations for the tailored calculation of activity coefficients of organic solutes in random and block copolymers*. Industrial & Engineering Chemistry Research, 56(3): 774–787. (jan 2017). doi.
- [32] Snyder, L.. *Classification of the solvent properties of common liquids*. Journal of Chromatography A, 92(2): 223–230. (may 1974). doi.
- [33] Rohrschneider, L.. *Solvent characterization by gas-liquid partition coefficients of selected solutes*. Analytical Chemistry, 45(7): 1241–1247. (jun 1973). doi.
- [34] Cheng, T.; Zhao, Y.; Li, X.; Lin, F.; Xu, Y.; Zhang, X.; Li, Y.; Wang, R.; Lai, L.. *Computation of octanol-water partition coefficients by guiding an additive model with knowledge*. Journal of Chemical Information and Modeling, 47(6): 2140–2148. (nov 2007). doi.
- [35] Fang, X.; Vitrac, O.. *Predicting diffusion coefficients of chemicals in and through packaging materials*. Critical Reviews in Food Science and Nutrition, 57(2): 275–312. (apr 2015). doi.
- [36] Begley, T.; Castle, L.; Feigenbaum, A.; Franz, R.; Hinrichs, K.; Lickly, T.; Mercea, P.; Milana, M.; O'Brien, A.; Rebre, S.; Rijk, R.; Piringer, O.. *Evaluation of migration models that might be used in support of regulations for food-contact plastics*. Food Additives and Contaminants, 22(1): 73–90. (jan 2005). doi.
- [37] Ewender, J.; Welle, F.. *A new method for the prediction of diffusion coefficients in poly(ethylene terephthalate)—Validation data*. Packaging Technology and Science, 35(5): 405–413. (jan 2022). doi.
- [38] Fang, X.; Domenek, S.; Ducruet, V.; Réfrégiers, M.; Vitrac, O.. *Diffusion of aromatic solutes in aliphatic polymers above glass transition temperature*. Macromolecules, 46(3): 874–888. (jan 2013). doi.
- [39] Zhu, Y.; Welle, F.; Vitrac, O.. *A blob model to parameterize polymer hole free volumes and solute diffusion*. Soft Matter, 15(43): 8912–8932. (2019). doi.
- [40] Zhu, Y.; Guillemat, B.; Vitrac, O.. *Rational design of packaging: toward safer and ecodesigned food packaging systems*. Frontiers in Chemistry, 7. (may 2019). doi.
- [41] Vitrac, O.. *radigen: Python-based chemical kernel for simulating oxidation reactions from prompts*. GitHub repository. Available at <https://github.com/ovitrac/radigen> (accessed on on July 27, 2025). (2025). URL.